TÉCNICO LISBOA

Modelling and experimental validation of mattress modified with PCM to improve the thermal comfort of homeless

Gonçalo Carreira da Silva

Thesis to obtain the Master of Science Degree in

Mechanical Engineering

Supervisors: Dr. Rui Pedro da Costa Neto
Prof. Carlos Augusto Santos Silva

Examination Committee

Chairperson: Prof. Edgar Caetano Fernandes
Supervisor: Dr. Rui Pedro da Costa Neto
Member of the Committee: Prof. António Joaquim dos Santos Romão Serralheiro

November 2018

Abstract

In this study, the performance of Phase Change Materials (PCM) to improve thermal comfort of homeless people (outdoors) in Lisbon was studied. For this, several EnergyPlus simulations were performed. These simulations were made to check the feasibility and best-case scenario of a sleeping system, containing a sleeping bag and a sleeping mat, in the meteorological conditions of Lisbon. Two parameters were studied: PCM melting temperature and PCM quantity. This EnergyPlus model was validated using real measured data from experimental simulations in which a subject slept for 8 hours in an ambient controlled room. It was concluded that a PCM sleeping system (system composed of a normal sleeping bag and a PCM-filled sleeping mat) improves thermal comfort in the subject when in steady-state with the surroundings, whereas in the first 30 minutes it takes longer to heat up the system. For Lisbon winter meteorological conditions, the best tested PCM was one with melting temperature of 22 ºC. Ideal PCM melting temperature would be 28 ºC for outside mild temperatures around 20 ºC. It was corroborated that measuring skin and thermal surfaces' temperature was an appropriate tool to compare sleeping systems.

Keywords: Phase Change Materials; Thermal comfort; Sleeping System; Melting Temperature; PCM for Heat Storage.

Resumo

Neste estudo, o desempenho de Materiais de Mudança de Fase (em inglês “Phase Change Materials” ou apenas “PCMs”) foi estudada com o intuito de melhorar o conforto térmico de Pessoas Sem-Abrigo (a viver na rua) em Lisboa. Para isto, foram feitas simulações no EnergyPlus. Estas simulações foram feitas para verificar qual seria o melhor cenário possível para um sistema saco-cama/colchonete, onde PCMs seriam incorporados no colchonete, para a região de Lisboa. Os dois parâmetros estudados foram a temperatura de mudança de fase dos PCMs e a quantidade de PCMs a incorporar no colchonete.

O modelo em EnergyPlus foi validado usando simulações experimentais. Estas consistiam numa pessoa dormir 8 horas numa sala com ambiente controlado. Foi concluído que um sistema saco-cama/colchonete, com PCMs incorporados no colchonete, melhorava o conforto térmico da pessoa quando a pessoa já se encontra em equilíbrio térmico com o ambiente à sua volta, enquanto que nos primeiros 30 minutos o sistema com PCMs demora mais tempo a aquecer. Para as condições meteorológicas do Inverno de Lisboa, a melhor temperatura de fusão do PCM testada foi 22 ºC. A melhor temperatura de fusão do PCM seria 28 ºC para temperaturas exteriores amenas à volta de 20 ºC. Foi corroborado o facto de temperaturas superficiais do sistema saco cama/colchonete e temperaturas da pele serem uma ferramenta apropriada para comparar sistemas saco-cama/colchonete.

Palavras-chave: PCMs, Conforto térmico; Sistema saco-cama/colchonete; Temperatura de fusão; Armazenamento de calor em PCMs

To all the homeless people in Portugal, and to all those who live in precarious home conditions around the world.

Acknowledgments

To my family, especially my parents, for helping me to get where I am today.

To all my friends, particularly the ones who accompanied me in this university journey.

To my girlfriend, whose support in harsh times made it all more bearable and meaningful.

Special thanks to the main coordinator of my work, professor Rui, who always supported me in the best way possible.

I would also like to thank Eng. Ricardo Gomes for helping me in EnergyPlus issues and for the insights related to my work.

I want to express my gratitude to professor João Gomes Ferreira who lent the thermographic camera.

Contents

List of Figures xi
List of Tables xiii
Acronyms xiv
1. Introduction 1
1.1. Motivation 1
1.2. Objectives 2
2. State of the art 3
2.1. Phase Change Materials 3
2.3. Various PCM applications 5
2.3.1. Sleeping system applications 6
2.3.2. Medical applications 6
2.3.3. PCM in vests 7
2.4 Thermal comfort and ambient temperature 9
2.5 Thermal comfort models 11
2.5.1. Fanger model 12
2.5.2 Pierce Two-Node Model 14
2.5.4. Adaptive models 20
2.5.5. Thermal models in sleeping bags 22
2.6. Conclusions 25
3. Methodology 27
3.1. Experimental 27
3.1.1. Sleeping System Materials 27
3.1.2. Data acquisition 28
3.1.3. Experimental Setup and Procedure 30
3.2. Numerical 34
3.2.1. Heat and moisture transfer problem resolution 35
3.2.2. Input Data 37
4. Results and Discussion 42
4.1. Experimental 42
4.1.1. Pre-analysis with thermographic camera 42
4.1.2. Results of the 8-hour experiment 47
4.2. Numerical 56
4.2.2. Particular night in January 59
4.2.3. Summary of simulations for the 4 coldest months 67
4.3. Synthesis of the Results 68

5. Conclusions and Future Research....70
5.1. Conclusions....70
Bibliography....72
Appendices....76
Appendix A.1.: Input of PCM in EnergyPlus (HexaHydrated-CalciumChloride)....76
Appendix A.2.: Input of PCM in EnergyPlus (BioPCM)....77
Appendix B: Thermocouple information....78
Appendix C – Visual Instrument to run NI cDAQ-9172 Datalogger....79
Appendix D – Technical specifications of AC unit (Daikin FTXS60)....81

List of Figures

Figure 1 - Temperature vs. Energy Addition (Fleischer A.S., 2015) 3
Figure 2 - Classification of PCMs (adapted from Sharma et al., 2009)..... 3
Figure 3 – ASHRAE Standard 55 Winter and Summer Comfort Zones. Clothing insulation levels of 0.5 clo for summer and 0.9 clo for winter. 10
Figure 4 - Thermal interaction of human body and environment (ASHRAE Fundamentals, 2001).....12
Figure 5 – Sleeping bag thermal models displayed in graph (Huang, 2008). Left: Acceptable temperatures for 8h sleep. Right: Air temperatures for thermal comfort (steady-state). 24
Figure 6 - Sleeping mat (Decathlon website) 27
Figure 7 - Sleeping bag (Decathlon website) 27
Figure 8 - Fluke TiR27 Infrared Camera (Fluke website) 28
Figure 9 - Hobo Datalogger 28
Figure 10 - NI cDAQ-9172 Datalogger.....29
Figure 11 -Outside Meteorological conditions. Left: Temperature(ºC) vs. Time(hour). Right: RH(%) vs. Time(hour) . Source: MeteoIST 30
Figure 12 - Daikin AC unit model FTXS60 (Daikin Technical specifications).....31
Figure 13 - Thermocouple's location in the subject (adapted from www.getdrawings.com)...32
Figure 14 - Thermocouple's location in the sleeping system.....32
Figure 15 - Exploded view of the sleeping system (PCM, sleeping mat and sleeping bag) and thermocouple’s location. Left: Bottom surface's visualization. Right: Top surface's visualization.....33
Figure 16 - Sleeping mat with insertion of PCM 33
Figure 17 - Experimental Setup 34
Figure 18 – Annual temperature of Lisbon, 2017. Red line: Maximum temperature. Green: Average temperature. Blue: Minimum temperature. Source: MeteoIST. 34
Figure 19 - Google SketchUp model.....35
Figure 20 - Sleeping system in EnergyPlus 37
Figure 21 - Differential Scanning Calorimetry of $CaCl_2(H_2O)_6$ at the 100^{th} cycle (Tyagi, Buddhi, 2008).....38
Figure 22 - Enthalpy curve of $CaCl_2(H_2O)_6$ 39
Figure 23 - Upper torso of the subject inside the sleeping bag (subject horizontally oriented with the head on the right) 42
Figure 24 – Legs and waist of the subject inside the sleeping bag. Left: Legs zone. Right: Waist zone. 43
Figure 25 - Upper torso of the subject above the sleeping mat (subject horizontally oriented with the head on the right) 43
Figure 26 - Waist Zone of the subject above the sleeping mat.....44
Figure 27 - Legs Zone of the subject above the sleeping mat.....44
Figure 28 - Upper torso thermal impression in the sleeping mat 45
Figure 29 - Waist zone thermal impression in the sleeping mat 45
Figure 30 - Legs zone thermal impression in the sleeping mat 46
Figure 31 - Thermal impression 5 minutes after the subject left the sleeping mat 46
Figure 32 - Temperature of the system without PCMs 47
Figure 33 - Temperature of the system with PCMs 48
Figure 34 – Interior Sleeping System Temperature (orange and blue lines) and Room Air Temperature (yellow and purple lines).....49
Figure 35 - Ground Room temperature away from sleeping system (orange and blue lines) and Room Air Temperature (yellow and purple lines) 50

Figure 36 - Ground temperature below the sleeping system (orange and blue lines) and Room Air Temperature (yellow and purple lines) 51
Figure 37 -Sleeping bag/sleeping mat surface temperature (orange and blue lines) and Room Air Temperature (yellow and purple lines) 51
Figure 38 - Sleeping mat surface and Back temperature (orange and blue lines) and Room Air Temperature (yellow and purple lines) 52
Figure 39 - Nape skin temperature (orange and blue lines) and Room Air Temperature (yellow and purple lines) 53
Figure 40 - Chest skin temperature (orange and blue lines) and room temperature (yellow and purple lines) 53
Figure 41 - Thigh skin temperature (red and blue lines) and room temperature (yellow and purple lines) 54
Figure 42 - Left foot skin temperature (red and blue lines) and room temperature (yellow and purple lines) 55
Figure 43 - Humidity variation in the experiments 55
Figure 44 - Zone mean air temperature without PCM for both experimental and numerical simulations 57
Figure 45 - Zone mean air temperature with PCM for both experimental and numerical simulations 58
Figure 46 - Outside Air Temperature of 8-9 January night 59
Figure 47 - Outside Air humidity in 8-9 January night 59
Figure 48 - Zone Mean Air Temperature. Blue: Outside Air Temperature. Orange: Sleeping system without PCMs. Red: Sleeping system with PCM25-1 Kg. Grey: Sleeping system with PCM25-2Kg 60
Figure 49 - Fanger PMV. Blue: Sleeping system without PCMs. Orange: Sleeping system with PCM25-1 Kg. 61
Figure 50 - Pierce Model Effective Temperature PMV. Blue: Sleeping system without PCMs. Orange: Sleeping system with PCM25-1 Kg. 62
Figure 51 - KSU Model TSV. Blue: Sleeping system without PCMs. Orange: Sleeping system with PCM25-1 Kg. 63

List of Tables

Table 1 - Advantages and Disadvantages of different types of PCMs..... 5
Table 2 - Sleeping bag thermal models 24
Table 3 - Test Room properties 31
Table 4 - Thermocouple's location.....32
Table 5 - Ground and sleeping system material properties.....37
Table 6 - PCM Properties 39
Table 7 - Parameters in EnergyPlus People's Section.....40
Table 8 - Properties used in EnergyPlus for model validation 56
Table 9 - Values of temperature and thermal model scales at 23h of 8 January.....64
Table 10 - Values of temperature and thermal model scales at 07h of 9 January.....65
Table 11 – Mean values of temperature and thermal model scales from 8-9 January night..66
Table 12 – Mean values of temperature and thermal comfort scales for the 4 month's nights studied 67

Acronyms

ACH	Air Changes per Hour
AMI	International Medical Association (*Associação Médica Internacional*)
EU	European Union
ET*	Effective Temperature
FEANTSA	European Federation of National Organisations working with the Homeless (*Fédération Européenne d'Associations Nationales Travaillant avec les Sans-Abri*)
ISS	Portuguese Institute for Social Security (*Instituto de Segurança Social*)
LMIC	Low and Middle-Income Countries
MET	Metabolic Equivalent of Task
OECD	Organisation for Economic Co-operation and Development
PCM	Phase Change Material
PMV	Predicted Mean Vote
RMSE	Root Mean Square Error
SET*	Standard Effective Temperature
SD	Sleep Deprivation
TES	Thermal Energy Storage

1. Introduction

1.1. Motivation

It is considered a homeless person who, independently of its nationality, racial or ethnical origin, religion, age, sex, sexual orientation, socioeconomical condition, physical and health condition is found without a roof, living in the public space, accommodated in emergency shelters or in precarious living conditions; or without a home, in temporary shelters destined to the effect (Minister Council Resolution, nº 107/2017, 25 July, Portugal).

According to the Organisation for Economic Co-operation and Development (OECD), there are more than 1.8 million homeless people in 29 of the 35 OECD countries. Data of many countries in this study only considers homeless people sleeping in the streets, not in emergency accommodation or temporary shelters.

According to the European Federation of National Organisations working with the Homeless (FEANTSA - *Fédération Européenne d'Associations Nationales Travaillant avec les Sans-Abri*), estimations show that 410 thousand homeless people (roofless and houseless) exist on any given night in the European Union, which suggests that 4.1 million people in the EU are exposed to this kind of homelessness each year for a shorter or longer period. Data also shows that these numbers are increasing in the EU.

In 2009, the Portuguese Institute for Social Security (ISS) launched a national survey addressed at all inland municipalities, and a total of 2133 people were found to be in a homelessness situation (including both homeless and houseless people) in the responding 53 municipalities out of the 308. More than half of this number was situations in Porto and Lisbon. In a study made by AMI (*Associação Médica Internacional*), 52% of the enquiries said they consumed addictive substances (Annual Report, Lisbon 2006).

Poor sleep habits, such as deficient sleep quantity or inconsistent sleep times might be associated with lower self-control (habits generally seen in homeless people). This can lead to compromised decision making and worse attentive capacity (Pilcher et al., 2015). Sleep deprivation has a negative impact on metabolism and endocrine function (Spiegel et al., 1999).

The hippocampus is an area of the brain that is affected by sleep deprivation (SD). Disrupted sleep can contribute to cognitive disorders and psychiatric diseases (Kreutzmann et al., 2015).

A possible solution to improve thermal comfort and thermal perception of homeless can be the insertion of PCMs in the sleeping system, as they undergo phase change at temperatures within thermal comfort range. PCMs work as thermal energy storage systems (TES), storing and releasing large amounts of latent heat, up to 300 $kJ.Kg^{-1}$.

1.2. Objectives

In this work, the performance of a PCM incorporated in a sleeping system will be studied. To do this, a series of simulations in EnergyPlus were done to check the feasibility of the system in terms of thermal improvement, as well as to check which melting temperature would be the best for the studied conditions. This model was validated through an experimental test in which a subject laid down in a controlled room temperature, and comparisons of both models were done. It was made a comparison also to PCM vs. non PCM sleeping system in both the experimental as well as in the numerical part.

In other words, the main objectives of this work were to study the performance of PCM sleeping systems and compare them with non-PCM sleeping systems, to check the best PCM melting temperature for winter in Lisbon, and to validate a numerical model.

2. State of the art

2.1. Phase Change Materials

Phase Change Materials (PCMs) are materials that go through phase change at a temperature within the operating interval of a selected thermal application. Many of these materials are chosen due to their large latent heats of fusion when melting and solidifying. For engineering applications, it is generally used the solid-liquid phase change. This phase change is used as a buffer in a system. The amount of energy absorption or release during the melting-solidification cycle is correlated with the value of the material's latent heat of fusion. This value is commonly expressed in $J.g^{-1}$ or $kJ.Kg^{-1}$. In figure 1, it can be seen the standard heating curve of a material:

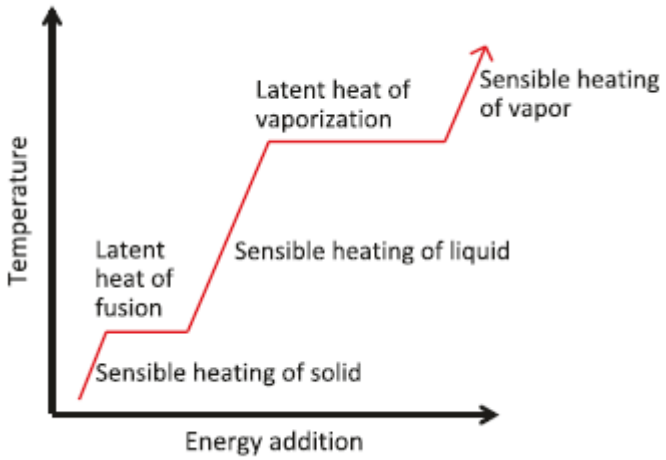

Figure 1 - Temperature vs. Energy Addition (Fleischer A.S., 2015)

There are some applications using latent heat of vaporization, but that often requires boilers and condensers, which cannot be used in most situations. Also, there is a large volume change in that phase-change, which is not ideal for most applications. A possible classification of PCMs is the following (figure 2):

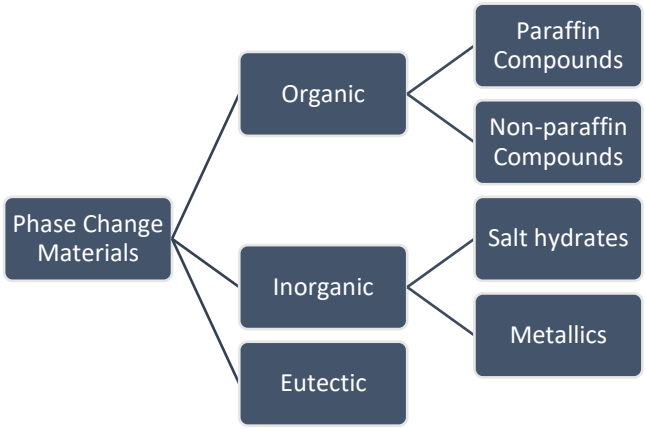

Figure 2 - Classification of PCMs (adapted from Sharma et al., 2009)

Organic PCMs

Paraffins

Consist of mostly chain n-alkanes CH3–(CH2)–CH3. Crystallization of this chain releases a large amount of latent heat. It is safe, reliable, not too expensive (up to 2€.Kg^{-1}), non-corrosive and chemically inert. In addition, it shows little volume change. The disadvantages of paraffins are low thermal conductivity and moderate flammability.

Non-paraffins

These materials consist in some esters, fatty acids, alcohols and glycols. In terms of properties, these have higher heat of fusion than paraffins, although they are flammable and have low thermal conductivity. Also, non-paraffins are more expensive.

Inorganic PCMs

Salt hydrates

Salt hydrates are alloys of inorganic salts and water, forming a crystalline solid with a chemical formula similar to $XY.nH_2O$. The solid-liquid transformation of a salt hydrate is a dehydration of the salt, although similar to a melting or freezing thermodynamically. Therefore, a salt hydrate melts to one of two options: a salt hydrate with fewer moles of water or to its anhydrous form. These have high latent heat of fusion per unit volume, higher thermal conductivity than organic PCMs and small volume changes on melting. These are not too corrosive nor expensive.

The biggest disadvantage of salt hydrates is incongruent melting due to density difference. There are some ways to reduce this problem, such as adding nucleating agents or encapsulating the PCM, therefore reducing separation. Examples of salt hydrates are hexa-hydrate magnesium chloride ($MgCl_2.6H_2O$) and tri-hydrate potassium fluoride ($KF.3H_2O$).

Metallics

Metallic PCMs have high heat fusion per unit volume and a high thermal conductivity. The biggest disadvantage is the large weight. Metals used in low temperature applications are caesium and gallium, whereas in high temperature applications zinc and magnesium are used.

Eutectics

Eutectics are mixtures of two or more components, where each component melts and freezes congruently. These seldom segregate when phase-changing, have sharp melting points and good latent heat storage capability. More research needs to be done in these materials, so they can be used more consistently. An example of eutectic alloy is Bi/Pb/Sn/In used by Pal, Joshi (1997).

A summary of the main advantages and disadvantages of different types of PCM is now presented in Table 1:

Table 1 - Advantages and Disadvantages of different types of PCMs

	Advantages	Disadvantages
Paraffins	• High heat of fusion • No tendency to segregate • Chemically stable	• Flammable • Low thermal conductivity • Relatively high price • Significant volume change • Melting point not well-defined
Fatty acids	• Sharp phase transformation	• Mildly corrosive • Cost-intensive (2 to 3 times more than paraffines)
Metallic	• High thermal conductivity • Able to store large latent heat per unit volume	• High cost • Store small amount of heat per unit mass
Salt hydrates	• High phase change enthalpy • High volumetric storage density	• Super-cooling • Phase segregation
Eutectic	• Sharp melting points • Good latent heat storage capabilities	• Few information about physical and thermal properties

2.3. Various PCM applications

PCMs are being used in several technologies. Some applications will be briefly discussed. Then, some specific applications with closer relation to the topic will be analysed thoroughly.

PCM applications can be divided into three major categories (adapted from Xia et al., 2014):

Use of latent heat associated with phase transition

PCM storage processes are increasing, as PCMs provide high storage density with small temperature difference when storing and releasing heat. For this application, paraffin waxes, eutectic compounds, salt hydrates and fatty acids have been used.

PCMs are chosen depending on the respective melting temperature. For instance, PCMs with melting temperatures between 20-90 ºC are used for solar energy storage applications (Baran, Sari, 2003). Latent heat storage has been useful to create systems that utilize off-peak electricity. This is a way to reduce peak load and therefore costs of electricity (Bakos, 2000). Use of PCM wallboards or active floor systems are some of the effective ways.

Nowadays, the capability of removing heat in an efficient way presents a big challenge, in systems such as engines or electronic devices. Nanoparticles made of PCMs have been added to fluids to improve their heat capacity (Hu, Zhang, 2002).

Use of state change involved in phase transition

PCMs are utilized in temperature-regulated drug-delivery systems, as they are thermosensitive materials, transitioning from solid to liquid at a given temperature, controlling diffusivity of a drug or its

carrier. Most suitable PCMs for this application are fatty acids and fatty alcohols due to their biocompatibility and degradability (Choi et al., 2010).

Theranostics, a new field of medicine that combines targeted therapy based on specific targeted diagnostic tests, uses PCM mixtures and drugs encapsulated by inorganic components. This technique uses irradiation either with near-infrared laser or high-intensity focused ultrasounds. These theranostic systems can be used for in vivo molecular imaging and chemo- and photothermal therapy (Yang et al., 2007; Xia et al., 2013).

Use of the fixed temperature/heat involved in phase transition

PCMs with sharp melting peaks are used as thermal signatures to fabricate a PCM-based system for simultaneous detection of multiple biomarkers. This is done using differential scanning calorimetry. It has the potential to be an effective tool of cancer detection (Wang et al., 2011). Also, barcoding of many small objects is currently very expensive. Metal PCM nanoparticles may be used during a linear thermal scan with this intention (Wang et al., 2012).

2.3.1. Sleeping system applications

There is not much research available about PCMs in sleeping system's applications.

Quesada et al. (2017) studied the impact of phase change materials (PCMs) in mattresses. For this, it was compared the performance between conventional mattresses and the ones filled with PCM, in this case microencapsulated paraffin with a concentration of 0.75 $Kg.L^{-1}$ and 90% of absorption. It was made an evaluation of the thermal perception, thermal comfort and skin temperature of the participants in the study, which were required to lay down 20 minutes in each type of mattress. The thermal perception and thermal comfort were indicated in the last minute of the test, whereas the temperature measurement was in the back of the subject. Results showed that the PCM mattress had an increase of the sheet temperature between 0.2-1.6 ºC and an increase in skin temperature between 0.3-1.0 ºC. It was concluded that measuring superficial (both skin and sheet) temperature was an appropriate tool to observe thermoregulatory differences between different mattresses. Although mattresses filled with PCMs increased heat dissipation of the human body between 2.7 - 25.6%, thermal comfort and perception of the participants was not changed during the test (20 minutes). These tests were done in mild environmental conditions: room temperature of about 24.3 ºC and 38% relative humidity.

2.3.2. Medical applications

PCMs are being used in beds for infants with perinatal asphyxia in developing countries. Perinatal asphyxia is failure to initiate and sustain breathing at birth (World Health Organization).

Hypoxic Ischemic Encephalopathy (HIE) refers to multi-organ dysfunction in the neonate and the neurological dysfunction inherent to perinatal asphyxia.

Around 4 million babies die every year in the neonatal period (first 28 days of life) globally and asphyxia accounts for 23 % of these neonatal deaths (Perlman, 2004). Many survivors of asphyxia (between 15-28%) have cerebral palsy in their lives.

Therapeutic Hypothermia (TH) has been proven to be effective in reducing morbidity associated with HIE and has become the standard of care for HIE in developed countries (Bhat et al., 2017). Cooling appears to reduce DNA damage induced by oxidative stress and improve neurodevelopmental outcome (Jacobs S. et al., 2013).

Iwata et al. (2009) studied the impact of effective, safe, low-maintenance and low-cost cooling methods to induce and maintain moderate therapeutic hypothermia in a piglet model, with the aim of helping infants with perinatal hypoxia-ischaemia with neurodevelopmental outcome at 18 months. Results showed that both water bottles with tepid water at 25 ºC and PCM mattresses with a melting point of 32 ºC can be used as low-cost devices to maintain the required constant temperature. Furthermore, the PCM mattress maintained a more stable hypothermia, although compared with water bottles these mattresses represent higher costs and a fine refinement of melting temperature is needed to optimise the results for the human new-borns.

Thomas et al. (2015) analysed the use of PCM (2.4 Kg of OM 32^{TM} or HS 29^{TM}, with melting points of 32 ºC and 29 ºC, respectively) as cooling method for therapeutic hypothermia in 41 babies with hypoxic ischaemic encephalopathy (HIE). The PCM bed was made of a hollowed-out foam mattress lined with extruded polystyrene (insulating layer) and covered with nylon (good conducting layer). The cost of the bed with the PCM was about 40€ and lasted on average for at least 20 babies.

The study's conclusion is that PCM provides an effective and low-cost method to maintain therapeutic hypothermia. Despite this, during induction and rewarming phases careful monitoring is required to avoid hypothermia outside the therapeutic range of temperature.

Thayyil et al. (2013) did the same analysis to 13 infants with neonatal encephalopathy, cooling the body with PCM. Results indicated that PCM with a melting point of 32 ºC was only effective when ambient temperature was below or equal to 28 ºC. Nevertheless, the conclusion of the study was that PCM was a good low-cost alternative to cool the infant's body, suitable for use in some low and middle-income countries (LMIC) neonatal units.

2.3.3. PCM in vests

Gao et al. (2010) investigated cooling vests with PCM and effects of melting temperature on heat strain alleviation in hot environments. The cooling vests were made of polyester with separate pockets that had 21 PCM kits. The PCM was made of salt mixtures (including sodium sulphate and water) and additives. The PCM melting temperatures were 24 and 28 ºC. The total PCM in each vest was 1.74 Kg. The tested environment was a fire reproduction (subjects had firefighting ensembles) and the subjects were 6 male firefighting-trainees. To represent fire conditions, subjects entered a climatic chamber (air temperature of 55 ºC, relative humidity of 30%, vapour pressure of 4725 Pa and 0.4 m.s^{-1} of air velocity). Results concluded that the PCM vest alleviated the rise in torso temperature (lower maximum temperature). Besides alleviating the rise in local skin temperature, PCM vests also mitigated mean skin

and mean body temperature, as well as the peak core temperature rise during the resting recovery period (maximum rectal temperature was obtained after 10-13 mins of the exercise). These vests alleviated 0.4 ºC of the peak rectal temperature. Moreover, heart rate, thermal sensation and sweat production were moderately lower with the lower melting temperature PCM. The authors point out that, even though the peak temperature lowered (which was in the break after the exercise), there was no alleviation in core temperature increase during the exercise. However, the vests provide lower torso temperatures that can provide a higher heat transfer gradient from core to periphery.

Gao et al. (2012) examined personal cooling with PCMs to improve thermal comfort from a heat wave perspective. For this, it was used a cooling vest made of polyester containing 21 PCM kits (salt mixtures including sodium sulphate, water and additives), with a melting temperature of 21 ºC. Total vest weight was 2.2 Kg. To represent heat wave conditions, a climatic chamber air was regulated to 34 ºC, 60% of relative humidity and air velocity of 0.4 $m.s^{-1}$. Both manikins and real subjects were used in this investigation. Results on the thermal manikin with constant heating power (20 $W.m^{-2}$) demonstrated that, with the PCM vest, average manikin torso temperature was 3ºC lower than temperatures in other unveiled areas. Torso skin temperatures on the subjects stayed about 2-3ºC lower compared with skin temperatures on other parts of the body, and rectal temperature was not influenced by the vest. Additionally, when wearing the cooling vest, subjects said that skin wetness sensation decreased, but the whole-body thermal comfort was relatively stable and not much affected by the torso cooling. The authors state that PCM cooling vest can be used as a personal cooling measure in heat waves and can be helpful to groups such as the elderly, chronic disease patients or situations where sweat production, physical activity and evaporation are not high. As such, it is declared that PCM cooling can contribute to energy savings in buildings and mitigate detrimental health effects of heat waves.

Zhao et al. (2012) studied torso cooling of vests with PCMs in a sweat evaporation perspective. For this, two hot environments were used: hot humid (HH, 34 ºC, 75% relative humidity) and hot dry (HD, 34 ºC, 37% relative humidity) and a thermal manikin with a pre-wetted torso fabric was used for the simulation. 3 PCMs (Glauber's salt) with 21, 24 and 28ºC melting temperatures were tested (MIL21, MIL24 and MIL28, respectively). Five simulations were made, one with fabric skin only, another with military ensemble without the cooling vest, and three others with cooling vests with each PCM. Results showed that the manikin with fabric skin only presented the highest torso heat loss and evaporative rate. With the military ensemble worn over the fabric skin, cooling power was reduced by 64% and 58% in HH and HD, respectively. When cooling vests were used, torso heat loss in HH increased by 100% for MIL21, 77% for MIL24 and 58% for MIL28. However, in HD environment, torso heat loss increased 1% for MIL21, decreased by 5% for MIL24 and decreased by 8% for MIL28. The authors concluded that, when using garments with low evaporative resistance and high sweat production, PCM vests were effective in the HH condition, but not in the HD condition.

House et al. (2012) studied the impact of a phase-change cooling vest on heat strain and the effect of different cooling pack melting temperatures. For this objective, ten participants were recruited. Room conditions were controlled to a climate of 40 ºC and 46 % relative humidity, and participants undertook a stepping exercise for 45 minutes, followed by a post-exercise seated recovery period for 45 minutes as well. Participants did the test in five different conditions, one for control (without cooling vest) and the other four with cooling packs melting at 0, 10, 20, 30 and 40ºC (CV0, CV10, CV20, CV30 and CV40, respectively). Each cooling vest had 2 Kg of coolant and every participant was required to dress a fire fighting coverall and shoes. Subjective preferences showed that all vest conditions were preferred to the control simulation. Furthermore, CV10 was preferred over the other vest conditions and subjects stated that CV0 was “too cold”, with a cold induced erythema due to the vest over the simulation day. Oxygen uptake was not changed in the five conditions, so there was not an increase in heat production due to wearing the vests. Recovery from the imposed heat strain was improved with all the cooling vests, with CV0 having a decrease in the temperature during the exercise, and the others only reducing heat strain during recovery. The authors conclude that a cooling vest can provide a heat strain reduction during resting recovery conditions where thermoregulation is not possible.

2.4 Thermal comfort and ambient temperature

Fanger (1970) stated that skin temperatures of 33 to 34 ºC are comfortable at sedentary activities. This range of temperatures can decrease with increase of activity. Hypothalamus, which is a part of the brain, controls the body temperature. It receives thermal information from temperature sensors in the skin and other parts of the body. It controls the body temperature by regulating various physiological processes of the body (Hensel, 1981). Its control behaviour is PID (proportional, integral, derivative) but primarily proportional to deviations from the set temperature (ASHRAE Fundamentals, 2013).

The heat produced by a resting adult is around 100 W. Most of the heat is transmitted to the environment through the skin, so metabolic activity is often characterized in terms of heat production per unit area of skin. For a resting person, based on the average male European, with a skin surface of 1.8 m^2 (female Europeans have an average surface of 1.6 m^2), this is about 58 $W.m^{-2}$ and can be named as one Metabolic Equivalent of Task, or 1 Met (ASHRAE Fundamentals, 2013). Clothing insulation can be expressed in clo units. 1 clo represents the amount of insulation a person needs to be in thermal equilibrium in an environment at 21 ºC in a normally ventilated room (0.1 $m.s^{-1}$). 1 clo equals 0.155 $m^2.K.W^{-1}$. ASHRAE Standard 55 assumes clothing insulation levels of 0.5 for summer conditions and 0.9 clo for winter conditions. In figure 3, it is possible to see comfort conditions both in Winter and Summer:

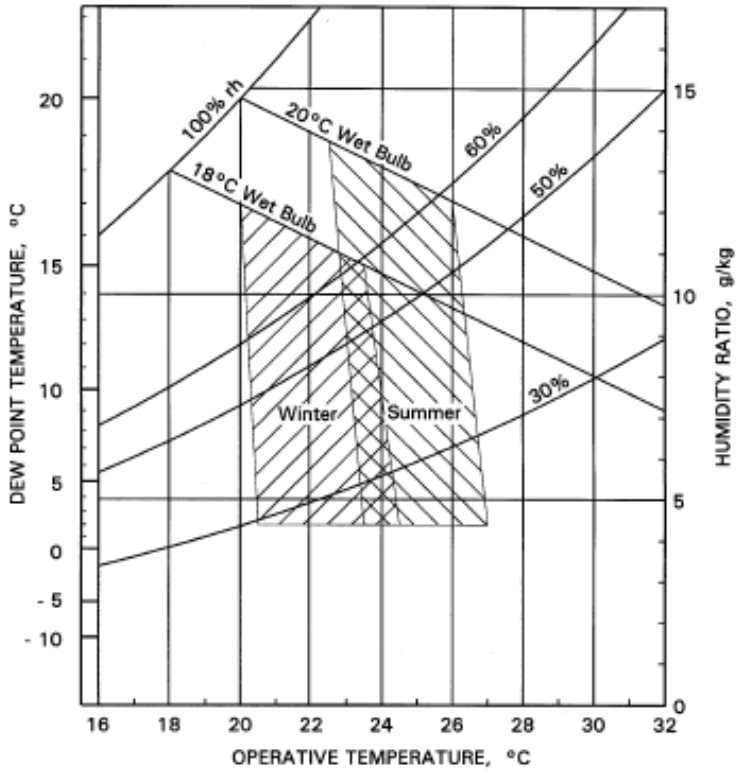

Figure 3 – ASHRAE Standard 55 Winter and Summer Comfort Zones. Clothing insulation levels of 0.5 clo for summer and 0.9 clo for winter.

Muzet et al. (1984) studied the range and impact of a thermal comfort zone. In this study, subjects had clothing and covering consisting of pyjamas, two cotton sheets and one wool blanket. With air and wall temperatures equal, varying from each experience between 16 ºC and 25 ºC, results showed that the microclimate temperature inside the bed varied from 28.6 ºC to 30.9 ºC. High nocturnal awakening was noted at ambient temperature of 13 ºC and a microclimate temperature of 26.1 ºC.
Conclusions from the authors are that thermal neutral zone (condition where a person would not want more heat or cold) in the bedding microclimate is around 30 ºC and the preferred ambient room temperature is 19 ºC. When temperatures move away from the thermal neutral zone the number and wakefulness periods during sleep increase. In addition, cold ambient temperatures are worse to sleep than warm ambient temperatures.

Amrit (2007) studied bedding textiles and their influence on sleep and thermal comfort. The three main factors found by the author which influence human thermal comfort are physical activity, environmental climate and clothing. Environmental climate changes thermal awareness in one of various factors, such as air temperature, relative humidity and air movement near the body. Clothing properties that change thermal comfort are thickness of the material, type of material, air permeability, among others. The author presents that heat loss in bedding occurs due to the ventilation effect. For this reason, duvets should have moisture absorbing and insulating effects, as well as adaptiveness to body shape. Also, heat loss comes from leakage of microclimate air to the ambient temperature through bedding upper layers and because of heat conduction to the mattress. Another conclusion of the study is that the

thermal neutral zone, where a person would not want a higher or lower ambient temperature, has small variations compared to different characteristics of humans, such as sex, age or geographical location.

Zhang et al. (2002) studied the effect of clothing material properties on rectal temperature in different environments. Seven female subjects participated in the study. Only outerwear material was investigated, and it consisted of two different types of cotton and one of tencel (fibre made from cellulose found in wood pulp) with differences in moisture regain and air permeability between them. Results showed that rectal temperature decreased significantly during the cooling period and increased significantly when the temperature rose (with and without wind). Decrease of rectal temperature was significantly affected by clothing type during cooling period. Similarly, increase of temperature was affected by clothing type during heating period. The conclusions of this paper were the following: when ambient temperature is lower than skin temperature, air permeability of clothing has greater influence than moisture regain on the rectal temperature. This is explained by the fact that with less air permeability, the body cannot lose as much heat by convection and radiation. On the contrary, in ambient temperature higher than the skin temperature the body must lose heat through evaporation of perspiration, therefore making moisture regain important as well, as it can allow a better sweat removal. Furthermore, these results appeared to be true whether there was wind or not, although with wind there was a higher influence of moisture regain.

Haskell et al. (1981) studied the effects of high and low environment temperatures on human sleep stages. For this, six male subjects between the ages of 18 to 30 years slept nude except for shorts on a bed made from nylon webbing at 5 different environment temperatures: 21, 24, 29, 34 and 37ºC. For the analysis, a standard somnograph was used, electrocardiogram and strain gauge activity were recorded and various skin and rectal temperatures, sweat rate and O_2 consumption were also monitored. Results showed that ambient temperature outside thermoneutrality, where a person would feel comfortable with its surroundings (in this case assumed to be around 29 ºC), did not significantly affect the time taken to fall asleep. What changed the most with greater difference of temperature from thermoneutrality was sleep disruption manifested by increased amounts of wakefulness, as well as lesser time in Rapid Eye Movement (REM) and Stage 2 sleep. Cold proved to be worse to sleep than heat.

2.5 Thermal comfort models

According ASHRAE Standard 55, thermal comfort is the mind condition that expresses satisfaction with the thermal surrounding environment.

Analytical calculations from thermal comfort based on climatic chamber studies present 6 variables that influence thermal comfort: Activity level, clothes' thermal insulation, air temperature, mean radiant temperature, air velocity and partial water vapour pressure. The following equations from Fanger, Pierce and KSU models are adapted from the equations EnergyPlus uses to its simulations.

2.5.1. Fanger model

Fanger (1970) describes thermal neutrality as the condition in which a person does not prefer neither more heat nor cold in its surrounding environment. In a physical state, this signifies that every heat that is generated by the body through metabolism is exchanged in equal proportion with the surrounding environment, not having neither heat gain nor excessive loss of it, keeping a constant corporal temperature. It can be stated that thermal neutrality is a necessary, but not sufficient, condition towards thermal comfort.

The Fanger model is considered a passive model because it considers humans as simple passive receptors of the thermal ambient.

Figure 4 presents the thermal interactions of human body in relation to the environment:

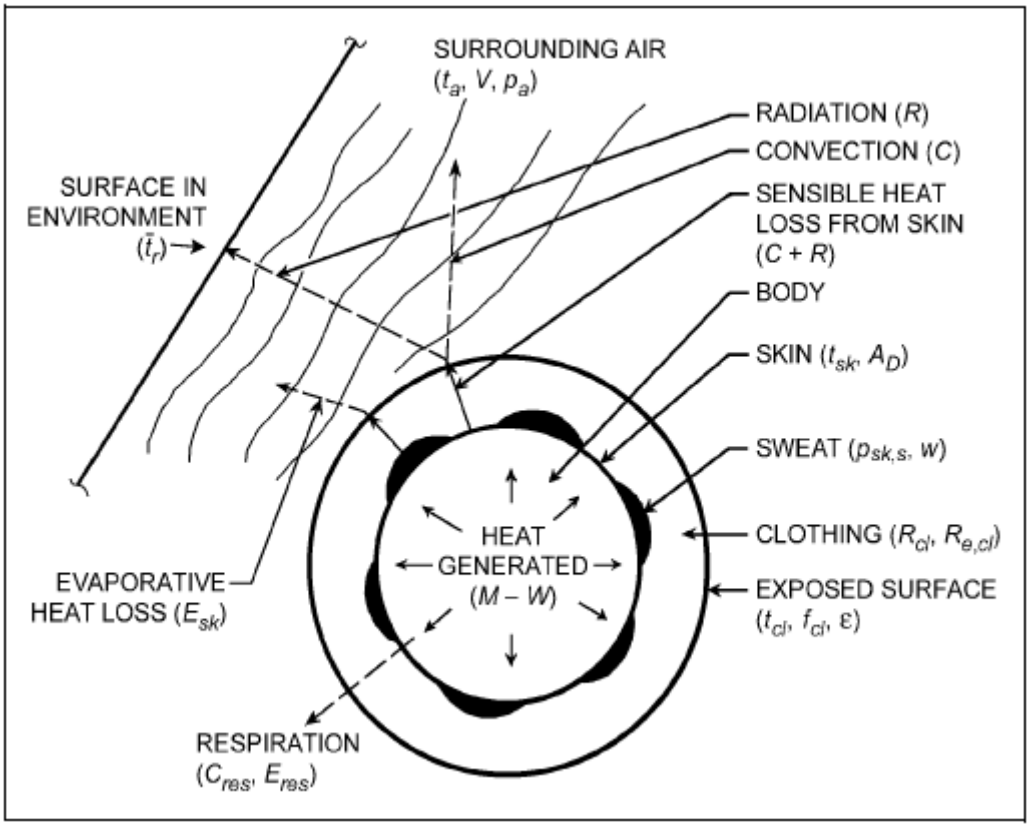

Figure 4 - Thermal interaction of human body and environment (ASHRAE Fundamentals, 2001)

ISO 7730 uses the stationary state stated by Fanger to model the body-environment relation:

$$M - W = Q_{sk} + Q_{res} = (C + R + E_{sk}) + (C_{res} + E_{res}) \quad (1)$$

where Q_{sk} is the heat skin loss, Q_{res} is the respiratory heat loss, M is the metabolic rate of heat production, which depends on the level of activity of the person (in the sleeping case, it is around 45 W. m^{-2}), and W is the work done by the body. Q_{sk} and Q_{res} can also be subdivided in heating loss mechanisms, where $C + R$ are the convection and radiation skin losses, respectively, which both combined give an equal value to the heat loss by conduction to clothes' external surface; E_{sk} is the latent

heat skin loss through evaporation, C_{res} is the breathing sensible heat loss through convection and E_{res} is the breathing latent heat loss through evaporation. Units of W.m^{-2} are usually used.

It is important to state that the terms of the previous equation are usually stated in energy per unit area, and this area is the naked body surface area. This area can be calculated by DuBois surface area through the following expression:

$$A_{Du} = 0.202 * m^{0.425} * l^{0.725} \quad (2)$$

Where A_{Du} is the body surface area, or DuBois area, in m^2, m is the body mass, in Kg, and l is the body height, in m.

The heat losses are emulated through the following empirical equations:

$$E_{sk} = 3.05 * (5.73 - 0.007(M - W) - p_a) + 0.42 * \big((M - W) - 58.15\big) \quad (3)$$

$$E_{res} = 0.0173M(5.87 - p_a) \quad (4)$$

$$C_{res} = 0.0014M(34 - t_a) \quad (5)$$

$$K_{Cl} = C + R = \frac{\big(35.7 - 0.028(M - W)\big) - t_{cl}}{0.155 * I_{cl}} \quad (6)$$

$$R = 3.96 * 10^{-8} * f_{cl} * ((t_{cl} + 273)^4 - (t_r + 273)^4) \quad (7)$$

$$C = f_{cl} * h_c * (t_{cl} - t_a) \quad (8)$$

where t_a is air temperature, in ºC, t_{cl} is the superficial clothes' temperature, in ºC, I_{cl} is the thermal insulation of clothes, in clo units, f_{cl} is the quotient between clothed surface area and naked surface area, t_r is the mean radiant temperature, in ºC, and h_c is the convection coefficient between air and clothes, in W.m^{-2}.K^{-1}. Substituting all the variables and rearranging, the following equation can then be written:

$$t_{cl} = 35.7 - 0.0275M - 0.155I_{cl} * \big(3.96 * 10^{-8} * f_{cl} * ((t_{cl} + 273)^4 - (t_r + 273)^4) + f_{cl} * h_c * (t_{cl} - t_a)\big) \quad (9)$$

with $h_c = 2.38 * (t_{cl} - t_a)^{0.25}$ or $h_c = 12.1 * \sqrt{v_{air}}$, whichever is the greatest, with v_{air} the relative air velocity in m.s^{-1}, given by: $v_{air} = v_a + 0.0052(M - 58)$;

$f_{cl} = 1 + 0.2 * I_{cl}$ for $I_{cl} \leq 0.5$ Clo,

$f_{cl} = 1.05 + 0.1 * I_{cl}$ for $I_{cl} > 0.5$ Clo.

In cases where thermal balance expression is not verified, there is a thermal gradient, and the difference of generated heat from the body and heat exchanged with the environment can be denominated as a thermal load over the body (L):

$$L = M - 3.05(5.73 - 0.007M - p_a) - 0.42(M - 58.15) - 0.0173M(5.87 - p_a) - 0.0014M(34 - t_a) - 3.96 * 10^{-8} * f_{cl} * ((t_{cl} + 273)^4 - (t_r + 273)^4) - f_{cl} * h_c * (t_{cl} - t_a) \quad (10)$$

The Predicted Mean Vote (PMV) is an index created through statistical analyses according to results obtained by Fanger in climatized chambers where people would register their votes over the 7th scale of ASHRAE, which has the following possibilities: +3 - Hot; +2 – Warm; +1 – Slightly warm; 0 – Neutral; -1 – Slightly cool; -2 – Cool; -3 – Cold.

The real sensation from the person is then represented by the PMV equation, which is the following:

$$PMV = (0.303 * e^{-0.036M} + 0.028) * L \quad (11)$$

where PMV is the Predicted Mean Vote, M is the metabolic rate and L is the thermal load over the body.

For instance, if a person would feel slightly cool in certain room conditions, her choice (in this case -1) would be an input in the statistics used to produce the PMV.

PPD is the Predicted Percentage of Dissatisfied, which establishes the estimated quantity of unsatisfied people with the given thermal environment. It can be analytically determined as:

$$PPD = 100 - 95 * e^{-(0.03353*PMV^4 + 0.2179*PMV^2)} \quad (12)$$

This percentage is useful as it can quantify the percentage of people that would not be happy with the given thermal environment. It is noted that, due to individual differences, it is impossible to project an environment that satisfies every person, but this number can be minimized. It is usual to define a thermally acceptable environment that has PMV between -0.5 and 0.5, which is equivalent to 10% of unsatisfied people.

2.5.2 Pierce Two-Node Model

The Pierce Two-Node Model uses a finite difference procedure to do an estimation of physiological parameters for given thermal data. It models the human body as two concentric cylinders, the outer one representing the skin shell and the interior one representing the body core. Passive heat conduction from the core to the skin can then be simulated. The boundary between both compartments, or nodes, is controlled by skin blood flow rate per unit skin surface area (Doherty and Arens, 1988; Gagge et al., 1986).

The fraction of total body mass attributed to the skin shell is described as:

$$\alpha = 0.0417737 + \frac{0.7451832}{(SKBF + 0.585417) * 10^{-3}} \quad (13)$$

where α is the fraction of mass attributed to the skin and $SKBF$ is the skin blood flow in $m.h^{-1}$.

Regulatory sweating, shivering and skin blood flow are defined in terms of thermal signals by the following equations:

$$SIG_{cr} = T_{cr} - 36.8 \quad (14)$$

$$SIG_{sk} = T_{sk} - 33.7 \quad (15)$$

$$SIG_b = T_b - 36.49 \quad (16)$$

where SIG_{cr}, SIG_{sk}, SIG_b are thermal signals of the core, skin and body, respectively, in ºC, and T_{cr}, T_{sk}, T_b are the temperatures of the core, skin and body (mean temperature), respectively, in ºC.

Skin blood flow rate is estimated using the following equation:

$$SKBF = \frac{6.3 + C_{dil} * SIG_{cr}}{1 + S_{tr} * SIG_{sk}} \tag{17}$$

where $SKBF$ is the skin blood flow rate, in L.h^{-1}.m^{-2}, C_{dil} is a constant for skin blood flow, SIG_{cr} and SIG_{sk} are the thermal signals of the core and skin, respectively, and S_{tr} is a constriction constant of skin blood flow. Regulatory sweating is determined with the following equation:

$$SW_{reg} = C_{sw} SIG_b e^{\frac{SIG_{sk}}{10.7}} \tag{18}$$

where SW_{reg} is the rate of regulatory sweating, in g.h^{-1}.m^{-2}, C_{sw} is the proportionality constant for sweat control, in g.h^{-1}.m^{-2}, SIG_b and SIG_{sk} are the thermal signals of body and skin, respectively, in ºC.

Shivering can be calculated with the following equation:

$$M_{shiv} = 19.4 * SIG_{cr} * SIG_{sk} \tag{19}$$

where M_{shiv} is the shivering response, in W.m^{-2}, SIG_{cr} and SIG_{sk} are the thermal signals of the core and skin, respectively, in ºC.

Metabolic rate per unit area can be partitioned as:

$$M = M_{act} + M_{shiv} \tag{20}$$

where M is the metabolic rate per unit area, M_{act} is the metabolic rate due to activity, M_{shiv} is the metabolic rate due to shivering, all in W.m^{-2}. Total energy loss is partitioned as the following:

$$L = Q_{res} + Q_{dry} + E_{sk} + W \tag{21}$$

where L is the total rate of energy loss, Q_{res} is the total rate of respiratory heat loss, Q_{dry} is the sensible heat flow from skin, E_{sk} is the total evaporative heat loss from skin, W is the rate of heat loss due to work. All units are W.m^{-2}.

Total rate of respiratory heat loss can be calculated from:

$$Q_{res} = E_{res} + C_{res} = 0.017251 * M * (5.8662 - P_a) + 0.0014 * M * (34 - T_a) \tag{22}$$

where E_{res} is the rate of latent respiratory heat loss, in W.m^{-2}, C_{res} is the rate of dry respiratory heat loss, in W.m^{-2}, M is the metabolic rate per unit area, in W.m^{-2}, P_a is the water vapour pressure in ambient air, in KPa, T_a is the air temperature, in ºC.

Sensible heat flow from skin, Q_{dry}, can be calculated using the following equations:

$$Q_{dry} = Q_c + Q_r \tag{23}$$

$$Q_c = h_c * f_{cl} * (T_{cl} - T_a) \tag{24}$$

$$Q_r = h_r * f_{cl} * (T_{cl} - T_r) \tag{25}$$

where Q_c is the rate of convective heat loss, in W.m^{-2}, Q_r is the rate of radiative heat loss, in W.m^{-2}, h_c and h_r are the convective and radiant heat transfer coefficients, respectively, in W.m^{-2}.K^{-1}, f_{cl} is the ratio of clothed body (dimensionless), T_{cl}, T_a, T_r are the clothing surface, air and mean radiant temperatures, respectively, in ºC.

The model uses the maximum value of equations 26 and 27:

$$h_c = 8.6 * v^{0.53} \tag{26}$$

$$h_c = 5.66\left(\frac{M}{58.2} - 0.85\right)^{0.39} \tag{27}$$

where h_c is the convective heat transfer coefficient, in W.m^{-2}.K^{-1}, M is the metabolic rate per unit area, in W.m^{-2}, v is the air velocity, in m.s^{-1}. Radiant heat transfer coefficient, h_r, is calculated using:

$$h_r = 4 * f_{eff} * \epsilon * \sigma\left(\frac{T_{cl} + T_r}{2} + 273.15\right)^3 \tag{28}$$

where f_{eff} is the fraction of surface effective for radiation (dimensionless), ϵ is the emissivity of clothing-skin surface (dimensionless), σ is the Stefan-Boltzmann constant, in W.m^{-2}.K^{-4}, T_{cl} and T_r are the clothing surface and mean radiant temperatures, respectively, in ºC. The clothing surface temperature, T_{cl}, is iteratively estimated by the following equation:

$$T_{cl} = \frac{\left(\frac{T_{sk}}{I_{cl}} + f_{cl}(h_c T_a + h_r T_r)\right)}{\frac{1}{I_{cl}} + f_{cl}(h_c + h_r)} \tag{29}$$

where T_{sk}, T_a, T_r are the skin, air and mean radiant temperatures, respectively, in ºC, f_{cl} is the ratio of clothed body (dimensionless), I_{cl} is the clothing insulation, in m^2.K.W^{-1}, h_c, h_r are the convective and radiant heat transfer coefficients, respectively, in W.m^{-2}.K^{-1}.

Total evaporative heat loss from skin, E_{sk}, can be calculated with the following equations:

$$E_{sk} = E_{rsw} + E_{diff} \tag{30}$$

$$E_{rsw} = 0.68 * SW_{reg} \tag{31}$$

$$E_{diff} = w_{diff} * E_{max} \tag{32}$$

$$w_{diff} = 0.06(1 - w_{rsw}) \tag{33}$$

$$E_{max} = h'_e(P_{sk} - P_a) \tag{34}$$

$$w_{rsw} = \frac{E_{rsw}}{E_{max}} \tag{35}$$

where E_{rsw}, E_{diff} are the rate of heat loss from evaporation of regulatory sweating and from diffusion of water vapour through the skin, respectively, in W.m^{-2}, SW_{reg} is the rate of regulatory sweating, in g.m^{-2}.hr^{-1}, w_{diff} is the skin wettedness due to diffusion through the skin (dimensionless), w_{rsw} is the skin wettedness due to regulatory sweating (dimensionless), E_{max} is the maximum evaporative heat loss, in W.m^{-2}, P_{sk}, P_a are the saturated water vapour pressure at required skin temperature and water vapour pressure in ambient air, respectively, in Torr.

The heat transfer between the internal core compartment and the outer skin shell, Q_{crsk}, in W.m^{-2}, can be determined with the following equation:

$$Q_{crsk} = (5.28 + 1.163 * SKBF)(T_{cr} - T_{sk}) \tag{36}$$

where $SKBF$ is the skin blood flow rate, in dm^3.m^{-1}.hr^{-1}, T_{cr} and T_{sk} are the temperatures of the core and skin, respectively, in ºC.

New temperatures of core, skin and body are calculated from each iteration from rates of heat storage:

$$S_{sk} = Q_{crsk} - Q_c - Q_r - E_{sk} \tag{37}$$

$$S_{cr} = M - W - Q_{res} - Q_{crsk} \tag{38}$$

where S_{sk}, S_{cr} are the heat storage in skin and core compartments, respectively, Q_{crsk} is the heat flow from core to skin, Q_c, Q_r are the rates of convective and radiative heat loss, respectively, E_{sk} is the total evaporative heat loss from skin, M is the metabolic rate, W the rate of heat loss due to work, Q_{res} the rate of respiratory heat loss. All units in W.m^{-2}.

Pierce Model converts the actual environment to a standard environment. Standard Effective Temperature (SET*) is the dry-bulb temperature with 50% RH, with subjects wearing appropriate clothing for the activity in real conditions. On the other hand, Effective Temperature (ET*) is the dry-bulb of a hypothetical environment at 50% RH and uniform temperature, which means air temperature equal to the Mean Radiant Temperature, and where the subjects would have the same physiological strain as in the real environment.

Predicted Mean Vote for ET* and SET* can be determined using:

$$PMV_{ET} = (0.303e^{-0.036M} + 0.028)(H - L_{ET}\ ) \tag{39}$$

$$PVM_{SET} = (0.303e^{-0.036M} + 0.028)(H - L_{SET}) \tag{40}$$

$TSENS$ is a classical index and function of the mean body temperature; $DISC$ is a relative thermoregulatory strain needed to bring about thermal equilibrium, function of heat stress and heat strain in hot environments and equal to $TSENS$ in cold environments. These variables can be calculated with the following equations:

$$T_{b-c} = \left(\frac{0.185}{58.2}\right)(M - W) + 36.313 \tag{41}$$

$$T_{b-h} = \left(\frac{0.359}{58.2}\right)(M - W) + 36.664 \quad (42)$$

where T_{b-c} is the mean body temperature when $DISC$ is zero (lower limit) and T_{b-h} is the mean body temperature when the blood flow rate is the maximum (upper limit).

If $T_b \leq T_{b-c}$,

$$TSENS_c = 0.68175(T_b - T_{b-c}) \quad (43)$$

Otherwise (when $T_b > T_{b-c}$):

$$TSENS_h = \frac{4.7(T_b - T_{b-c})}{T_{b-h} - T_{b-c}} \quad (44)$$

And $DISC$ is calculated using the following equation:

$$DISC = 5 * \frac{E_{rsw} - E_{rsw-comf}}{E_{\max} - E_{rsw-comf} - E_{diff}} \quad (45)$$

Where E_{rsw} is the rate of heat loss from evaporation of regulatory sweating, $E_{rsw-comf}$ is the rate of heat loss from evaporation of regulatory sweating at the state of comfort, $E_{\max}$ is the maximum evaporative heat loss, E_{diff} is the rate of heat loss from diffusion of water vapour through the skin. These have units of W.m^{-2}.

2.5.3. KSU Two-Node Model

The KSU Two-Node Model is comparable with the Pierce Two-Node Model. The biggest difference between the two models is that KSU model predicts the thermal sensation in a different manner for warm and cold environments: for warm environments, thermal conductance of the model is based on changes in skin wettedness, whereas in cold environments the model is based on changes that occur in the thermal conductance between core and skin (Azer and Hsu, 1977).

The core generates heat, which is exchanged with the interior environment by respiration. The interior environment also exchanges energy with the skin through evaporation of sweat or water vapour diffusion. Theses exchanges of energy are represented in this model by the following equations:

$$W_{cr}C_{cr}\frac{dT_{cr}}{dt} = M - W - Q_{res} - KS(T_{cr} - T_{sk}) \quad (46)$$

$$W_{sk}C_{sk}\frac{dT_{sk}}{dt} = KS(T_{cr} - T_{sk}) - Q_{dry} - E_{sk} \quad (47)$$

Where KS is the overall skin thermal conductance, in W.m^{-2}.K^{-1}, C_{cr} and C_{sk} are the specific heat of body core and skin, respectively, in W.hr.Kg^{-1}.K^{-1}, W_{cr}, W_{sk} are the mass of body core and skin per unit surface area, respectively, in Kg.m^{-2}, T_{cr}, T_{sk} are the core and skin temperatures, in ºC, Q_{res}, Q_{dry}, E_{sk} are the rates of respiratory, sensible and evaporative heat loss rates, in W.m^{-2}, M is the metabolic heat rate per unit area and W is the heat loss due to work, both in W.m^{-2}.

Sensible heat loss rate, Q_{dry}, is calculated with the following set of equations:

$$Q_{dry} = Q_c + Q_r = h f_{cl} F_{cl} (T_{sk} - T_o) \tag{48}$$

$$h = h_c + h_r \tag{49}$$

$$h_c = 8.3\sqrt{v} \tag{50}$$

$$h_r = \epsilon_{avg}(3.87 + 0.031 T_r) \tag{51}$$

$$T_o = \frac{h_c T_a + h_r T_r}{h_c + h_r} \tag{52}$$

Where h is the combined heat transfer coefficient, in W.m^{-2}.K^{-1}, ϵ_{avg} is the median emissivity (dimensionless), F_{cl} is the Burton thermal efficiency factor for clothing (dimensionless), T_r is the mean radiant temperature, T_a is the air temperature, T_o is the operative temperature, temperatures in ºC.

Evaporative heat losses, E_{sk} are defined by the following equations:

If $E_{sw} \leq E_{max}$:

$$E_{sk} = E_{sw} + (1 - w_{rsw}) E_{diff} \tag{53}$$

If $E_{sw} > E_{max}$:

$$E_{sk} = E_{max} \tag{54}$$

$$E_{diff} = 0.408(P_{sk} - P_a) \tag{55}$$

$$E_{\max} = 2.2 h_c F_{pcl} (P_{sk} - P_a) \tag{56}$$

where F_{pcl} is the permeation efficiency factor for clothing (dimensionless).

Controlling functions of skin conductance (KS), sweat rate (E_{sw}) and shivering (M_{shiv}) are based on deviations in skin and core temperatures, as follows:

$$KS = 5.3 + \frac{6.75 + 42.45(T_{cr} - 36.98) + 8.15(T_{cr} - 35.15)^{0.8}(T_{sk} - 33.8)}{1 + 0.4(32.1 - T_{sk})} \tag{57}$$

$$E_{sw} = \phi \frac{\big(260(T_{cr} - 36.9) + 26(T_{sk} - 33.8)\big) e^{\frac{(T_{sk} - 33.8)}{8.5}}}{1 + 0.05(33.37 - T_{sk})^{2.4}} \tag{58}$$

$$M_{shiv} = 20(36.9 - T_{cr})(32.5 - T_{sk}) + 5(32.5 - T_{sk}) \tag{59}$$

Where ϕ is a sweat supply factor (dimensionless).

Wettedness factor, ϵ_{wsw}, correlated with warm thermal sensations, is defined by:

$$\epsilon_{wsw} = \frac{w_{rsw} - w_{rsw-o}}{1 - w_{rsw-o}} \tag{60}$$

$$w_{rsw} = \frac{E_{sw}}{E_{\max}} \tag{61}$$

$$w_{rsw-o} = 0.2 + 0.4\left(1 - e^{-0.6\left(\frac{H}{58.2}\right)-1}\right) \quad (62)$$

where w_{rsw} is the skin wettedness due to regulatory sweating, w_{rsw-o} is the skin wettedness at thermal neutrality, H is internal heat production, in W.m^{-2}. On the contrary, it is created a vasoconstriction factor with cold thermal sensations, defined by:

$$\epsilon_{vc} = \frac{KS_0 - KS}{KS_0 - KS_{-4}} \quad (63)$$

Where KS_0 is the skin conductance at thermal neutrality, KS_{-4} is the skin conductance at very cold thermal sensation, both in W.m^{-2}.K^{-1}.

Thermal Sensation Vote (TSV) in a cold environment is, therefore, a function of the vasoconstriction factor (ϵ_{vc}):

$$TSV = -1.46 * \epsilon_{vc} + 3.75 * \epsilon_{vc}^2 - 6.17 * \epsilon_{vc}^3 \quad (64)$$

Whereas for warm environments, TSV is a function of both the wettedness factor, ϵ_{wsw}, and relative humidity, RH:

$$TSV = \left(5 - 6.56(RH - 0.5)\right) * \epsilon_{wsw} \quad (65)$$

It is to be noted that KSU model's TSV was developed for a wide temperature range and clo levels between 0.05 and 0.7 clo and for activities ranging from 1 to 6 Mets.

2.5.4. Adaptive models

These models differentiate themselves from the previous ones because of one primary reason: it considers the man as an active agent, which interacts with the surrounding environment in response to its own thermal preferences and sensations. While the first models shown (denominated passive models) are mainly static and developed in climatic chambers, adaptive models are more grounded on field studies. Humphreys (1979) identifies two main reasons adaptive models were created: the results in climatized chambers diverged somewhat in natural ventilated areas, especially in warm climates of low- and middle-income countries. Fanger, Toftum, (2002) describe an extension to Fanger model to account an expectancy factor for these warm climates, to describe better thermal sensations of humans in these areas. The second factor is that it seemed population accepted better a greater temperature interval than the proposed in other methods, hence the adaptation part of the model.

The adaptive approach considers the following adjustments to the human body:

- **Behavioural adjustments**: conscious or unconscious modifications from people; it can change the thermal exchange with the surrounding environment. These adjustments can be personal (clothes, posture), environmental and cultural;
- **Physiological adjustments**: those that include all changes in people physiological responses, including genetical adaptation and acclimation;

- **Psychological adjustments**: perceptions and reactions from sensorial information. This can be compared to the notion of habit.

To this approach, thermal comfort sensation is not only measured from internal ambient temperature, but also from a monthly mean outdoor temperature, as discomfort is translated as the difference between the expected ambient and the ambient they encounter.

Adaptive model based on ASHRAE Standard 55-2010

In this standard, the monthly mean outdoor air temperature is defined as the average of previous 30 daily average outdoor air temperatures. Furthermore, the model is only applicable between monthly mean outdoor air temperature of 10 to 33.5ºC. This model defines two comfort regions: 80% Acceptability and 90% Acceptability. The comfort temperature is defined as:

$$T_{ot} = 0.31 * T_o + 17.8 \quad (66)$$

Where T_{ot} is the operative temperature, in ºC, calculated as the average of indoor air dry-bulb temperature and mean radiant temperature of zone inside surfaces, T_o is the monthly mean outdoor air dry-bulb temperature, in ºC. Comfort regions are symmetric about the comfort temperature and are defined as:

90% Acceptability limits: $T_{ot} = 0.31 * T_o + 17.8 \pm 2.5$

80% Acceptability limits: $T_{ot} = 0.31 * T_o + 17.8 \pm 3.5$

Adaptive model based on European Standard EN15251-2007

This model is intended for use with naturally ventilated buildings and determines the acceptability of indoor conditions given the 7-day weighted mean outdoor air temperature (T_o). In this model, people's clothing properties are not necessary, as the model accounts for people's adaptation to the space. In addition, no humidity or air-speed limits are necessary as input for this model. It defines three comfort regions: Category I (90% Acceptability), Category II (80% Acceptability) and Category III (65% Acceptability). This model is only applicable when T_o is in the specified domain of 10 to 30 ºC.

Comfort temperature is defined as:

$$T_{ot} = 0.33 * T_o + 18.8 \quad (67)$$

Category I, 90% Acceptability limits: $T_{ot} = 0.33 * T_o + 18.8 \pm 2$

Category II, 80% Acceptability limits: $T_{ot} = 0.33 * T_o + 18.8 \pm 3$

Category III, 65%Acceptability limits: $T_{ot} = 0.33 * T_o + 18.8 \pm 4$

Where T_{ot} is the operative temperature, in ºC.

2.5.5. Thermal models in sleeping bags

There are various models that determine air temperatures for thermal comfort of people using sleeping bags. Rohles and Munson (1980) made an equation to predict the lower thermal comfort limit of sleeping bags, with the help of a study of thermal comfort of 1600 subjects. Huang (2008) converted this equation to the variables compared in other models using data from research on awake subjects (Seppanen et al., 1972):

$$T_e = 35.07 - 7.29 * I_t \quad (68)$$

where T_e is the effective outside temperature, in ºC, and I_t is the total insulation of the sleeping system, in clo.

Holand (1999) used ISO 11079 equations. Metabolic rate was assumed to be 55 W.m^{-2}. The equation to calculate minimum environmental temperature for 8h of sleep was therefore created:

$$T_a = 30.08 - 7.85 * I_t \quad (69)$$

where T_a is the minimum environmental temperature, in ºC, and I_t is the total insulation of the system, in clo. This equation considered data retrieved from tests made to the sleeping bags with a thermal manikin and to human subjects (six males and six females). Subjects were required to fill out a questionnaire regarding the tested sleeping bags and to rate their thermal comfort, so that the researcher could estimate the comfortable temperature for each sleeping bag.

Hartog et al. (2001) estimated the minimum temperature for 8h of sleep as (TNO model):

$$T_a = T_{sk} - M * R_t \quad (70)$$

Where T_a is the lowest acceptable outside air temperature (ºC), T_{sk} is the mean skin temperature (assumed to be 32ºC), M is the metabolic rate, assumed 47.22 W.m^{-2} and R_t the total insulation of the sleeping bag system, in m^2.ºC.W^{-1}. It was also assumed that 4.2 J.g^{-1} was acceptable as minimal heat loss in a military soldier. Several manikin measurements and subject tests (three men and three women) were done to verify this model by the author, and the sleeping bags were evaluated with a sweat rate of the torso of 20 g.h^{-1}. It was found that a large difference occurred from the model prediction and the subject test, and it was concluded by the author that this difference was caused by moisture accumulation of the bags. With R_t quantified in clo units, Huang (2008) rewrote this equation as:

$$T_a = 32 - 7.32 * I_t \quad (71)$$

Goldman (1988) considered an average soldier of 70 kg, 173 cm and 1.8 m^2 of surface area, and this soldier produced 46.5 W.m^{-2}, from which 25% would be lost by body respiration and evaporation, following that 34.9 W.m^{-2} would be lost by conduction, convection and radiation.

In the author system, two concepts were defined: comfortable sleep, where a sleeping soldier could lose up to 34.9 W.m^{-2} by non-evaporating means, and six hours of restful sleep, where the soldier would lose 43.5 W.m^{-2}. In both systems, average skin temperature should not fall below 32 ºC and an amount of

body heat debt greater than 334944 J was not acceptable. Hence, the equations developed were the following:

For 8 hours of sleep: $T_a = 32 - 6.4 * I_t$

In steady-state: $T_a = 32 - 5.4 * I_t$

Where I_t is the total thermal insulation of the sleeping bag and surface air layer in clo and T_a is the expected outside air temperature for thermal comfort in ºC.

Huang (2008) derived the equation for 8h of sleep from his work:

$$T_a = 32 - 6.4 * I_t \quad (72)$$

KSU model assumes that the mean skin temperature for a comfortable, steady-state sleeping person is 33 ºC and uses metabolic rate of 46.6 W.m^{-2}. Assuming a heat debt of 163000 J.m^{-2}, the average skin temperature is 31.5 ºC for a typical person under an assumed number of sleeping hours. Four components of heat loss from the body were computed: dry heat loss and evaporative heat loss from respiration, and dry heat loss and evaporative heat loss from the skin. The general energy equation (ISO 2007) can be represented as:

$$M - W = C + R + E + C_{res} + E_{res} + S \quad (73)$$

where M is the metabolic rate, W is mechanical power (which is negligible in a person sleeping in a bag), C is the convective heat loss from skin, R is the radiation heat loss from skin, E is the evaporative heat loss from skin, C_{res} is the convective heat loss from respiration, E_{res} is the evaporative heat loss from respiration and S is the rate of body heat storage, all in W.m^{-2}. Under thermal equilibrium conditions, it can be assumed that body heat production is equal to body heat loss.

Solving the energy equation to infer the minimum air temperature for a specific insulation value, the following equations were derived from the KSU model (McCullough, 1994):

For 8 hours of sleep: $T_a = 31.43 - 5.78 * I_t$;

In steady-state: $T_a = 32.79 - 4.82 * I_t$

In European Standard 13537:2002, heat exchange equations were solved to know the lower limit temperature for a standard man, with metabolic rate of 47.5 W.m^{-2} and mean skin temperature of 32.9 ºC. Huang (2008) derived from the original model the following prediction:

$$T_a = 31.81 - 5.6 * I_t \quad (74)$$

, and for a standard woman with a metabolic rate of 44.4 W.m^{-2} and mean skin temperature of 32.8 ºC, it was obtained the following for the comfort temperature:

$$T_a = 32.24 - 4.8 * I_t \quad (75)$$

The comparison of the models discussed so far are presented in Table 2 (adapted from Huang, 2008):

Table 2 - Sleeping bag thermal models

Models	Metabolic rate ($W.m^{-2}$)	Skin temperature (ºC)	Equations (steady-state)	Equations (8 h sleep)
Goldman	46.4	32	$T_a = 32 - 5.4 * I_t$	$T_a = 32 - 6.4 * I_t$
KSU	46.6	31.5	$T_a = 32.79 - 4.82 * I_t$	$T_a = 31.43 - 5.78 * I_t$
Europe (limit)	47.5	32.9	$T_a = 31.81 - 5.6 * I_t$	NA
Europe (comfort)	44.4	32.8	$T_a = 32.24 - 4.8 * I_t$	NA
Holand	55	NA	NA	$T_a = 30.08 - 7.85 * I_t$
TNO	47.2	32	NA	$T_a = 32 - 7.32 * I_t$

It can be seen from Table 2 that average skin temperature varied between 31.5 ºC and 32.9 ºC, and metabolic rates varied from 44.4 $W.m^{-2}$ to 55 $W.m^{-2}$. None of the models predict air temperature for optimum thermal comfort since these models use skin temperatures lower than those needed for thermal neutrality. Figure 5 gives other view for the air temperatures for 8h sleep and thermal comfort (adapted from Huang, 2008):

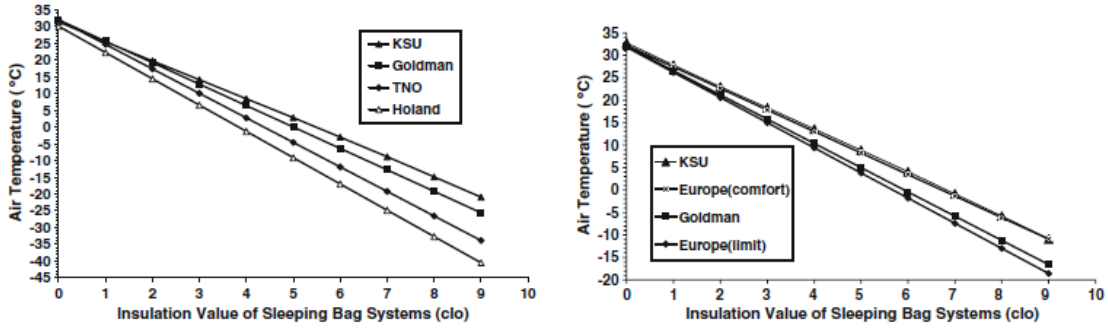

Figure 5 – Sleeping bag thermal models displayed in graph (Huang, 2008). Left: Acceptable temperatures for 8h sleep. Right: Air temperatures for thermal comfort (steady-state).

One conclusion from figure 5 is that all models display a trend of decreasing the minimum outside air temperature when increasing the insulation value of the sleeping bag system. Predictions are diverging as the insulation values increase.

As can be seen from figure 5 (left), KSU model has the highest acceptable temperature predictions. This is in line with the fact that this model was created for recreational users, hence it is reasonable that the model gives the most conservative results.

In figure 5 (right), it can be observed that both KSU and European models give similar and the most conservative results. This can be explained from the fact that these models were grounded on identical assumptions.

Huang (2008) refers that condensation of moisture vapor is a dominant issue for wearer comfort. The intensity of condensation is mainly dependent on vapor permeability of the sleeping bag materials. Usage of semipermeable cover materials has been used as it is an efficient method of reducing moisture accumulation.

2.6. Conclusions

Some conclusions can be taken out from the research done:

Measurement and analysis of PCM performance

Both mattress and surface temperatures are useful to verify thermoregulatory differences. Moreover, both mattress and skin temperatures increase when using PCMs, which is ideal in the case at hand, where the objective is to increase thermal comfort in homeless people in Lisbon.

PCM beds are currently used for infants in low- and middle-income countries with success.

PCM vests can be very useful for personal use in heat strain alleviation. Thermal manikins are widely used as human models and thermal sensation of the body with PCM vests is improved.

Factors affecting PCM performance

PCM melting temperature is very important, as the PCM performance in certain applications depends majorly on this factor. For the application at hand, PCM melting temperature between 18ºC and 32ºC should be ideal, as skin temperature and surface temperature is inside these values.

PCM performance is dependent on the climate at study. It seems that PCM performs better in humid conditions, as seen earlier for instance in Zhao et al. (2012).

PCM quantity is also significant, as energy storage is correlated with it. It seems that 1 to 2 Kg of PCM for this case should be ideal, as used in House et al. (2012) and Gao et al. (2010). More quantity would also mean carrying more weight in the sleeping system, which is not ideal.

Clothing properties

Thermal comfort might be changed by clothing properties. The most important clothing properties are material thickness, material type and air and moisture permeability.

When ambient temperature is lower than skin temperature, air permeability of clothing has greater influence than moisture regain on rectal temperature. This is the case in the winter for the homeless, which means air permeability of clothing might play an important role.

Sleeping system properties

For experiments with wall and air temperatures of 16 ºC-25 ºC, microclimate temperature of the sleeping system was around 28-30 ºC. Also, with a microclimate temperature of 26.1 ºC, high nocturnal awakening happened. If simulations are done with this temperature conditions, a comparison can be made to perceive thermal comfort of the subject.

Heat loss in the sleeping system occurs because of the ventilation effect. The sleeping system should have moisture absorbing and insulating effects, as well as adaptiveness to body shape. Furthermore, sleeping system's heat loss comes from leakage of microclimate air to ambient temperature through bedding upper layers and because of heat conduction to the ground.

Human comfort and thermal models

It can be concluded that in thermal comfort, skin temperature in sedentary activities, such as office activities, ranges between 33ºC to 34 ºC and this temperature can be lower with increase of activity. In relation to the simulations to be done, it is expected a skin temperature of 34 ºC or higher in core temperature, as the person should be asleep, thus having no activity besides the necessary to keep the internal temperature stable.

There are some models to verify human thermal comfort. Fanger is the most known model but presents some discrepancies when modelling thermal comfort of people inside natural ventilated buildings, which is the closest to outdoors. Both Pierce Two-Node Model and KSU Model use concentric cylinders and simulate the core and periphery of the body. This presents a higher level of complexity comparing to Fanger model.

In relation to the adaptive models, the one that seems more relevant to this work is the European Standard EN15251-2007, as it was designed for naturally ventilated buildings. The disadvantage of these adaptive models is the fact that they are only available to outdoor temperatures above 10 ºC. This means that for the coldest nights in Lisbon, which can easily be 5 ºC or lower, the models cannot predict a comfort region.

In terms of thermal models in sleeping bags, these are only useful to see the required outside temperature vs. the total insulation of the sleeping system. These have few information about the material's permeability and moisture accumulation.

3. Methodology

This work consists in two different parts: numerical and experimental analyses. In both sections, the sleeping system consists in the sleeping bag and sleeping mat, as well as PCMs when they are present in the system.

3.1. Experimental

3.1.1. Sleeping System Materials

Figure 6 presents the sleeping mat chosen for this test. It was the cheapest one (5 €) found in a sports store:

Figure 6 - Sleeping mat (Decathlon website)

The sleeping mat is made of a polyester foam. With the weight and volume stated in the site, the density was found to be 0,033 $Kg.m^{-3}$. A polyester foam with the same density was found in CES Edupack 2013, a database of materials. The other properties of the sleeping mat were taken from this software too.

Similarly, the sleeping bag used was one akin to the cheapest one (8 €) found in a sports store (figure 7):

Figure 7 - Sleeping bag (Decathlon website)

With the weight and dimensions of the sleeping bag, as well as the material information provided by the seller, density was calculated and the material with similar properties in CES Edupack 2013 was chosen to be the reference. This is a bag for comfortable conditions in 20 ºC, which means (with the European norm given in section 2.5.5.) this sleeping bag has 2.55 clo. This sleeping bag is not ideal for winter in Lisbon. However, it can represent extreme clothing conditions from homeless.

3.1.2. Data acquisition

Thermographic Camera

A thermographic camera (see figure 8) was used to evaluate the sleeping system and the different parts of the body, to decide which parts would be analysed in more detail with thermocouples.

Figure 8 - Fluke TiR27 Infrared Camera (Fluke website)

Camera model is Fluke TiR27 Infrared Camera. This camera has a temperature measurement range of -20 ºC to 150 ºC, and a temperature measurement uncertainty of ± 2°C or 2%, whichever is greater. For the temperature range of this test (maximum 40 ºC), the uncertainty is therefore ± 2°C. It is important to state that uncertainty also depends on the distance from the thermographic camera to the object being analysed. Precautions and minimum possible distance to the sleeping system were used to reduce uncertainty.

Temperature/Humidity Datalogger

Two Onset® HOBO Temperature and Relative Humidity Data Logger – U10-003 were used to measure temperature and humidity (figure 9):

Figure 9 - Hobo Datalogger

Temperature uncertainty is ± 0.53°C from 0° to 50°C, humidity uncertainty is ± 3.5% from 25% to 85% over the range of 15° to 45°C, which are the ranges of temperature and humidity present in the executed experiments. For these experiments, a frequency of 1 sample per minute was chosen, to accurately represent data from the 8-hour experiments. Hoboware® software, from the same company, was used

to read data gathered in the experiments. Then, Matlab was used to process this data and produce graphs.

Thermocouples

The most accurate thermocouples are the ones that have the biggest $\frac{mV}{°C}$ ratio for the range of temperatures needed (see Appendix B for temperature-millivolt graph of thermocouples).

Thermocouples used were type T, with an uncertainty of ± 0.5 ºC for the temperature range of these experiments, which would be at most 0-40 ºC. Not only are T thermocouples one of the best in terms of sensitivity to change in temperature ratio (3rd highest slope in $\frac{mV}{°C}$ ratio), but they are also precise where moisture is present, which is necessary when measuring skin temperatures (Omega® Encyclopedia).

For the thermocouple calibration process, a mercury thermometer was not available. Therefore, calibration was done using a SuperMeter® HHM290 as reference. Two K-thermocouple probes were plugged in the SuperMeter, and the reference was the average of both. After the temperature of the reference stabilized, difference in temperature of the thermocouple to the reference was recorded. This value was then used in results' treatment.

To measure temperature in several locations at the same time, a NI cDAQ-9172 was used (figure 10):

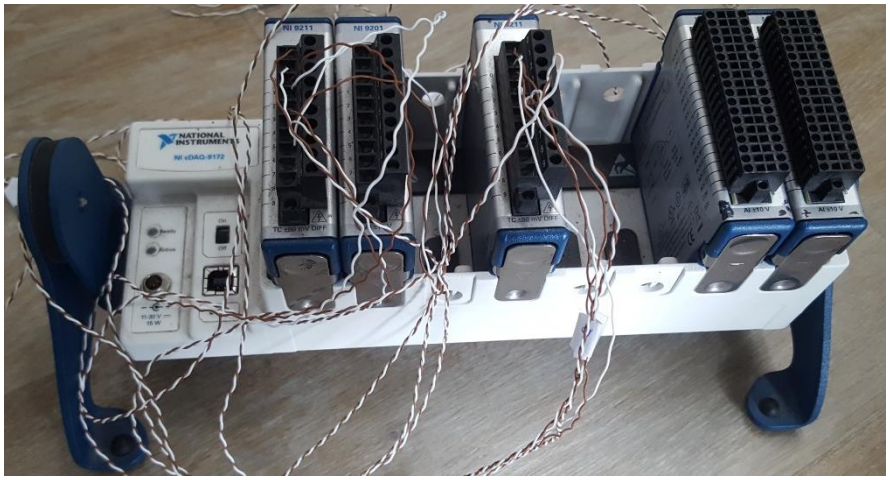

Figure 10 - NI cDAQ-9172 Datalogger

With 2 temperature decks available, this DAQ could have 8 thermocouples gathering data simultaneously.

To program the DAQ, a Virtual Instrument (VI) was made in LabView®, a software of the same company (see Appendix C). The VI was necessary to make the DAQ record the desired temperatures, with the T thermocouple design, and store it in a PC. Thermocouples were measuring 3 times per minute and giving an average for each minute. These mean temperatures were then saved to the computer at each time interval for a .lvm file. The processing of files and the output of results were done in Matlab.

For DAQ to work and save data, it had to be connected to a PC. This was a heat source near the subject (about 2m of distance), which was a source of errors in the experiment.

3.1.3. Experimental Setup and Procedure

Thermographic camera analyses

A preliminary analysis was done with the thermographic camera. It was made a small-period test in a temperature-controlled room. The room temperature was 21 °C.

Firstly, a test was done with a person laid down in the sleeping mat. For these experiments with the thermographic camera, the subject was wearing a t-shirt, jeans and sneakers.

The subject was inside the sleeping bag and above the sleeping mat for 7 minutes. Then, photos were taken of the body divided in 3 parts: upper torso zone, waist zone and legs. After this, some photos were taken to the sleeping mat right after the subject left the sleeping mat, to check the thermal impression left by the subject in the sleeping mat. These tests were done without PCM.

When revising literature about the tests made in subjects and thermal manikins, very different approaches were noted. For instance, Okamoto-Mizuno et al. (2016) measured the foot, hand, back and thigh skin temperatures of the subjects. On the other hand, Wu, Fan (2009) measured 22 different places with sensors in a thermal manikin, from head to calves.

Given the results of the experience and the knowledge based on the papers reviewed, thermocouples were put on chosen parts of the subject's body in the 8-hour experiment with thermocouples.

Night experiments

It was done a two-night experiment (28-29 and 29-30 August) with similar outside weather conditions of the building, so as not to have disproportional thermal gains over both nights, and with the same conditions in both nights. The only exception was that in one night the sleeping system contained PCM, in this case hexa-hydrated calcium chloride that melts at 28 ºC, and in other night it does not have PCMs. The weather in the evening and nights of the experiment (day prior and respective days) was the following (figure 11):

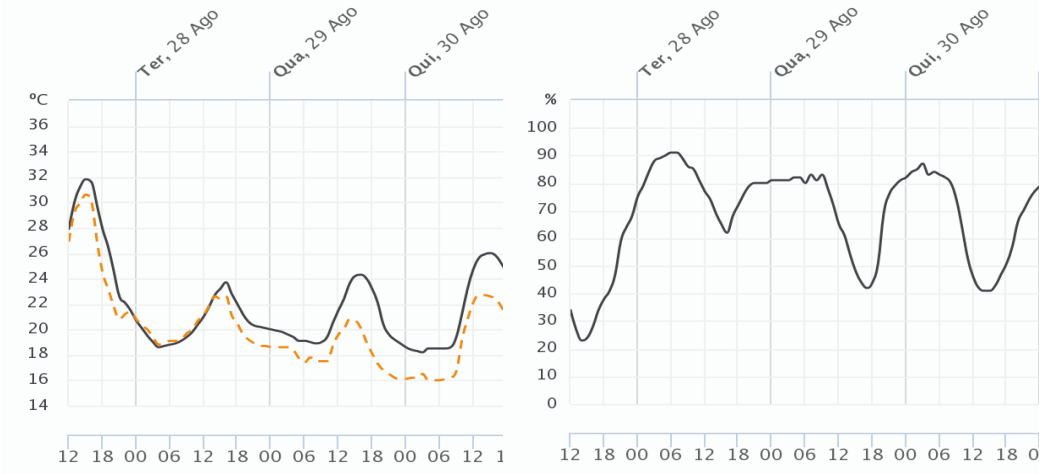

Figure 11 -Outside Meteorological conditions. Left: Temperature(ºC) vs. Time(hour). Right: RH(%) vs. Time(hour) . Source: MeteoIST

Analysing figure 11, it can be observed that the temperature varied only slightly (maximum temperature was 24ºC on Tuesday 28 August versus 26 ºC on Thursday 30 August), and RH was not much different either. Also, solar gains were checked in www.meteo.tecnico.ulisboa.pt and there was not a significant difference in both days. These parameters were important to verify since the building itself (walls, roof, floor) could have very different temperatures from one day to the other. As the differences were not relevant, the experiments were done in these days.

The experiment was done in a room with the following AC unit (figure 12):

Figure 12 - Daikin AC unit model FTXS60 (Daikin Technical specifications)

This AC unit is from Daikin, model is FTXS60-71GV1B. Looking at the technical specifications and knowing the volume of the room, it can be calculated the Air Changes per Hour (ACH) with the following expression:

$$ACH = \frac{60 * Q}{Volume} \tag{76}$$

where Q is the air flow rate in $m^3.min^{-1}$ and volume is in m^3. Table 3 presents the test room properties:

Table 3 - Test Room properties

Mode	Room Volume (m^3)	Air Flow Rate ($m^3.min^{-1}$)	Air Changes per Hour (ACH)
Low (cooling)	39.65	5.5	8.32
Medium (cooling)		7.4	11.20
High (cooling)		9.4	14.22

It was turned the air conditioning on about 4 hours earlier than the test was conducted to stabilize room conditions.

Temperature/RH dataloggers

The 2 dataloggers were used to record the mean test-room temperature and RH, as well as the temperature and air RH on the inside of the sleeping system. The recording of the inside's sleeping system was made with the assumption that it was equivalent and comparable to the zone mean air temperature: it was at the lower torso of the subject's body, and some cardboard was used to separate the body from the datalogger to have a mean RH value of the sleeping system.

Thermocouples location

The subject was laid down on his back (chest upwards) for the entirety of the test. It was necessary so that thermocouples would not easily detach from the body.

Table 4 presents the thermocouple's location. Figures 13, 14 and 15 help visualize where thermocouples were inserted in the system. After the preliminary analyses with the thermographic camera, the 8 available thermocouples were put in the following places:

Table 4 - Thermocouple's location

No.	Location
1	Nape
2	Chest
3	Thigh
4	Left foot
5	PCM/Back
5**	Sleeping mat surface (test without PCM)/ Back
6	Sleeping bag surface/ sleeping mat surface
7	Ground/sleeping bag surface
8	Ground (away from sleeping system)

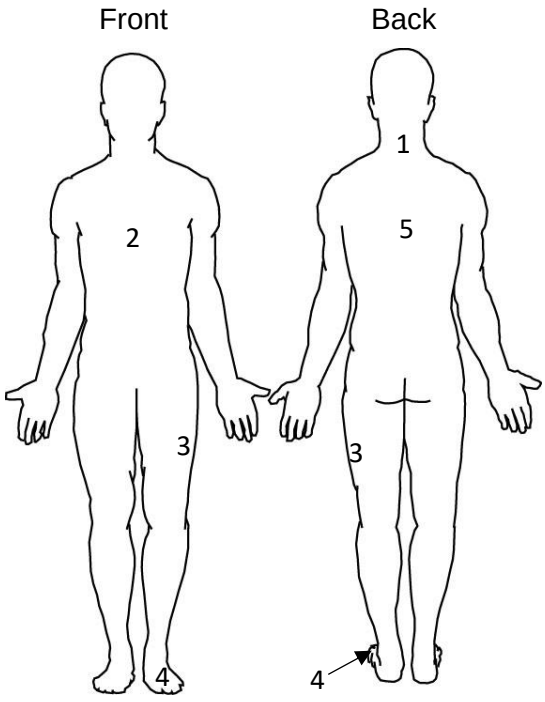

Figure 13 - Thermocouple's location in the subject (adapted from www.getdrawings.com)

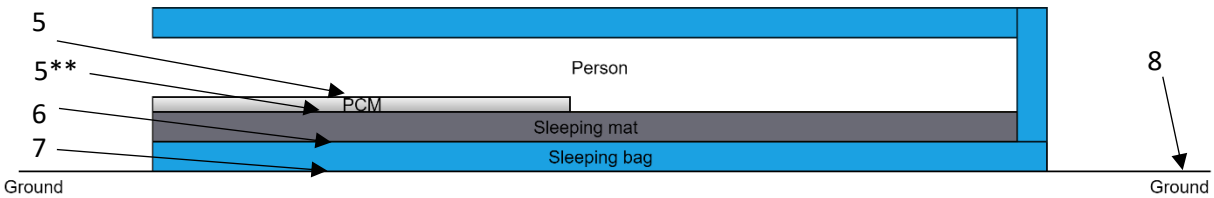

Figure 14 - Thermocouple's location in the sleeping system

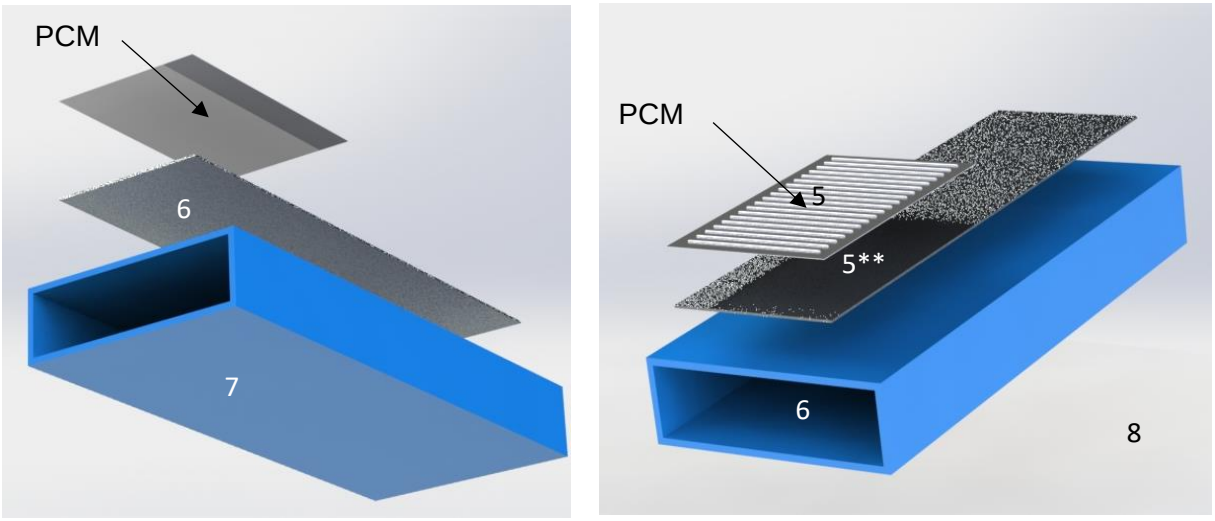

Figure 15 - Exploded view of the sleeping system (PCM, sleeping mat and sleeping bag) and thermocouple's location. Left: Bottom surface's visualization. Right: Top surface's visualization.

PCM properties

The PCM chosen for testing was the hexa-hydrated calcium chloride ($CaCl_2.6H_2O$), which is a hydrated salt. This PCM was chosen due to several reasons (Kaygusuz, 1994): its high heat of fusion (about 188000 $J.Kg^{-1}$), good thermal stability and resistance to corrosion. Another advantage is its low price (0.3 €.Kg^{-1}). The PCM was packed inside water-balloons and then was wrapped up in aluminium tape, with the spacing equal to the cuts done in the sleeping mat prepared to have these PCMs above it. The sleeping mat with PCMs can be seen in figure 16:

Figure 16 - Sleeping mat with insertion of PCM

These cuts were necessary to have minimum contact of PCMs with the human subject, to avoid leakages of the PCM. In the experiments, 1 Kg of PCM was used.

In figure 17, it can be seen the experimental setup:

Figure 17 - Experimental Setup

In the 1st experiments made, the thermocouples disattached from the human body easily. They would only be attached a maximum of 1 hour, being necessary to put again aluminium tape to reattach the thermocouples. In order to avoid this occurrence, the skin of the subject was defatted with ethylic alcohol. Even though some disattachments still occurred (see Results and Discussion section), there was a clear improvement in this matter.

3.2. Numerical

The numerical part was done using EnergyPlus 8.9.0. To use EnergyPlus, a model was done in Google SketchUp 2017, and OpenStudio 2.5.0 was used to link the model with the EnergyPlus simulation. It was simulated the last 2 months of the year and the first 2 months, November, December, January and February, respectively. These correspond to 4 of the 5 coldest months in Lisbon, Portugal, as can be seen in the figure 18:

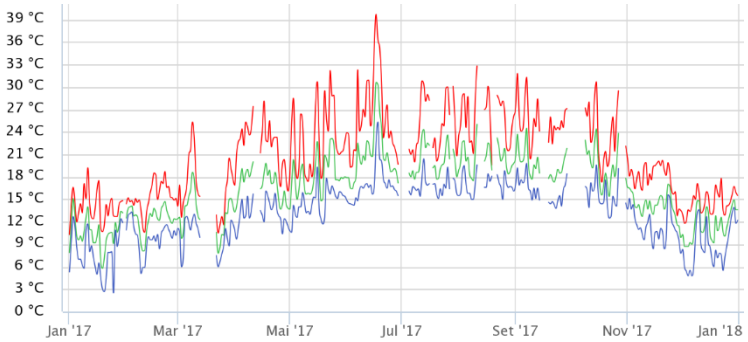

Figure 18 – Annual temperature of Lisbon, 2017. Red line: Maximum temperature. Green: Average temperature. Blue: Minimum temperature. Source: MeteoIST.

The Google SketchUp model can be seen in figure 19:

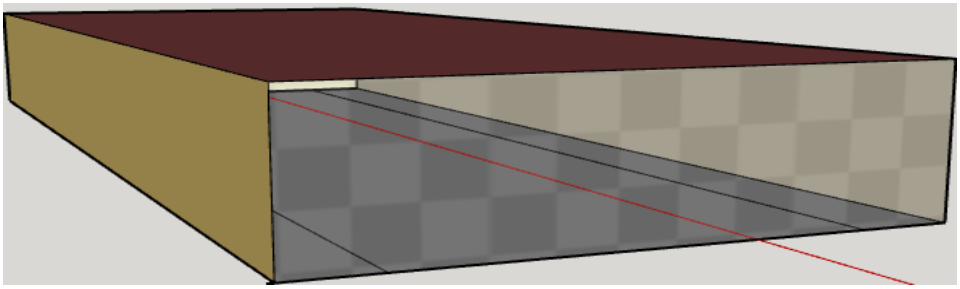

Figure 19 - Google SketchUp model

EnergyPlus was utilized to test different parameters, such as the PCM material (with different conductivity, density and specific heat), PCM melting temperature and sleeping system properties in Lisbon. Also, as this thesis was done throughout the warm season of the year, the numerical simulation helped to understand what could be done to improve the thermal and isolation properties of the sleeping system in cold conditions, which was not possible to do in the experimental part.

3.2.1. Heat and moisture transfer problem resolution

According to Incropera, DeWitt (2016), "Heat transfer (or heat) is thermal energy in transit due to a spatial temperature difference." This means that the existence of a temperature difference implies that heat transfer is occurring. The different modes of heat transfer are the following: conduction, convection and thermal radiation. Conduction is when heat transfer occurs when there is a temperature gradient in a stationary medium. The amount of energy transferred per unit time is described by Fourier's law:

$$q''_x = -k\left(\frac{dT}{dx}\right) \tag{77}$$

The equation above is for one-dimensional plane-wall. This equation implies that the heat flux per unit area, q''_x, in W.m^{-2}, is equal to symmetric of the conductivity of the material, k, in W.m^{-1}.K^{-1}, times the temperature gradient in the studied direction, $\frac{dT}{dx}$, in K.m^{-1}.

Convection is heat transfer that occurs between a surface and a moving fluid at different temperatures. The rate equation for this heat transfer mode is the following (Newton's law of cooling):

$$q'' = h(T_s - T_\infty) \tag{78}$$

Where the heat flux per unit area, q'', in W.m^{-2}, is equal to the convection heat transfer coefficient, h, in W.m^{-2}.K^{-1}, times the temperature difference between the surface and fluid temperatures, T_s and T_∞, respectively, in K.

Thermal radiation is the heat transfer in the form of electromagnetic waves between two surfaces at different temperatures. The heat flux emitted by a real surface is given by:

$$E = \epsilon\sigma T_s^4 \tag{79}$$

Where the surface emissive power, E, in W.m^{-2}, is equal to the emissivity of the surface, which ranges from 0 to 1, times the Stefan-Boltzmann constant, σ, which is equal to 5.67*10^-8 W.m^{-2}.K^{-4}, times the 4th power of the surface temperature, T_s, in K^4. Thus, the net rate of radiation heat transfer from the surface is given by:

$$q''_{rad} = \epsilon\sigma(T_s^4 - T_{sur}^4) \quad (80)$$

Where the units are the same as in equation 79, and T_{sur} is the surrounding temperature.

For the moisture part, there are several different properties that can be used. For example, the algorithm in EnergyPlus that solves both heat and moisture transfer, named HeatAndMoistureTransfer (HAMT) utilises the following set of properties: Sorption Isotherm, Suction, Redistribution, Diffusion and Thermal Conductivity.

Sorption Isotherm relates the water content density, in Kg.m^{-3} with Relative Humidity (RH). It expresses the way water content of a material changes with a change in RH. Suction relates the liquid transport coefficient, under suction, in m^2.s^{-1}, to the water content of a material, in Kg.m^{-3}. The Diffusion property relates the vapour resistance factor, which is dimensionless, to the RH. Finally, the Thermal Conductivity property of this algorithm relates the thermal conductivity, in W.m^{-1}.K^{-1}, with water content, in Kg.m^{-3} (adapted from EnergyPlus Engineering Reference document).

There are various models in EnergyPlus that solve the heat transfer equations in different ways. The one mentioned before is the Heat And Moisture Transfer algorithm, and it would be the ideal one for this case, as both heat and moisture are important to analyse the sleeping bag model. However, only one algorithm in EnergyPlus can incorporate the PCM phase-change properties in the simulation, and that algorithm is the Conduction Finite Difference (CondFD). Therefore, CondFD was the algorithm used. Results of moisture in the simulations made with this algorithm have many approximations.

The Crank-Nicholson scheme was used for this work, which is semi-implicit and second-order in time. In this case, it uses an implicit finite difference scheme coupled with an enthalpy-temperature function to account for phase change energy accurately. The implicit formulation for an internal node is the following:

$$\frac{C_p\rho\Delta x\left(T_i^{j+1} - T_i^{j}\right)}{\Delta t} = \frac{1}{2} * \left(\frac{k_W\left(T_{i+1}^{j+1} - T_i^{j+1}\right)}{\Delta x} + \frac{k_E\left(T_{i-1} - T_i^{j+1}\right)}{\Delta x} + \frac{k_W\left(T_{i+1}^{j} - T_i^{j}\right)}{\Delta x} + \frac{k_E\left(T_{i-1}^{j} - T_i^{j}\right)}{\Delta x}\right) \quad (81)$$

Where T is the node temperature, i represents the node being modelled, $i+1$ the adjacent node to interior of construction, $i-1$ the adjacent node to exterior of construction, $j+1$ the new time step, j the previous time step, Δt the calculation time step, Δx the finite layer thickness, C_p the specific heat of material, k_w the thermal conductivity for interface between i node and $i+1$ node, k_E the thermal conductivity for interface between $i-1$ node and i node, ρ the density of the material. Equation 81 is accompanied by the enthalpy-temperature function that the user inputs to the program.

The discretization used in the CondFD algorithm is the following:

$$\Delta x = \sqrt{C\alpha\Delta t} \tag{82}$$

Where C is the inverse of the Fourier number and α is the thermal diffusivity of the material. It was decided to use the C with the value of 1, as sub-hourly timesteps were desired.

When PCMs are being modelled, CondFD also calculates the specific heat from the tabulated input data of temperature/enthalpy pairs given by the user, in the form:

$$C_p = \frac{h_{i,new} - h_{i,old}}{T_{i,new} - T_{i,old}} \tag{83}$$

3.2.2. Input Data

Ground and Sleeping System

A scheme of the sleeping system can be seen in figure 20:

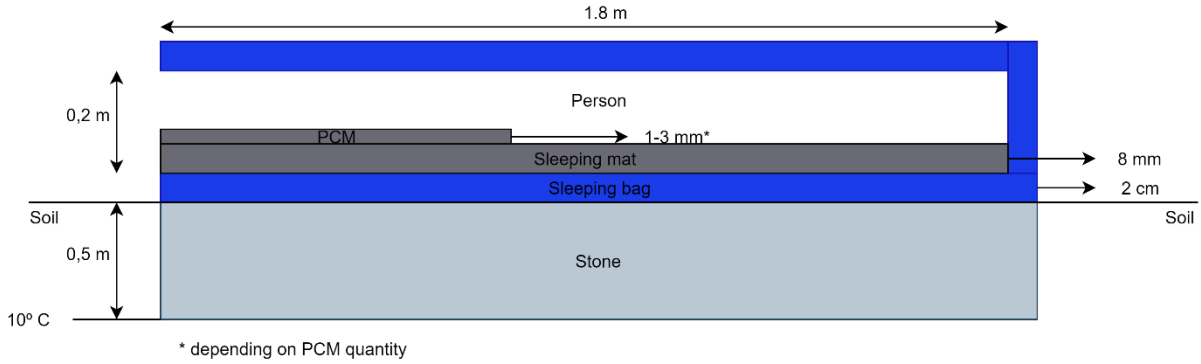

Figure 20 - Sleeping system in EnergyPlus

It was done a simulation outdoors (without any constructions to protect the sleeping bag) to represent homeless conditions in the streets of Lisbon.

The temperature of the rock at 0.5 meters was assumed to be 10ºC in the 4 months, on average, based on Morais (1955). Stone properties were decided to be equal to hard limestone, which is common in Lisbon. These properties were found in Pina dos Santos, Matias (2006).

The sleeping bag and sleeping mat properties put in EnergyPlus were the same as the ones found in CES Edupack for the experimental part. Table 5 presents the material properties:

Table 5 - Ground and sleeping system material properties

Material	Thickness(m)	Density ($Kg.m^{-3}$)	Conductivity ($W.m^{-1}.K^{-1}$)	Specific Heat ($J.Kg^{-1}.K^{-1}$)	Emissivity (ϵ)
Soil (Hard limestone) -	0.5	1842	0.23	837	0.6
Sleeping mat (Polyethylene)	0.008	33.33	0.04	2025	0.9
Sleeping Bag (Polyester PET-foam)	0.02	150	0.03155	1200	0.9

PCM

It was used two PCMs in EnergyPlus simulations: hexa-hydrated calcium chloride and BioPCM. The BioPCM enthalpy-temperature curve was found in the technical specifications of the manufacturer, whereas for hexa-hydrated calcium chloride some calculations were done to find its enthalpy-curve, based on the Differential Scanning Calorimetry (DSC) analysis of the material.

It can be seen in figure 21 the DSC curve of hexa-hydrated calcium chloride at the 100th cycle (Tyagi, Buddhi, 2008):

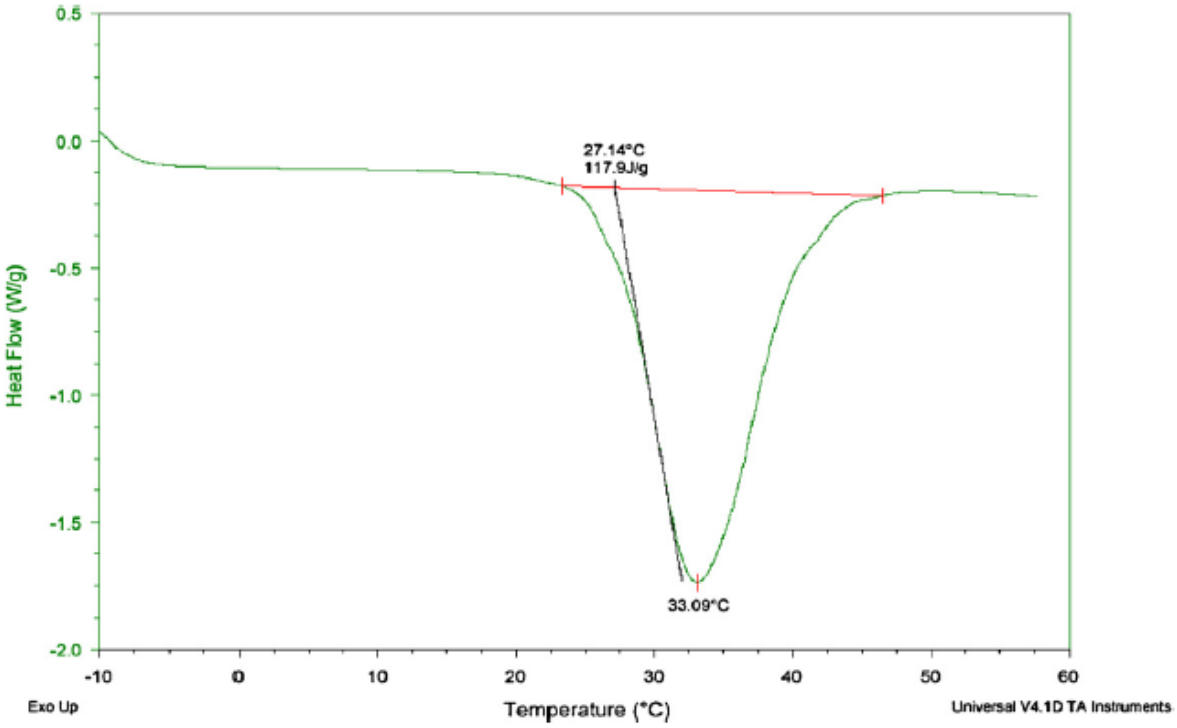

Figure 21 - Differential Scanning Calorimetry of $CaCl_2(H_2O)_6$ at the 100th cycle (Tyagi, Buddhi, 2008)

Points were taken from the DSC curve using PlotDigitizer® software. After the information was processed, it was made an integral and an accumulated integral of the curve. For this, the following equation was used:

$$integral = (T_{i+1} - T_i) * \frac{HF_{i+1} - HF_i}{2} * 1000 * \frac{60}{7} \quad (84)$$

Where $integral$ is in $J.Kg^{-1}$, which is the unit used in EnergyPlus, T_{i+1} and T_i is the temperature of two adjacent points, in ºC, HF_{i+1} and HF_i is the heat flux in two adjacent points, in $W.g^{-1}$, the additional part of the equation is conversion of units for EnergyPlus used units and the rate (7 $ºC.min^{-1}$) used in the experiment. The accumulated integral is just the sum of all the previous integrals.

Figure 22 presents the calculated enthalpy curve of the calcium chloride ($CaCl_2.6H_2O$):

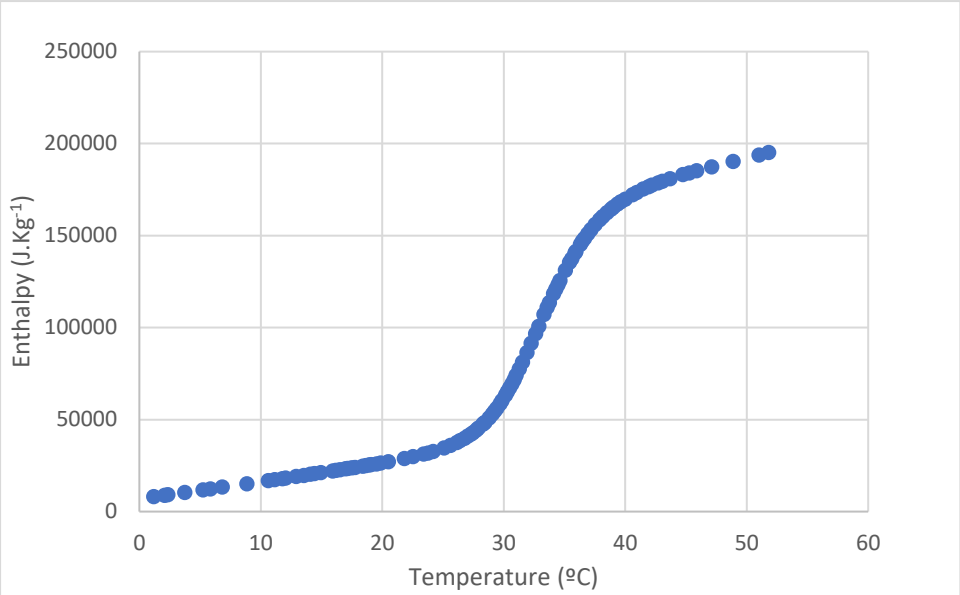

Figure 22 - Enthalpy curve of $CaCl_2(H_2O)_6$

The melting temperature of the calcium chloride in this experiment was 27.14 ºC, though the temperature usually used as reference for the melting temperature of the calcium chloride is 28 ºC (Kaygusuz, 1994).

The enthalpy curve of Bio PCM is given in the technical specification. It is used the BioPCM with melting temperature of 29 ºC (see appendix A.2.).

To be able to compare different melting temperatures, both enthalpy curves were shifted the necessary degrees. Enthalpy-temperature points introduced in EnergyPlus are in Appendix A.

Table 6 contains the other PCM properties:

Table 6 - PCM Properties

	Conductivity of the solid ($W.m^{-1}.K^{-1}$)	Conductivity of the liquid ($W.m^{-1}.K^{-1}$)	Specific heat ($J.Kg^{-1}.K^{-1}$)	Density ($Kg.m^{-3}$)	Latent heat ($J.g^{-1}$)
Calcium chloride	1.09	0.54	1757	1500	140
BioPCM	2.5	0.15	3350	1125	230

The tests made in EnergyPlus (besides the Control simulation, without PCM) were with the following melting temperatures and quantity: Calcium Chloride melting at 22, 25, 28, 31 (all with 1 and 2 Kg), BioPCM melting at 22 ºC (2 Kg), 25 ºC (2 Kg), 28 (1 and 2 Kg).

PCM quantity

It was tested all materials with 2 different weights (1 and 2 Kg) to check the importance of the quantity in the simulations. Furthermore, it was decided to put no more than 2 Kg, as the sleeping system would be too heavy to carry with ease.

Weather file

It was used the EnergyPlus file of Lisbon, for the 4 months of testing: November, December, January and February.

Timestep

It was utilised 60 timesteps per hour (1 per minute). This was decided because a detailed analysis of the night's system behaviour was necessary.

People Section:

In table 7, parameters of EnergyPlus people's section are shown:

Table 7 - Parameters in EnergyPlus People's Section

Parameter	Value
Sleeping bag occupancy time	23h to 07h
Occupancy	1 person sleeping (72 W)
Fraction Radiant	1
Mean Radiant Temperature Calculation Type	Zone Averaged
Air Velocity	0 $m.s^{-1}$

The occupancy time inside the sleeping system is 8 hours. It was decided to put them between 23h to 07h, which is a normal sleeping schedule in Portugal. The occupancy of the sleeping bag is only 1 person, as each sleeping bag studied in this project is made for 1 person only. The metabolic rate is 72 W for a person at sleep (ASHRAE 2013). Fraction Radiant, which is radiant fraction of sensible heat released by people in a zone, in this case the sleeping bag, must be 1 as the person is close to all the surfaces of the sleeping bag.

Boundary Conditions

Boundary Conditions of the outside of the sleeping bag surfaces are all in "Outdoors". Only the surface exposed to the ground has the "Ground" boundary condition. The sleeping system is wind exposed and it has no sun in the simulation.

Clothing

In the EnergyPlus simulation, the person has 1.0 clo in clothe ensemble, which is equivalent to be wearing trousers, a long-sleeved shirt, a long-sleeved sweater and a t-shirt.

Output variables

The most important output variables from EnergyPlus were the following: Zone Mean Air Temperature, to know the micro-climate temperature inside the sleeping system. Fanger, Pierce Two-Node and KSU Model output variables (such as PMV) to verify and compare the thermal comfort between different sleeping system conditions. In addition, CEN 15251 Adaptive Model outputs were chosen to see if the

conditions used in these simulations are acceptable or not in terms of these models. The European model was used because it was mostly made for naturally ventilated buildings, which is the closest to outdoor conditions.

4. Results and Discussion

In this section, all numerical and experimental results will be introduced and discussed.

4.1. Experimental

In the experimental part, a pre-analysis was done with the thermographic camera, to check the system and its different variables as well as to decide where the thermocouples would be installed in the system.

4.1.1. Pre-analysis with thermographic camera

In this analysis, the subject was wearing trousers, a t-shirt and sneakers. The subject was on his chest (back upwards). This was done in a temperature-controlled room with AC at the maximum ACH possible, and a fixed temperature of 20 ºC. The picture was taken 7 minutes after the subject was inside the sleeping system.

The first analysis made was beneath the sleeping bag (and above the sleeping mat). Figure 23 shows the upper torso of the subject:

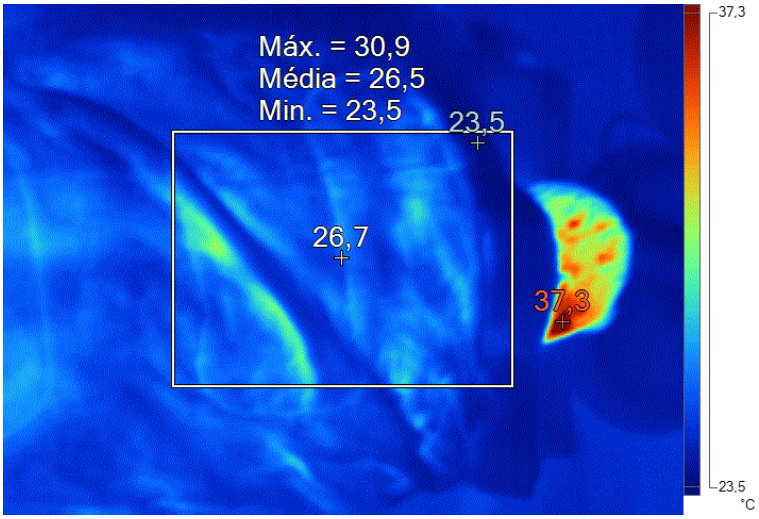

Figure 23 - Upper torso of the subject inside the sleeping bag (subject horizontally oriented with the head on the right)

In figure 23, it can be seen that the sleeping bag isolates well the body, as the temperature in it is about 26.5 ºC. The temperature of the subject's head is near 37 ºC which is in line with literature. Figure 24 presents the waist zone and legs of the subject inside the sleeping bag:

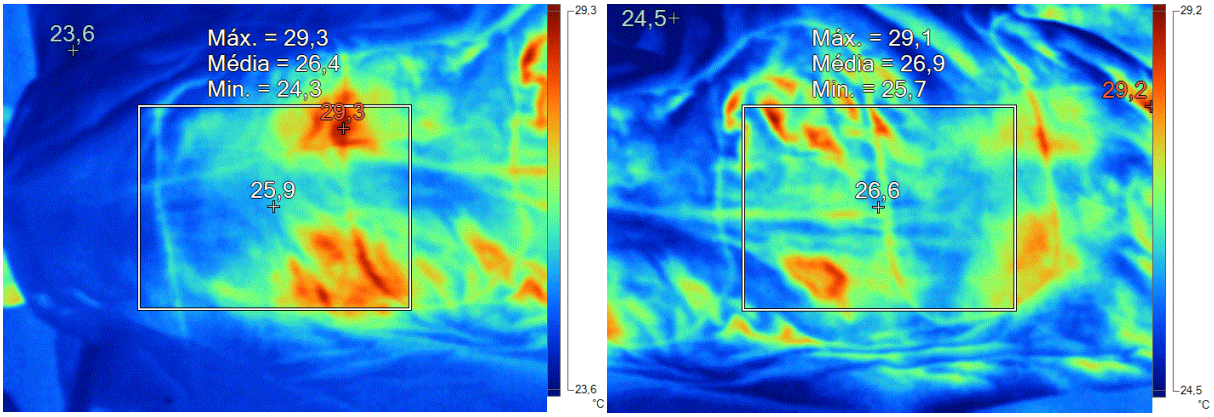

Figure 24 – Legs and waist of the subject inside the sleeping bag. Left: Legs zone. Right: Waist zone.

In figure 24, it can be seen the heat spread out through the inside of the sleeping bag, and as the sleeping bag has zones with more stuffing material than others, body heat is viewed from the outside of the sleeping bag in some zones, with temperatures above 29 ºC and an average temperature near 26.5 ºC. The waist zone muscles and fat, as well as the calves seem to dissipate more energy to the exterior.

After the first analysis with the sleeping bag, some analysis was done taking out the sleeping bag and seeing the temperature of the person that was inside the sleeping bag. The subject was inside the sleeping bag for 7 minutes, and then the sleeping bag was taken off to see the temperatures of the body. In figure 25, it can be seen the subject above the sleeping mat:

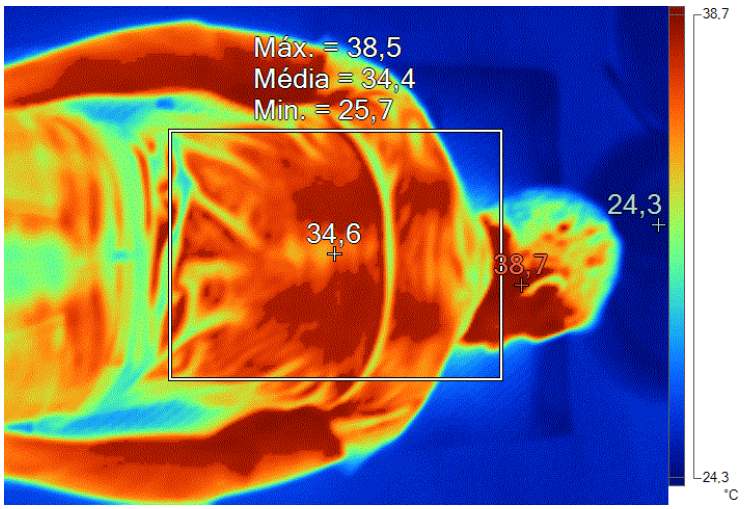

Figure 25 - Upper torso of the subject above the sleeping mat
(subject horizontally oriented with the head on the right)

In this upper torso part, it can be observed that the t-shirt already had a temperature of 32.1 ºC, and the head temperature was 38.7 ºC. The arms are between the temperatures described earlier, near the head temperature but lower. It can be seen some colder parts between the upper back and the waist of the subject. This has to do with the fact that the t-shirt of the subject was larger in this area, having some infiltrated air in this zone, which is around 26 ºC from the surroundings.

In figure 26, the intermedium part of the body was analysed:

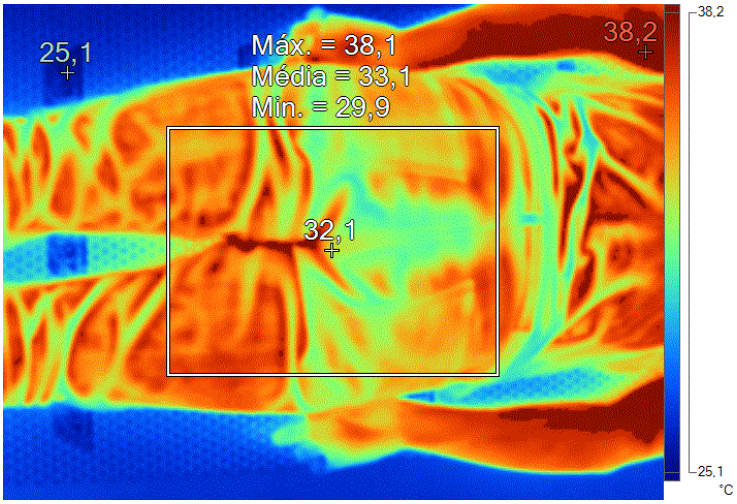

Figure 26 - Waist Zone of the subject above the sleeping mat

It can be observed in figure 26 that the average temperature is lower, which makes sense because the upper torso contains all the vital organs of the body. Also, the rectal temperature can be observed, which is about 38 ºC. The thighs seem to have major importance in the dissipation of body's heat, as they have a relative high temperature. The thighs have a temperature above 34 ºC. It is reasonable, as they are one of the biggest muscles in the human body.

Looking now at the lower legs zone (figure 27):

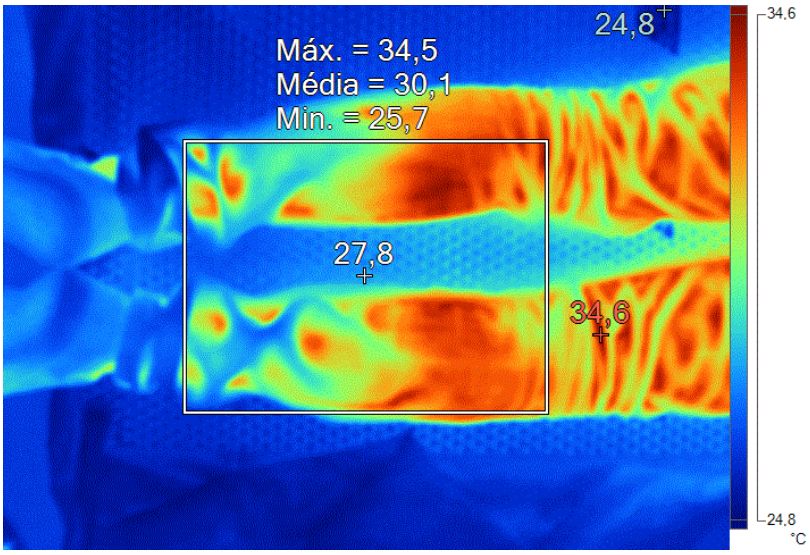

Figure 27 - Legs Zone of the subject above the sleeping mat

In figure 27 it can be seen a clear drop of temperature in the ankles and foot of the subject. This is the part that is already in balance with the surroundings, and it only has a temperature of about 26ºC. In addition, the part of the ankles is also cold, as cold air is trapped inside the subject's trousers.

After the subject left the sleeping system, it was pictured the thermal impression left on the sleeping mat (figure 28):

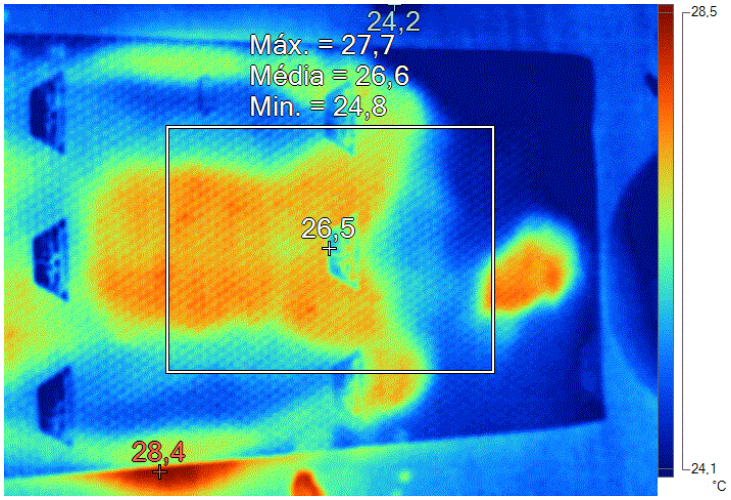

Figure 28 - Upper torso thermal impression in the sleeping mat

It can be seen in figure 28 a clear thermal impression left by the body, which indicates that the subject heats up fast the sleeping system (only 7 minutes in the sleeping mat) and the energy leaving the body is stored by both components of the sleeping system. In this case, it can be seen the thermal impression of the head and torso of the subject, which stays 3.1 ºC above the other zones with no contact to the body, in this case 27.7 ºC to 24.8ºC.

The thermal impression left by the waist zone is in figure 29:

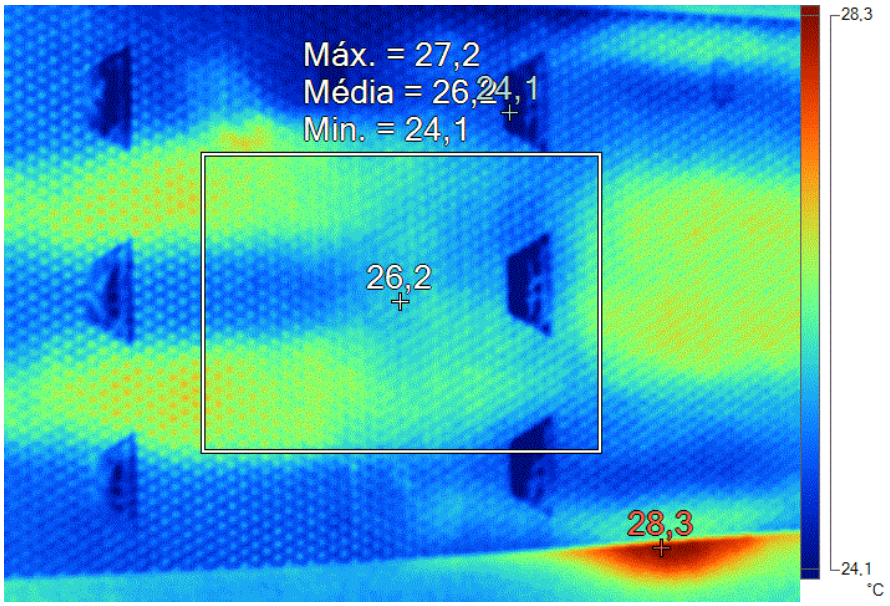

Figure 29 - Waist zone thermal impression in the sleeping mat

It is clearly shown in figure 29 that the waist zone does not leave an intense thermal impression of the body. However, the thighs do, which is in line with the comments previously made of the thigh's energy production.

Figure 30 presents the thermal impression in the legs zone:

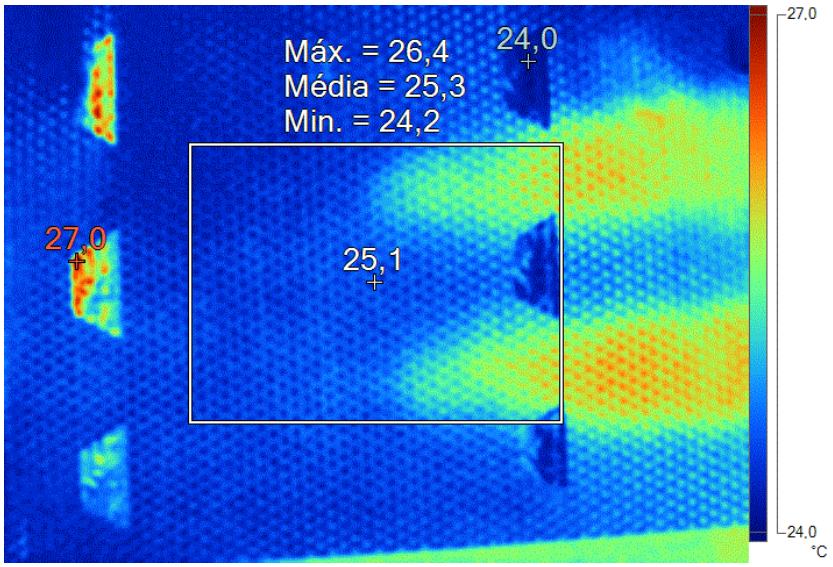

Figure 30 - Legs zone thermal impression in the sleeping mat

In figure 30, it can be observed that the lower part of the legs leave no thermal impression on the sleeping mat, which makes sense as the legs in this zone are at the same temperature of the sleeping mat.

The following picture (figure 31) is taken 5 minutes after the previous ones:

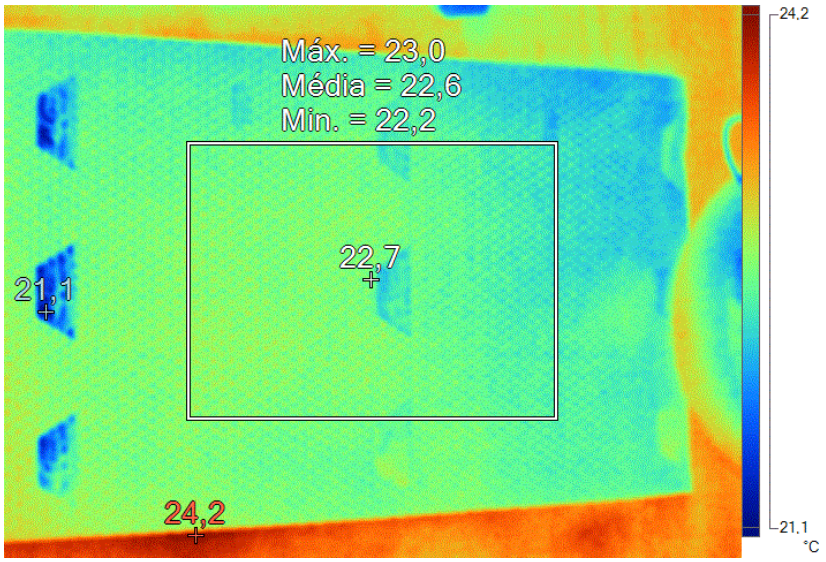

Figure 31 - Thermal impression 5 minutes after the subject left the sleeping mat

It is clearly seen in figure 31 that the heat had already been dissipated by the surroundings, with no thermal impression of the human body in the sleeping mat.

4.1.2. Results of the 8-hour experiment

The conditions of the room and the sleeping system were defined in section 3.1.3..

Figure 32 presents the temperatures from the night without PCMs:

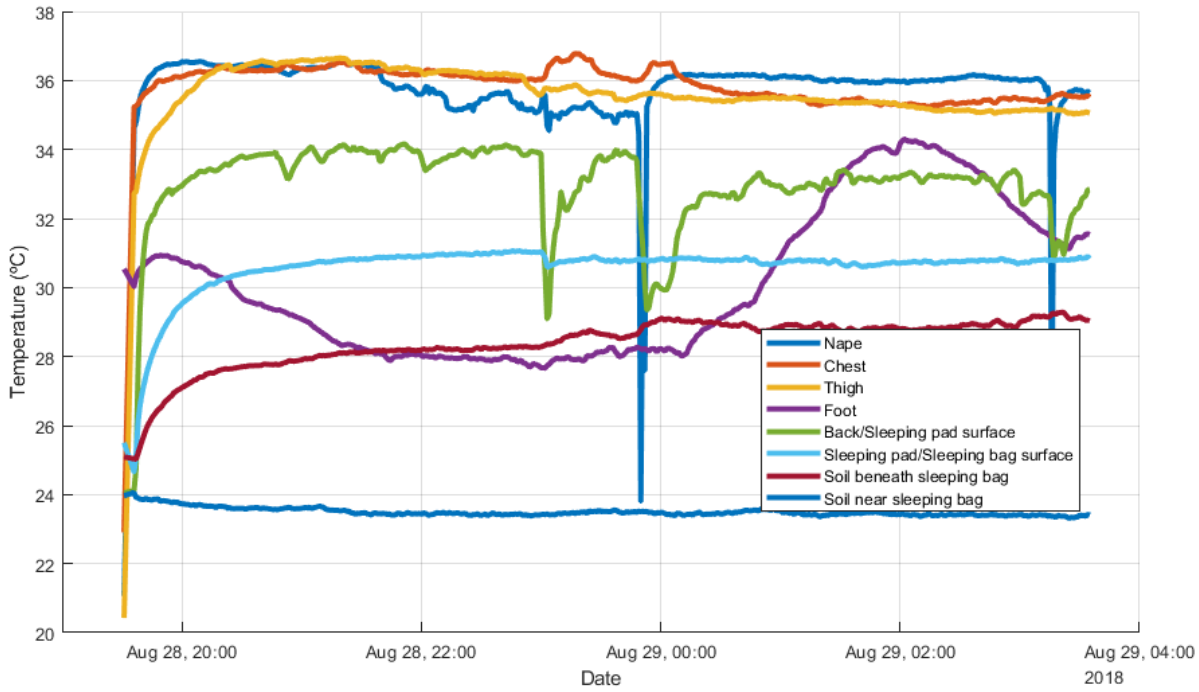

Figure 32 - Temperature of the system without PCMs

It can be noted that the highest temperatures are clearly from the nape, chest and thigh. After these three, the 4th highest mean temperature is the sleeping pad surface where there is contact with the subject's back. It is followed by the surface between the sleeping mat and the sleeping bag, then the foot skin temperature, soil (ground) beneath the sleeping bag and lastly the soil (ground) near sleeping bag.

There are some perturbations in temperature, which can be seen in abrupt negative peaks. This is due to a detachment in some of the thermocouples connected to the subject's skin, particularly the nape. These detachments were provoked by random movements of the body, for example back movement in the sleeping mat, or head movement. When something like this occurred, another aluminium tape would be put in the thermocouple and a reattachment would be made to the skin.

It can be verified that the ground beneath the sleeping bag effectively warms up more than the ground with nothing above it. There is a heating of 4 ºC of this ground comparing to the ground with nothing above, right after the half-hour.

The following graphic is from the night with PCMs (figure 33):

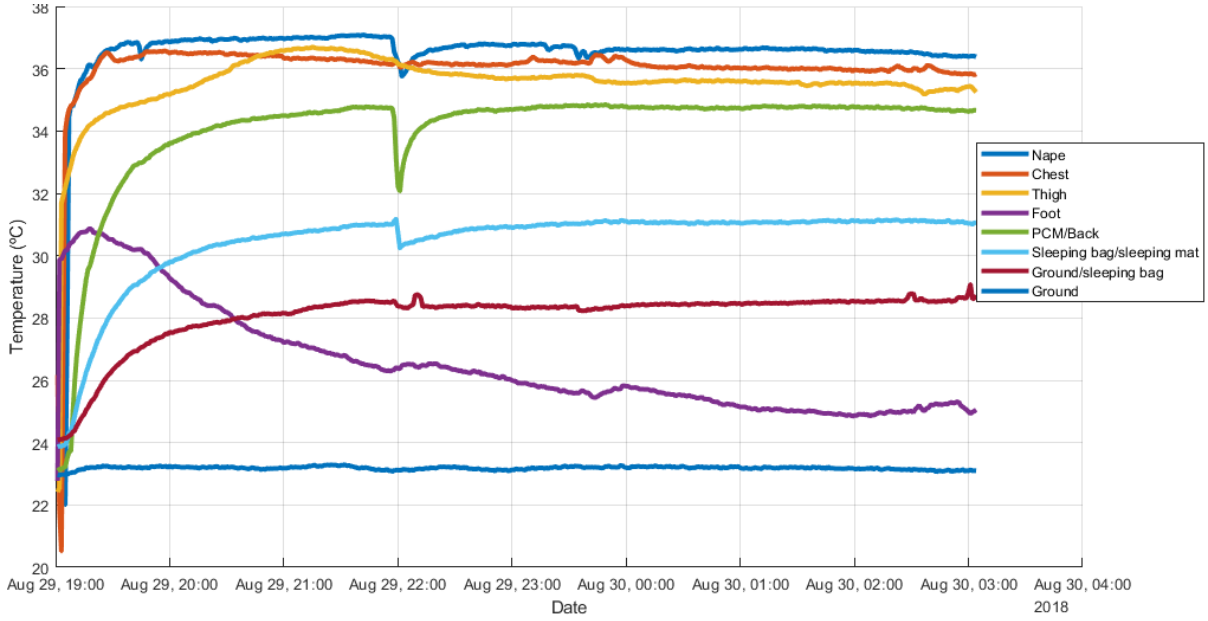

Figure 33 - Temperature of the system with PCMs

It can be perceived in the figure above that the 4 highest temperatures are still the same, although there is a bigger gap between the first three, which are nape, chest and thigh, in comparison from the figure without PCMs.

The datalogger temperatures, which measured the room temperature (indicated as exterior air temperature) and the sleeping system mean air temperature (indicated as interior air temperature) were measured and gave the following results (figure 34):

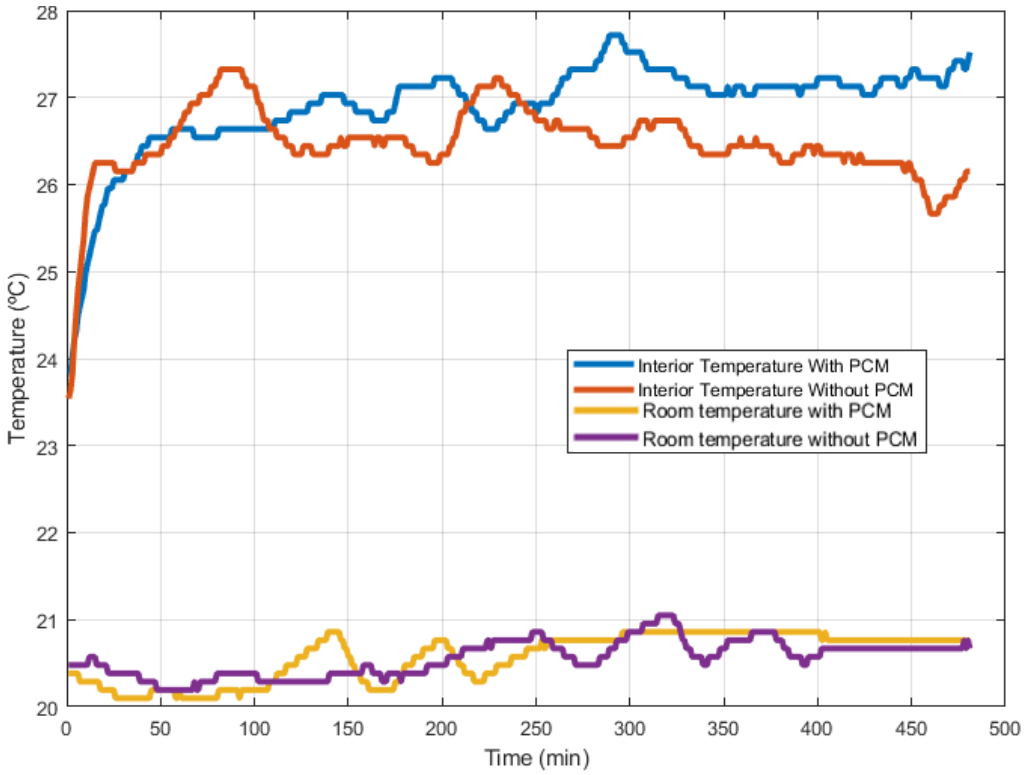

Figure 34 – Interior Sleeping System Temperature (orange and blue lines) and Room Air Temperature (yellow and purple lines)

It can be noticed in the figure above that room temperature did not vary much in both nights, which is favourable to have reasonable comparisons between other temperatures measured during both nights.

About interior sleeping system air temperature, the transient without PCM is always faster than the transient with PCM, which makes sense since PCMs absorb energy that is coming out of the body. Hence, it takes more time to heat up the rest of the sleeping system. After the first 2 hours of experiments, the system with PCMs is almost always above the sleeping system without PCMs. Furthermore, from the middle of the night onwards, interior air temperature with PCM is higher than without PCM with a difference of about 1 ºC on average.

The sleeping system interior air temperature is assumed to be equivalent to the Zone Mean Air Temperature.

Comparing the temperatures of the Ground inside the test-room (figure 35):

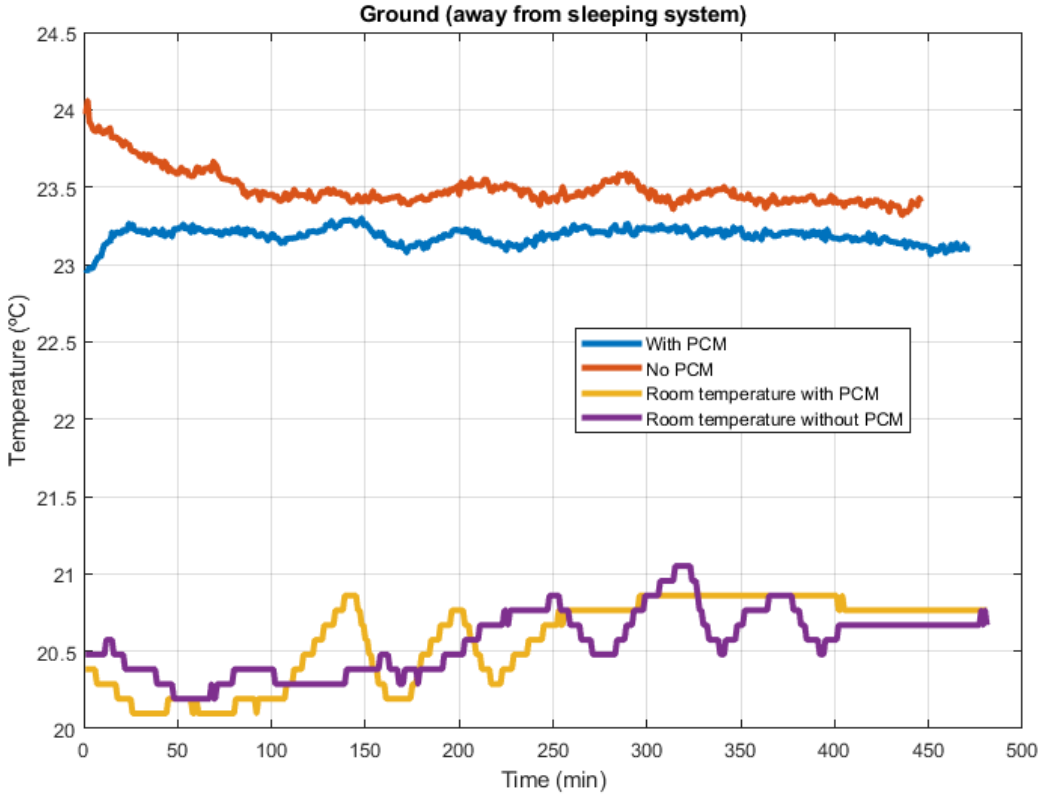

Figure 35 - Ground Room temperature away from sleeping system (orange and blue lines) and Room Air Temperature (yellow and purple lines)

It can be observed that the temperatures are not too different along the night. The reasoning behind the temperature being so close is because the exterior temperature for both days is very similar, and the AC was put at the same temperature during the night and 4 hours before the test. This temperature was measured to compare with the temperature of the ground below the sleeping bag. Also, to check if there was not much difference between both nights, to be able to compare the other measured temperatures.

At the beginning, the temperature has a difference between both nights of about 1 ºC, but it fades away as time goes by, having a difference of about 0.2 ºC at the end of the night, with temperatures constant at around 23.3 ºC. This difference can be related with distinct thermal gains from the ground in the different days of the experience.

Comparison of temperatures from both nights

As seen previously, room temperature of both nights and Ground temperature was similar, so a comparison can be made between the temperatures of the sleeping system and subject's body with and without PCM.

Comparing the temperatures of the Ground below the sleeping bag (figure 36):

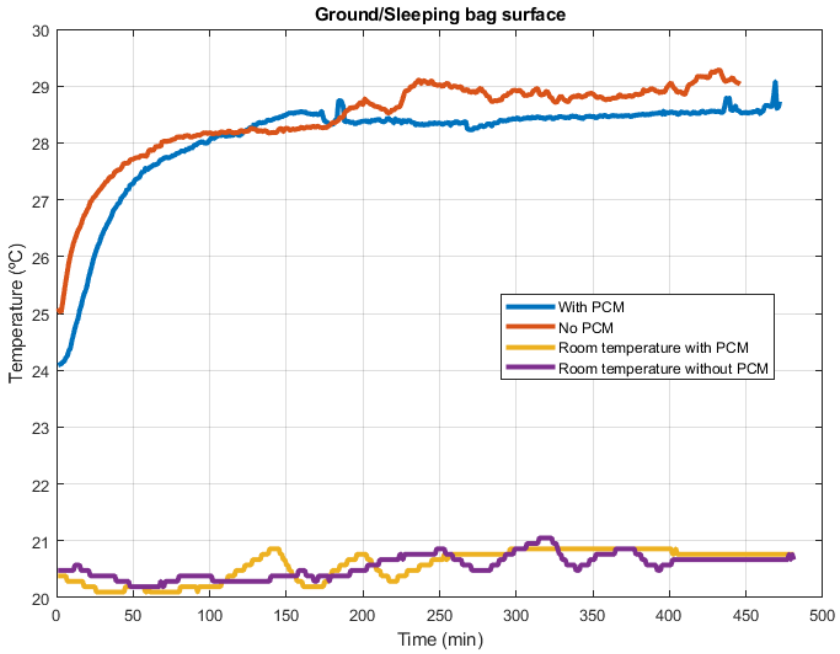

Figure 36 - Ground temperature below the sleeping system (orange and blue lines) and Room Air Temperature (yellow and purple lines)

It can be seen in figure 36 that at the start of the night there is a difference in temperature of 1 ºC. After some time of the test, the ground heats up until 28-29 ºC. It can be observed that the Ground temperature is maintained at a temperature of 28 ºC when PCMs are present in the test, which is lower than the temperature of the sleeping system without PCMs, possibly derived from the absorption of additional heat from PCMs as well as from the fact that this is the melting temperature of the PCM, thus remaining a more constant temperature throughout the night.

The temperature variation throughout the night of the interior sleeping bag surface with contact to the bottom sleeping pad surface is the following (figure 37):

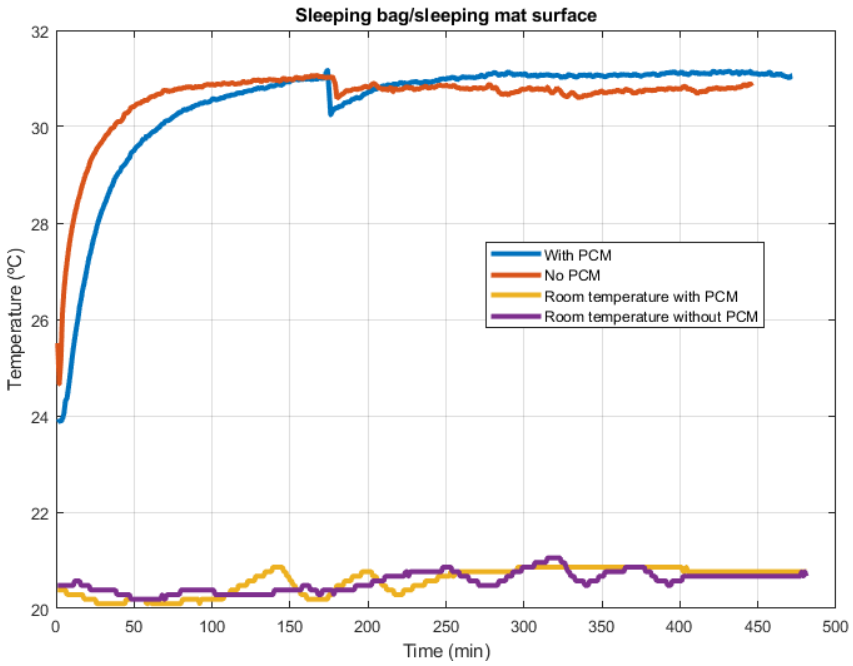

Figure 37 -Sleeping bag/sleeping mat surface temperature (orange and blue lines) and Room Air Temperature (yellow and purple lines)

In figure 37, it can be seen the slower transient of the PCM sleeping system, as PCMs use energy from the body to heat up and change phase. Furthermore, it can be observed that the sleeping system with PCMs is hotter and remains constant after the 3 first testing hours.

About the thermocouple attached to the sleeping pad surface, with the contact of the back (figure 38):

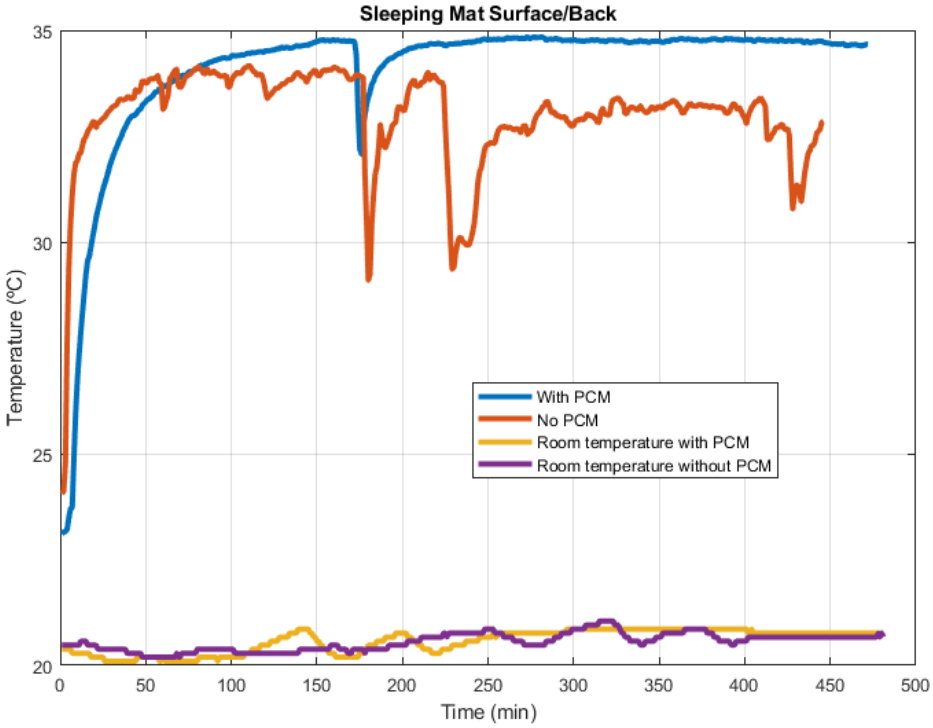

Figure 38 - Sleeping mat surface and Back temperature (orange and blue lines) and Room Air Temperature (yellow and purple lines)

In figure 38, it is important to notice that this temperature is the closest temperature to the PCMs, as it is attached to the aluminium that contains the PCMs and is a good conductor (in the night without PCMs, thermocouple is attached to the sleeping pad only), so it represents accurately the temperature inside the PCMs. It can be seen the time lag from the sleeping system with PCM in the first hour of testing, and it maintains a higher temperature than the sleeping system without PCMs throughout the night.

It can also be observed that temperature of the sleeping system without PCMs is erratic due to the movement of the body (in this case, the back), which makes the temperature oscillate. Nevertheless, it is a lower temperature without PCM for majority of the night, with a higher steady-state temperature of the PCM sleeping system of more than 2 ºC.

The nape skin temperature variation was the following (figure 39):

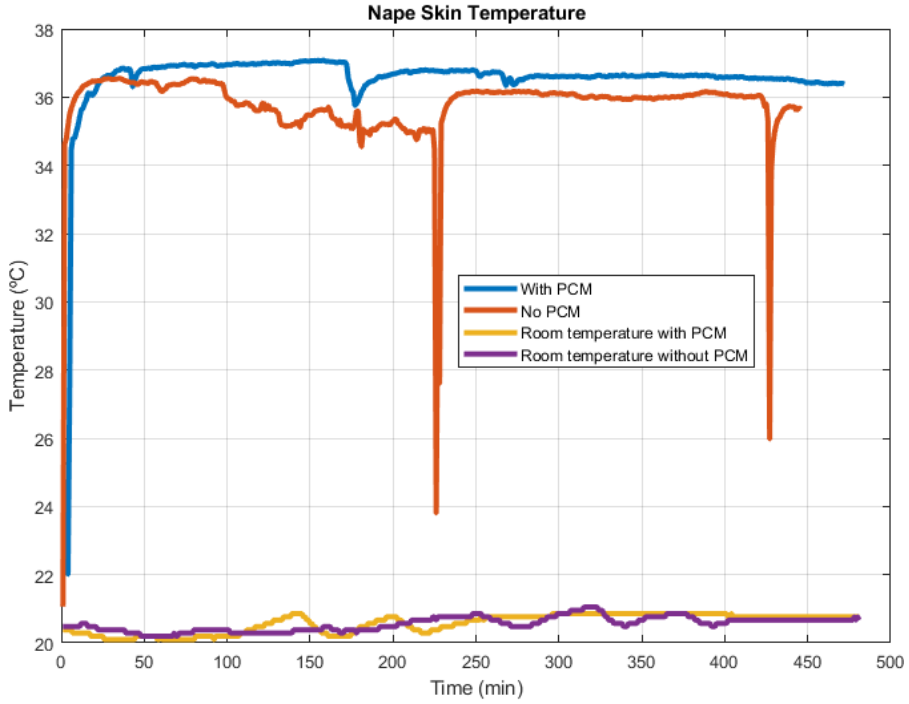

Figure 39 - Nape skin temperature (orange and blue lines) and Room Air Temperature (yellow and purple lines)

In figure 39, the nape skin temperature transient is analogous to the transient of the overall sleeping system, as the existence of PCMs in the system makes it slower to heat up in the 1st hour.

Even though there are some perturbations in the non-PCM sleeping system, due to detachment of the nape's thermocouple and respective reattachment, nape skin temperature of PCM-sleeping system remains around 0.5 ºC above the non-PCM-sleeping system throughout the night.

About the chest skin temperature (figure 40):

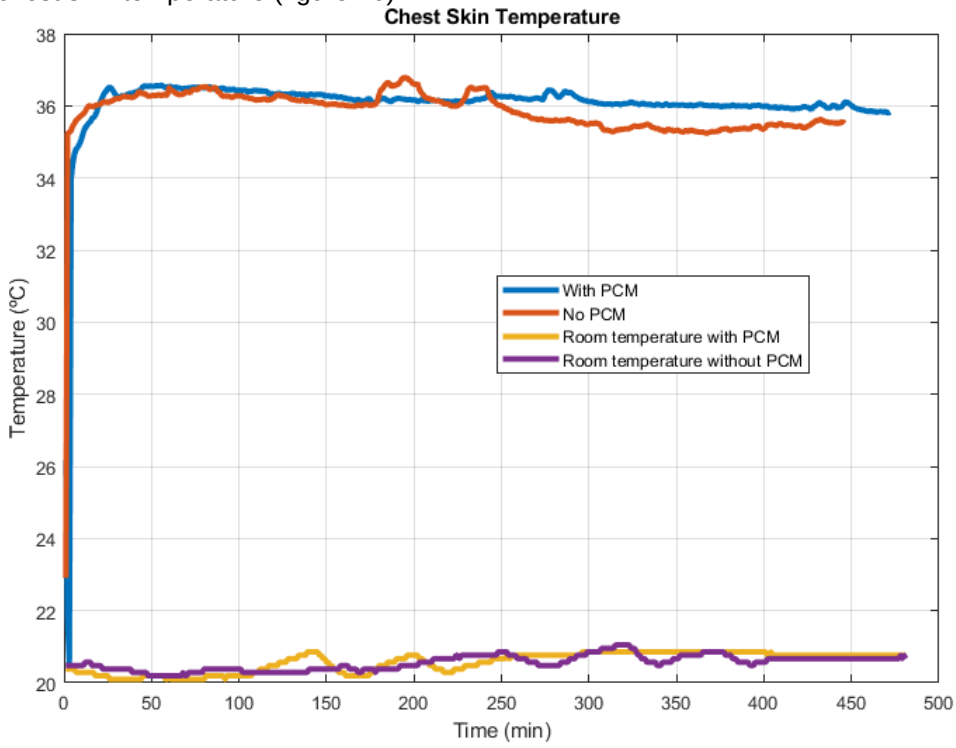

Figure 40 - Chest skin temperature (orange and blue lines) and room temperature (yellow and purple lines)

After the delayed transient of the PCM-sleeping system, it can be noted a similar temperature until half of the test, where the chest temperature seemed to decrease almost 1ºC for the non-PCM sleeping system and a less variant temperature in the PCM-sleeping system occurred. This is a significant variation.

About the thigh skin temperature, the following variations occurred (figure 41):

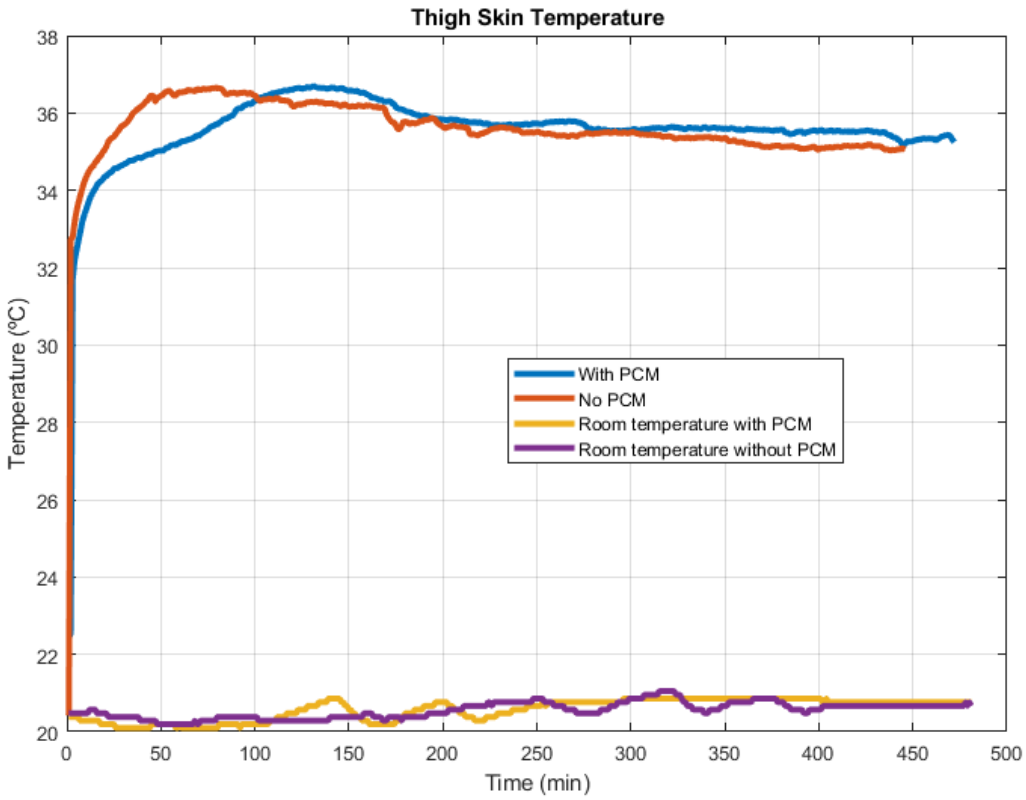

Figure 41 - Thigh skin temperature (red and blue lines) and room temperature (yellow and purple lines)

In this case, even though the thigh does not have PCMs underneath it, it is only a few centimetres short of it. This explains the transient being slower in the PCM-sleeping system. After the first one and half hours of the test, there is not a large difference in both systems, with a slight bigger temperature for the PCM-sleeping system. Both temperatures plateaued between 35 and 36 ºC.

About the foot skin temperature variation (figure 42):

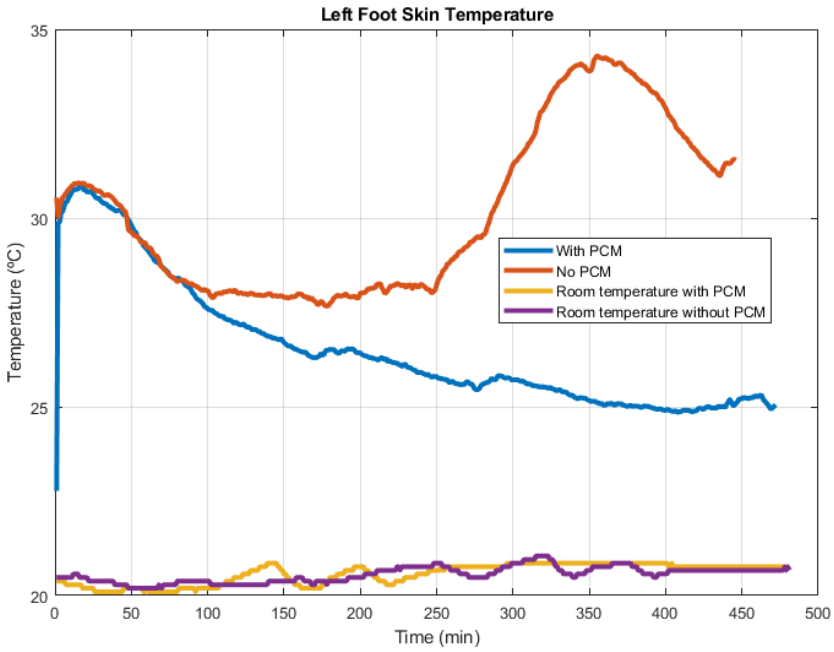

Figure 42 - Left foot skin temperature (red and blue lines) and room temperature (yellow and purple lines)

It can be seen in figure 42 that the foot skin temperature has the same behaviour in the first testing hour, but after that there is a difference in the behaviour of both experiments. PCM-sleeping system declines temperature until the end of the test, whereas non-PCM-sleeping system gets higher at half of the test. It is important to refer higher frequency of movement of the subject's legs in the non-PCM sleeping system test, which may have helped to increase foot temperature and increase variation in temperatures from both nights. Also, PCMs are only at the upper part of the body, so they don't seem to have made a big difference in this body part. The humidity variations throughout the experiment were the following (figure 43):

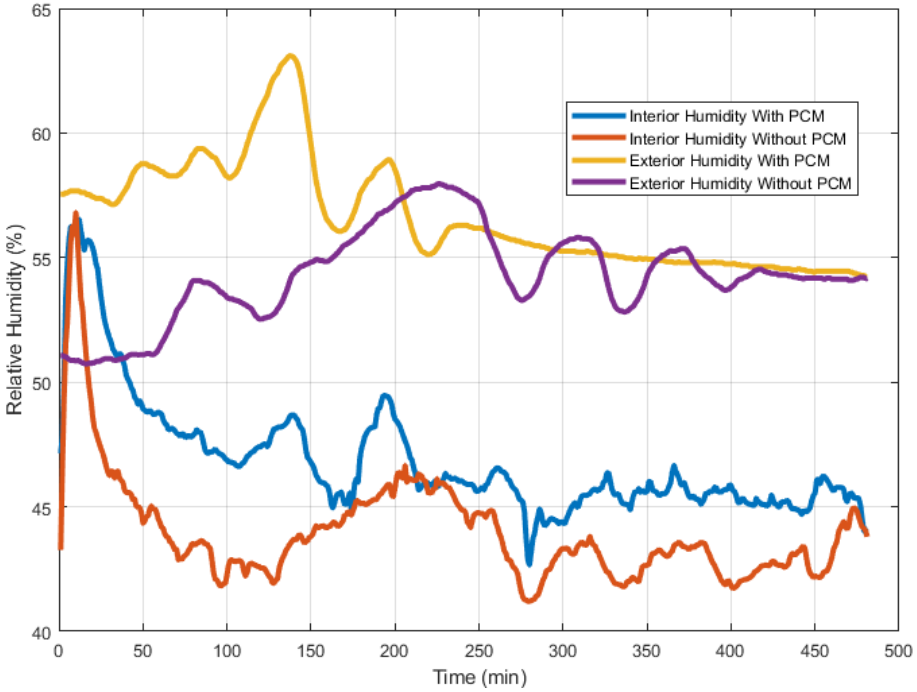

Figure 43 - Humidity variation in the experiments

It can be seen in figure 43 that the exterior humidity at the beginning of the experiment is different in both nights, with a difference of about 5% of Relative Humidity (RH). After the initial hours, it begins to intersect until it reaches the same point of about 55% in the final moments of the night. The interior humidity behaves in the same way in the initial minutes, getting higher, and then the PCM sleeping-system takes longer to diminish humidity, staying higher than the non-PCM sleeping system for the rest of the night. It is hard to take any conclusions from this data, as the humidity variation inside the sleeping system follows the humidity in the room, both with and without PCMs.

4.2. Numerical

Several simulations were made in EnergyPlus to verify the importance of different properties in the efficiency of the sleeping system (consisting of sleeping bag, sleeping mat and PCMs when they are present), such as PCM properties or outside weather conditions. Properties and characteristics of the simulations done are available in the methodology (see section 3.2.).

4.2.1. Model Validation

Table 8 shows the changes made in EnergyPlus for the model validation:

Table 8 - Properties used in EnergyPlus for model validation

Properties	Changes
Weather file	Temperature and Humidity equal to room air conditions, in both days of the experiments (28 and 29 August)
Clothing insulation	For t-shirt, walking shorts, ankle-length athletic socks and men's briefs totalized 0.22 clo
Ground Temperature	According to Ground thermocouple, an average for the night was done. It was used 23.5 ºC for night without PCMs, and 23.3 ºC for night with PCMs
ACH	The AC was in medium cooling power, so 11.20 ACH was introduced in EnergyPlus model
PCM	The night with PCM was done with 1 Kg of hexa-hydrated calcium chloride, with melting temperature of 28 ºC.
1st night test hours	19h30 to 03h30 (8hours total)
2nd night test hours	19h05 to 03h05 (8 hours total)
Wind and Sun Conditions	No Wind and No Sun

It is important to refer that only the Zone Mean Air Temperature can be validated, as it is not possible to check various temperatures of the body in EnergyPlus.

Without PCM

The values of Zone Mean Air Temperature for the night without PCMs are the following (figure 44):

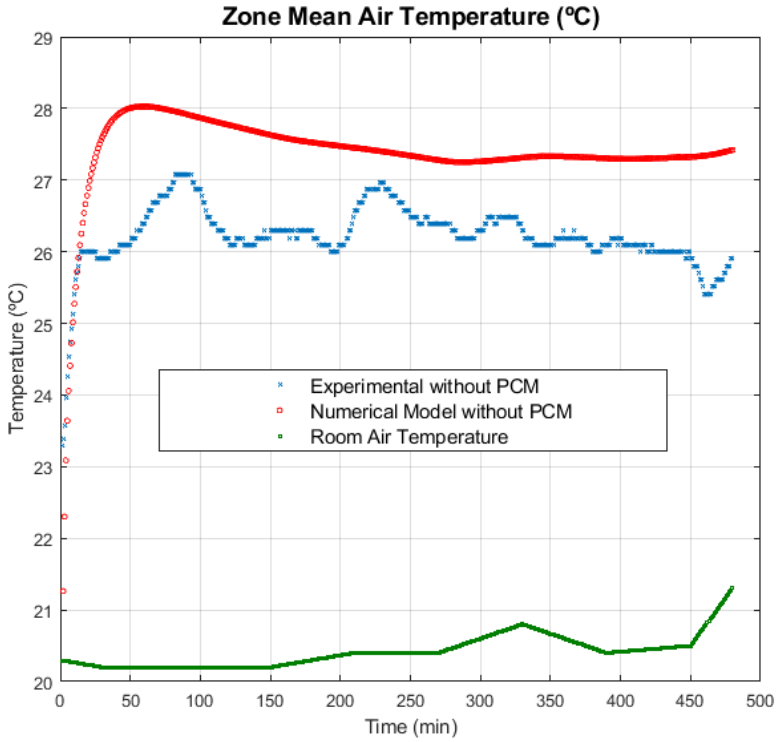

Figure 44 - Zone mean air temperature without PCM for both experimental and numerical simulations

It can be noted several things in figure 44: the transient behaviour seems to be similar in both models, in terms of variation of temperature per variation of time, as both experimental (blue) and numerical (red) lines have equal slopes, in the first 20 minutes of test. Although this is true, the numerical model assumes an initial temperature below the experimental one but assumes close values to the experimental temperature after the first 5 minutes, and the numerical model takes 20 more minutes to get close to the steady-state temperature. The steady-state response of the numerical model is always higher than the steady-state temperature of the experimental model. On average, there is a difference of 1.19 ºC, with a maximum difference of 1.93 ºC. The Root Mean Square Error (RMSE) is 1.25 ºC. There can be various reasons for this difference: firstly, the fact that the sleeping bag is open laterally to let thermocouples inside the sleeping bag, which is very hard to accurately model in EnergyPlus. Secondly, the movement of the arms and legs of the subject in the experimental model makes the system lose energy to its surroundings, as colder air enters the sleeping system due to this. Thirdly, it can be because of the way the sleeping system is positioned in the test room, as the walls dissipate energy that is not accounted in EnergyPlus model. Finally, it was assumed that the position of the datalogger inside the sleeping system was simulating the zone mean air temperature, which might not be true. It was in the centre of the waist, but the zone mean air temperature could be situated higher or lower in relation to the body.

It can be important to refer again that the datalogger accuracy is +- 0.53 ºC, which means that this error is on average just 2.25 times greater than the datalogger accuracy. For all the reasons stated and for the purpose of this study, the magnitude of this error was considered acceptable.

With PCM

The values of Zone Mean Air Temperature for the night with PCMs are the following (figure 45):

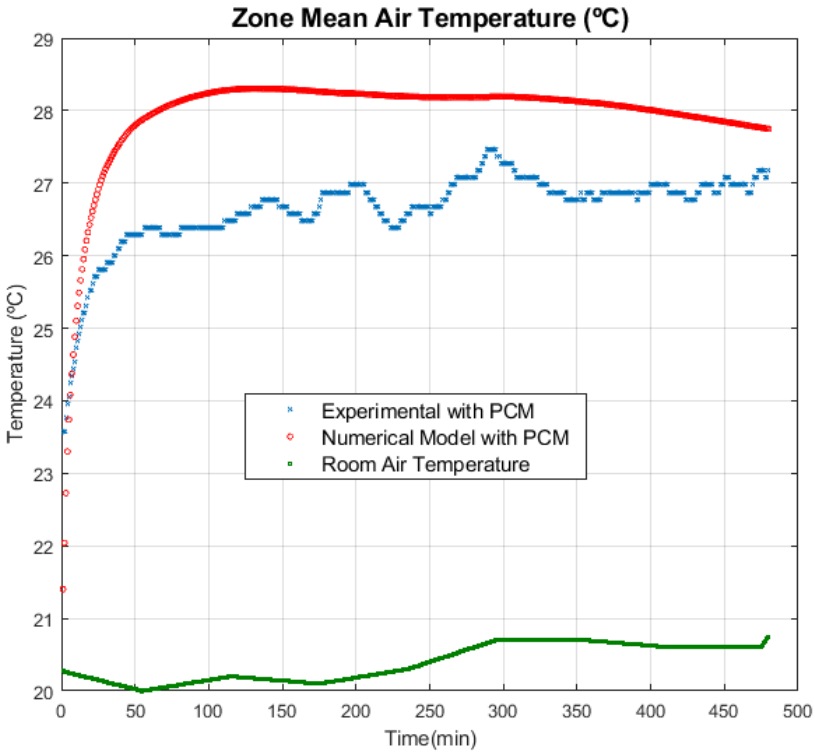

Figure 45 - Zone mean air temperature with PCM for both experimental and numerical simulations

In terms of validation of the sleeping system with PCM, in this case 1 Kg of hexa-hydrated calcium chloride, both models have similar transient time, as both models get to the steady-state temperature at about the first 60 minutes of the test. However, the variation of temperature per variation of time is higher in the numerical model.

In this case, the steady-state temperature of the numerical model is also higher, which is expectable due to the same reasons stated in the sleeping system without PCM. In this case, the average difference of steady-state temperature is 1.34 ºC and the maximum difference in steady-state temperature is 1.89 ºC. The Root Mean Square Error (RMSE) is 1.35 ºC.

It can be noted that there is a higher variability in the experimental model, which is expectable due to perturbations in the system, such as movement of the body and sleeping system, and consequently more fresh air going into the sleeping system. This magnitude of error is acceptable for the study at hand and the system with PCMs was also considered validated.

4.2.2. Particular night in January

It was decided to do check the results of the night between 8-9 January, from 23h to 07h. It was chosen this night because in the EnergyPlus weather file this is one of the coldest nights in this weather file, as can be seen in figure 46:

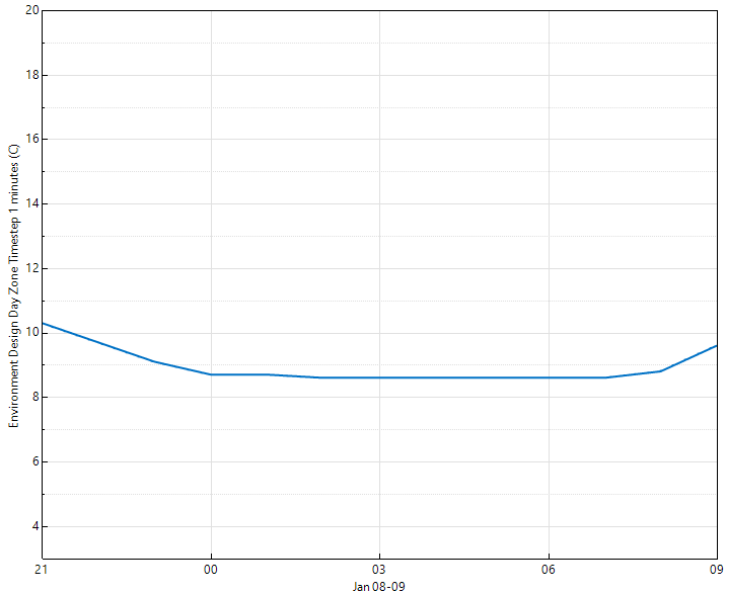

Figure 46 - Outside Air Temperature of 8-9 January night

As can be seen in figure 46, the average temperature in this night is less than 9ºC.

The outdoor Air RH(%) in this night is the following (figure 47):

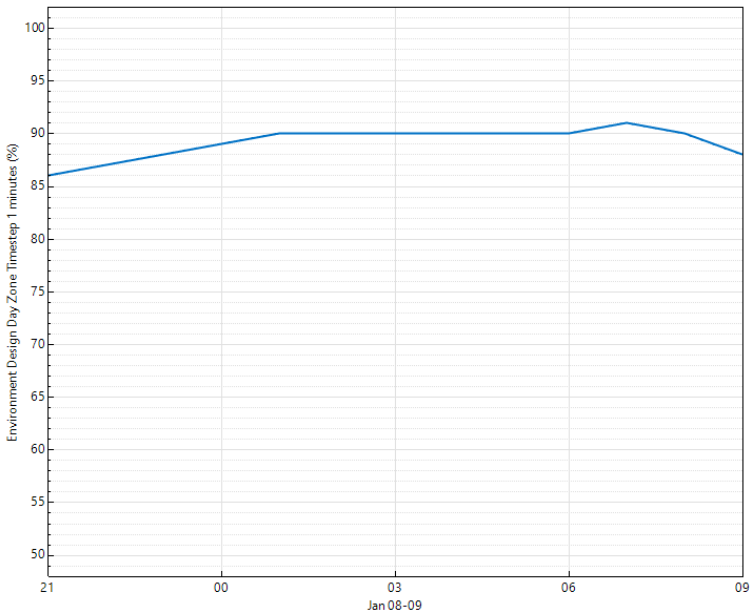

Figure 47 - Outside Air humidity in 8-9 January night

There is a high outside Air humidity in this night, with an average value around 90%.

The result given of the Zone Mean Air Temperature, when the sleeping system is without PCMs versus when it has PCMs is presented in figure 48 (the PCM is hexa-hydrated calcium chloride):

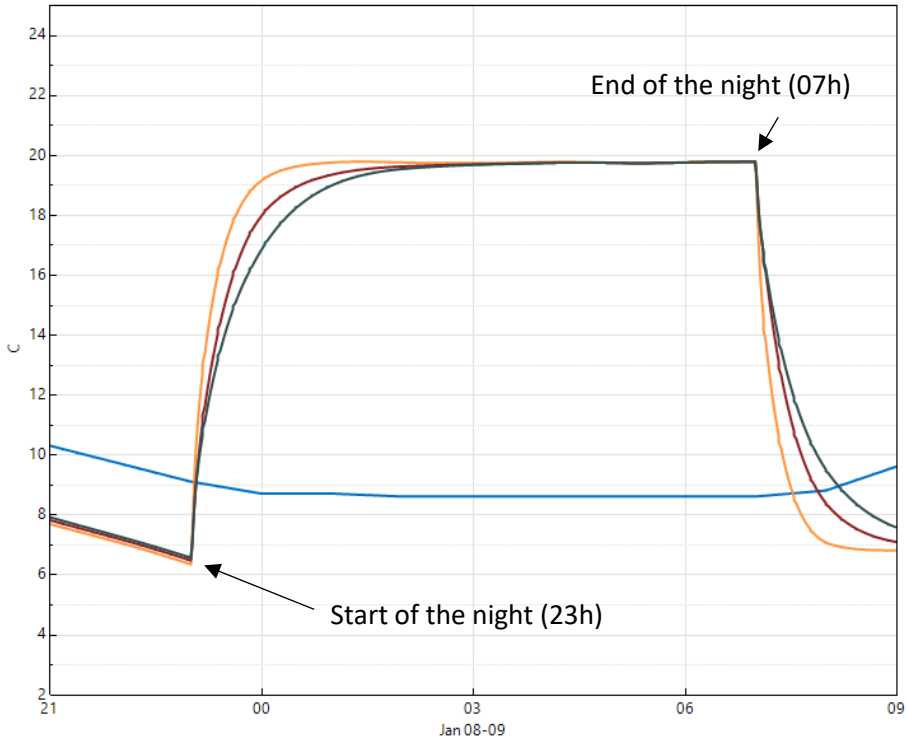

Figure 48 - Zone Mean Air Temperature. Blue: Outside Air Temperature. Orange: Sleeping system without PCMs. Red: Sleeping system with PCM25-1 Kg. Grey: Sleeping system with PCM25-2Kg.

As can be seen in figure 48, from 23h to 07h, hour that is defined as the person being inside the sleeping bag, the inside zone mean air temperature is always warmer than without sleeping bag, except for the first few minutes when the person warms up the sleeping system. It is important to refer the Ground is defined to have 10 ºC at 0.5 m depth and hard limestone is beneath the sleeping system, hence the beginning of the night with less temperature than the air-dry bulb temperature.

It is possible to observe that with PCM (in this case PCM with melting temperature of 25 ºC) takes much longer to warm up to the steady-state temperature without PCMs. So, PCMs take longer to reach the steady-state temperature that the sleeping system without PCMs reaches. In other words, the system with PCMs gets phased in time in relation to the system without PCMs. After this, in the following hours of sleep, in these conditions of temperature and humidity (low temperature and high humidity, see Figures 46 and 47) there is no significant difference between both systems, with and without PCM, although with PCMs the steady-state is slightly higher. It can also be seen that when the mean zone air temperature cools down after the person leaves the sleeping system (after 07h), the PCMs make the sleeping system decrease temperature slower. This makes sense, because it is the latent heat that PCMs absorbed when the sleeping system was warming up, now gets released also with a delay in time. There is not much advantage in this case though, the person is not in the sleeping bag to take advantage of this situation.

According to Muzet et al. (1984), this microclimate temperature would give frequent nocturnal awakening to the subject.

For thermal sensations scale, it is reminded that EnergyPlus uses a continuum approach to these scales. In other words, it does not round the results given. For example, Fanger scale is from -3 to 3, from “Cold” to “Hot”, respectively, with a 7-point scale (only integers). In this case, there are numbers with decimal digits, because EnergyPlus does not round to the closest integer neither does it have a maximum for these scales used (Pierce Two-Node Model, Fanger and KSU).

In terms of Predicted Mean Vote (PMV) in Fanger thermal sensations scale, the results for this night were the following (figure 49):

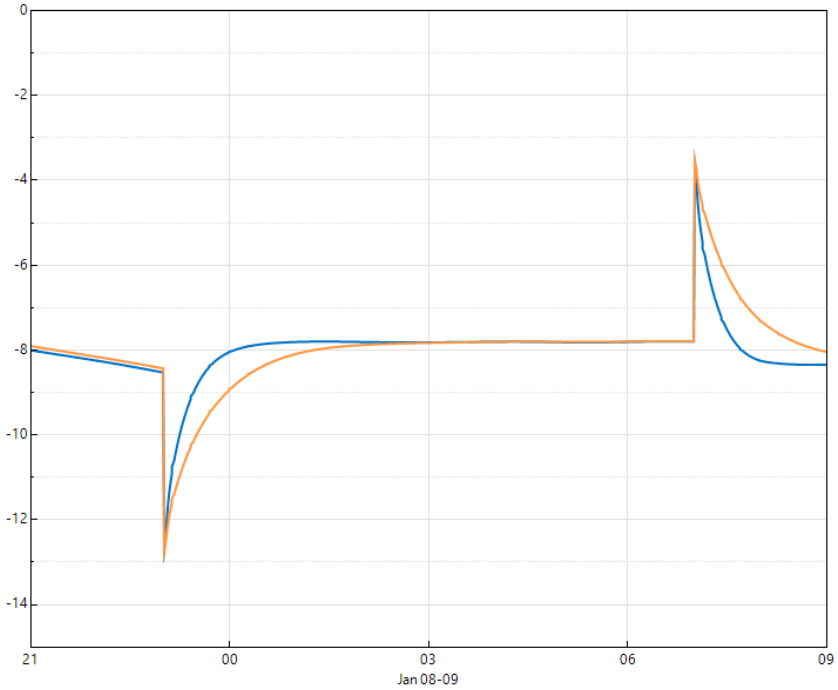

Figure 49 - Fanger PMV. Blue: Sleeping system without PCMs. Orange: Sleeping system with PCM25-1 Kg.

It can be seen that the thermal sensation scale has a minimum in the first few minutes of the night, which is when the person goes to the sleeping system. In this case, the Fanger PMV is close to -13, which would be in the category “Too Cold”, either with PCM or without PCM. It can also be seen that a steady-state of thermal index is reached more rapidly without PCM, which is in line with the previous graphs, as the PCM system has a higher transient time until it gets to the steady-state than the system without PCMs, and it also takes longer to cool down the sleeping system after 07h in the morning, when the person is out of the sleeping system. It can be concluded that this scale, in these conditions of temperature, humidity and occupancy has the same trend as the zone mean air temperature.

As the PMV is always lower than -3, it is obvious that 100% of the people would be discomfortable in this situation (the value of Percent People Dissatisfied, PPD). This can be due to various reasons, but one of them could be the fact that this sleeping bag is made for temperatures around 20 ºC, which is

considerably higher than the outdoor air drybulb temperature in this particular night (around 9 ºC). Furthermore, it is important to refer that this scale was not made for sleeping systems in outside conditions, so it makes sense that it would be a discomfortable night in that perspective.

The Pierce Two-Node Model Effective Temperature (ET) PMV is the following (figure 50):

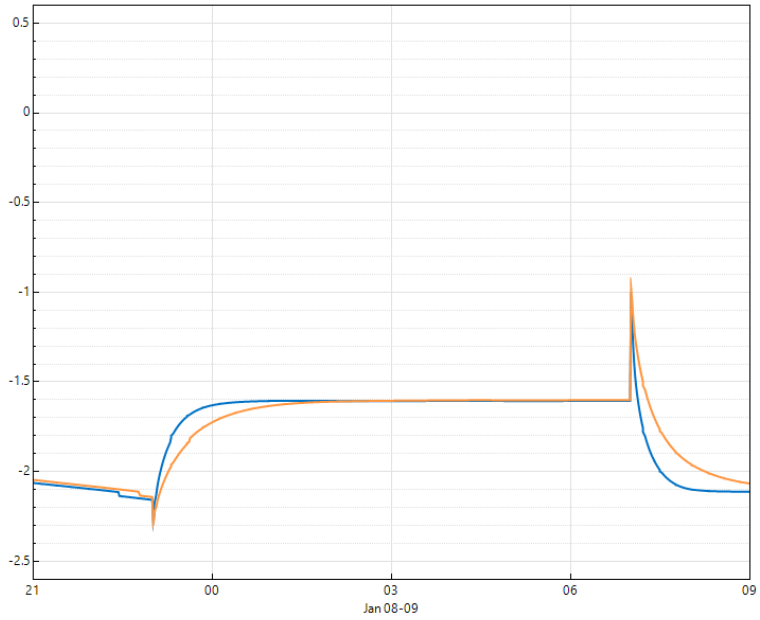

Figure 50 - Pierce Model Effective Temperature PMV. Blue: Sleeping system without PCMs. Orange: Sleeping system with PCM25-1 Kg.

It can be seen the same thing in this scale as in the Fanger one, such as the delay in time of the PCM curve, both in the warming and the cooling of the sleeping system. The important remark in this scale is that it does not represent it as cold as in Fanger scale, this time it is only considered “Cold” at the beginning of the night and the steady-state of both sleeping systems is between “Cool” and “Slightly Cool”. This has to do with the importance given to both temperature and humidity to the calculation of the scale, as well as other important factors such as the level of clothing insulation of the person and the outdoor air velocity. The Effective Temperature means that the Pierce model converts the actual environment to an environment at an Effective Temperature, which is a dry-bulb temperature of a hypothetical environment at 50% RH and uniform temperature where subjects would experience the same physiological strain as in the real environment.

KSU Thermal Sensation Vote (TSV) for this night gave the following result (figure 51):

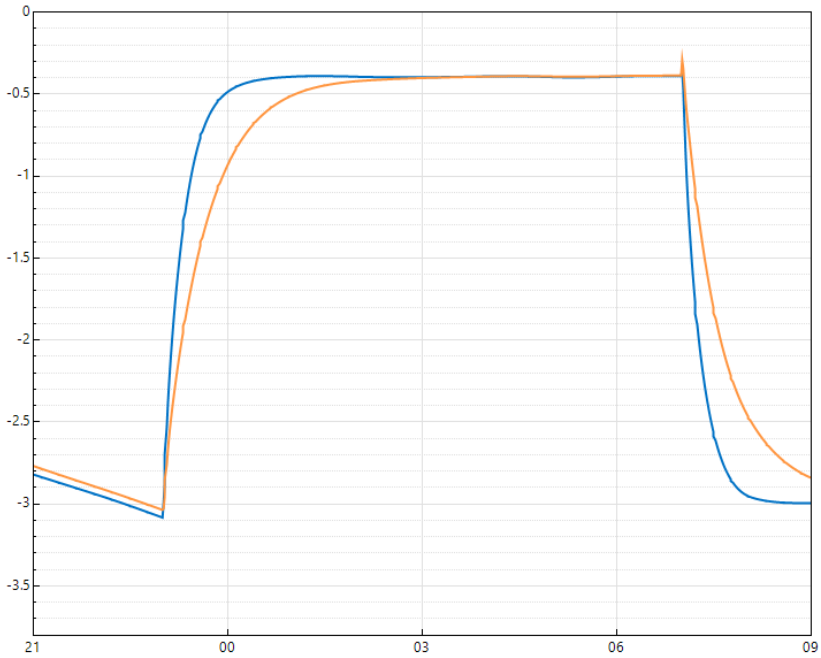

Figure 51 - KSU Model TSV. Blue: Sleeping system without PCMs. Orange: Sleeping system with PCM25-1 Kg.

In figure 51, it can be seen that there are no results out of the scale boundaries (this scale is between -4 and +4), much like the Pierce Two-Node Model ET PMV. This scale also produces a time lag between the PCM and non-PCM sleeping systems, both in the warm up of the sleeping bag, when the person is inside the sleeping system, and in the cooling phase, when the person leaves the sleeping system. The differentiating thing about this scale is that it gives a much wider range of values throughout the night (23h to 07h). Specifically, in the beginning of the night both systems begin with “Cold” (around the -3 mark) and reach a steady-state where the user of the system is neutral to slightly cool, in terms of thermal comfort. Basically, it is a much more sensitive scale, as it produces a worst outcome in the beginning of the night whereas in the steady-state a much more comfortable state is reached than in the other scales.

It was summarized in a table the information of the zone mean air temperature and thermal sensation scales for all the simulations made of this night. It was made a synthesis of the value of chosen output variables.

Beginning of the night

The outside Air temperature was, in the beginning of the night, 9.09 ºC. The scales of thermal comfort are dimensionless.

Table 9 presents the results from the beginning of the night (23h):

Table 9 - Values of temperature and thermal model scales at 23h of 8 January

		Fanger	Pierce	KSU
	Inside Zone Mean Air Temperature (ºC)	PMV	PMV (ET*)	TSV
Control (no PCM)	8,1	-12,50	-2,98	-2,88
Calcium Chloride 22 (1 Kg)	7,5	-12,64	-3,03	-2.97
Calcium Chloride 22 (2 Kg)	7,6	-12,62	-3,03	-2.96
Calcium Chloride 25 (1 Kg)	7,5	-12,64	-3,03	-2.97
Calcium Chloride 25 (2 Kg)	7,6	-12,62	-3,03	-2.96
Calcium Chloride 28 (1 Kg)	7,5	-12,64	-3,03	-2.97
Calcium Chloride 28 (2 Kg)	7,6	-12,62	-3,03	-2.96
Calcium Chloride 31 (1 Kg)	7,5	-12,64	-3,03	-2.97
Calcium Chloride 31 (2 Kg)	7,6	-12,62	-3,03	-2.96
BioPCM 22 (2 Kg)	7,6	-12,58	-3,01	-2.94
BioPCM 25 (2 Kg)	7,6	-12,58	-3,01	-2.94
BioPCM 28 (1 Kg)	7,6	-12,62	-3,03	-2.96
BioPCM 28 (2 Kg)	7,6	-12,58	-3,01	-2.94

It is shown that the Control simulation always starts in a better way than the PCMs. In terms of temperature, it starts out about 0.5 ºC warmer. In terms of thermal sensation scales, the control simulation is always the least negative one from the thermal sensations, which suggests that in the beginning of the night, having PCMs in the system is slightly worse.

Comparing PCM materials with same melting temperature and same quantity in the sleeping mat, it can be seen that BioPCM starts out with a slightly higher temperature than Hexa-hydrated Calcium Chloride, and the thermal scales follow the same trend, i.e. they are less negative, even if only decimal points.

Summarizing, though PCMs make the zone mean air temperature colder, there is not a real difference between sleeping systems with and without PCMs in the beginning of the night.

End of the night

The outside air dry-bulb temperature was, at the end of the night, 8.6 ºC.

At the end of the night (07h), the following values were taken from the simulations (Table 10):

Table 10 - Values of temperature and thermal model scales at 07h of 9 January

		Fanger	Pierce Two-Node	KSU
	Zone Mean Air Temperature (ºC)	PMV	PMV (ET*)	TSV
Control (no PCM)	19,8	-7,82	-1,79	-0,40
Calcium Chloride 22 (1 Kg)	19,8	-7,81	-1,79	-0,39
Calcium Chloride 22 (2 Kg)	19,8	-7,81	-1,79	-0,39
Calcium Chloride 25 (1 Kg)	19,8	-7,81	-1,79	-0,39
Calcium Chloride 25 (2 Kg)	19,8	-7,81	-1,79	-0,39
Calcium Chloride 28 (1 Kg)	19,8	-7,81	-1,79	-0,39
Calcium Chloride 28 (2 Kg)	19,8	-7,81	-1,79	-0,39
Calcium Chloride 31 (1 Kg)	19,8	-7,81	-1,79	-0,39
Calcium Chloride 31 (2 Kg)	19,8	-7,81	-1,79	-0,39
BioPCM 22 (2 Kg)	19,4	-7,95	-1,82	-0,45
BioPCM 25 (2 Kg)	19,8	-7,80	-1,78	-0,39
BioPCM 28 (1 Kg)	19,8	-7,81	-1,79	-0,39
BioPCM 28 (2 Kg)	19,8	-7,80	-1,78	-0,39

It seems that the Zone Mean Air Temperature is almost the same in all cases. In terms of Fanger PMV, it is still “Cold” in all cases (as seen in the previous graph of Fanger PMV), but the sleeping systems with PCM are slightly less discomfortable, which indicates that either the temperature or humidity (or both) provide more comfort in those cases, though it is only a very small change. In the other scales it exists the same trend, in spite of assuming a much less discomfortable steady-state stage, with Pierce Two Node assuming the person would be Slightly Cool to Cool, whereas KSU Thermal Sensation Vote assuming the person would be between Neutral and Slightly Cool.

Night Average

It is important to refer the mean outside air dry-bulb temperature was 8.66 ºC.

Next, the Night Average values were calculated (Table 11):

Table 11 – Mean values of temperature and thermal model scales from 8-9 January night.

		Fanger	Pierce Two-Node	KSU
	Zone Mean Air Temperature (ºC)	PMV	PMV (ET*)	TSV
Control (no PCM)	19,3	-8,01	-1,84	-0,49
Calcium Chloride 22 (1 Kg)	19,0	-8,13	-1,87	-0,55
Calcium Chloride 22 (2 Kg)	18,7	-8,24	-1,90	-0,61
Calcium Chloride 25 (1 Kg)	19,0	-8,12	-1,87	-0,55
Calcium Chloride 25 (2 Kg)	18,7	-8,22	-1,90	-0,60
Calcium Chloride 28 (1 Kg)	19,0	-8,12	-1,87	-0,55
Calcium Chloride 28 (2 Kg)	18,7	-8,22	-1,90	-0,60
Calcium Chloride 31 (1 Kg)	19,0	-8,12	-1,87	-0,55
Calcium Chloride 31 (2 Kg)	18,7	-8,22	-1,89	-0,60
BioPCM 22 (2 Kg)	18,2	-8,41	-1,94	-0,68
BioPCM 25 (2 Kg)	18,5	-8,30	-1,91	-0,64
BioPCM 28 (1 Kg)	18,9	-8,20	-1,88	-0,57
BioPCM 28 (2 Kg)	18,5	-8,30	-1,91	-0,64

Comparing the Zone Mean Air temperature with the mean air temperature of the exterior, all sleeping systems provide some thermal comfort, as inside the sleeping systems the temperature is about 10 ºC warmer than on the outside.

It can be seen in the table above that the Zone Mean Air Temperature is always higher without any kind of PCMs, as well as the thermal sensation scales. This has to do with the time lag previously discussed, as the PCMs absorb heat between the starting temperature of the sleeping system and the steady-state temperature, making the temperature change more slowly between the initial and the steady-state one and the overall zone mean air temperature lower than the control sleeping system's zone mean air temperature.

Considering the thermal sensation scales, it seems that the best case scenario is also the control sleeping system as it is the closest to neutral, which would be zero. Basically, the fact that PCMs thermal sensation scale being better than the control one at the end of the night does not make it better due to the time lag, i.e. the time lag seems to be the dominant factor in this specific example of thermal properties and chosen sleeping system.

Comparing PCM sleeping systems, BioPCM seems to have the most time lag because it has the most negative thermal scales as well as lower zone mean air temperature, which makes sense as this PCM has more phase-change enthalpy, thus requiring more energy to change its state from solid to liquid and

making its sleeping system take longer to reach steady-state temperature. Also, it is important to state that these results do not take into account the energy and time lag when the person has already left the sleeping system, as this energy is not used to warm the person, but most of this energy was given to the PCMs and it is released when there is a sudden drop of temperature in the system, in this case when the person leaves the system.

The CEN 15251 Adaptive Model Temperature, for this night, was 22.52 ºC. This means that most of the values given for the Zone Mean Air Temperature would be in the the 65% Acceptability limits, with the exception of BioPCM 22 (2 Kg), BioPCM 25 (2 Kg) and BioPCM 28 (2 Kg), since these have more than 4 ºC of difference to the reference temperature of 22.52 ºC.

4.2.3. Summary of simulations for the 4 coldest months

It was calculated the average of the same values for all of the nights of the 4 months studied (Table 12):

Table 12 – Mean values of temperature and thermal comfort scales for the 4 month's nights studied

		Fanger	Pierce Two-Node	KSU
	Zone Mean Air Temperature	PMV	PMV (ET*)	TSV
Control (no PCM)	20,8	-7,21	-1,54	-0,30
Calcium Chloride 22 (1 Kg)	20,4	-7,40	-1,61	-0,36
Calcium Chloride 22 (2 Kg)	20,1	-7,57	-1,67	-0,41
Calcium Chloride 25 (1 Kg)	20,5	-7,34	-1,58	-0,35
Calcium Chloride 25 (2 Kg)	20,2	-7,47	-1,62	-0,39
Calcium Chloride 28 (1 Kg)	20,5	-7,34	-1,58	-0,35
Calcium Chloride 28 (2 Kg)	20,2	-7,46	-1,62	-0,39
Calcium Chloride 31 (1 Kg)	20,5	-7,34	-1,58	-0,35
Calcium Chloride 31 (2 Kg)	20,2	-7,46	-1,62	-0,39
BioPCM 22 (2 Kg)	19,3	-7,97	-1,82	-0,51
BioPCM 25 (2 Kg)	19,9	-7,61	-1,68	-0,43
BioPCM 28 (1 Kg)	20,4	-7,39	-1,60	-0,37
BioPCM 28 (2 Kg)	20,0	-7,56	-1,65	-0,43

It seems that the trend of the zone mean air temperature is to be lower with the PCM-sleeping systems, which is similar to the particular night (8-9 Jan) considered, although in this table the temperature is higher, which proves that the night studied was one of the coldest in the weather file considered. The same analogy can be made to the thermal sensation scales, as this average is not as discomfortable as the average of the night considered, even though the values are at the same thermal scale, comparing both tables and comparing the same thermal scales with each other. For example, the KSU TSV is between 'Neutral' and 'Slighty Cool' in both tables, being more inclined to neutral in this averages' table.

Comparing PCMs, some things are different, as BioPCM 22 and BioPCM 25 seem to be the worst in terms of all night performance, analysing purely Zone Mean Air Temperature, which is in line with being the ones that have more latent heat being used in the system. In terms of weight differences between same PCMs, they also seem to have a worse perfomance in terms of temperature due to the fact that more energy is used to change their phase. The thermal scales follow this temperature trend as well.

4.3. Synthesis of Results

Experimental simulation:

- ➔ It can be seen a slower transient with the PCM sleeping system in every graph that is related with PCM performance. These include sleeping mat surface, nape, thigh, chest and interior sleeping bag surface temperature;
- ➔ The only steady-state temperature higher in the non-PCM sleeping system is the ground one. This is due to the fact that the PCMs absorb some of the energy that would go to the Ground;
- ➔ PCM sleeping system shows an overall higher steady-state temperature. This is in line with literature (Quesada et al., 2017);
- ➔ In terms of humidity, the sleeping system's inside RH is lower than outside in both experiments, with and without PCMs;
- ➔ Although it is a small difference, RH in PCM sleeping system is a bit higher than in non-PCM sleeping system;
- ➔ Interior RH follows the same trend as exterior room RH in the same night, which makes sense as it is not a totally insulated system;

Numerical Simulation:

- ➔ The simulation was validated through an experimental simulation;
- ➔ The zone mean air temperature is a good way to check thermal comfort of this sleeping system in particular, which contains sleeping bag, sleeping mat, PCMs and the person. This is in line with literature (Quesada et al., 2017);
- ➔ It was seen that the thermal comfort models behave in the same way as the zone mean air temperature in these meteorology conditions, material properties and subject's activity level (sleep), so it is a good comparison factor between different systems;
- ➔ The PCMs have a transient that is slower to heat up the sleeping system, and in return can give a higher level of steady-state temperature, even though it is an almost negligible increase, in this particular ambient and chosen material properties for the simulations;
- ➔ The best PCM melting temperature tested for this sleeping system and severe meteorology conditions in Lisbon was 22 ºC, as the temperature should allow more use of PCM's latent

energy, whereas for the conditions of the experimental simulation, 28 ºC (20 ºC of room temperature) would be the best;

- ➔ Comparing both PCMs, it can be noted that BioPCM has a higher latent energy, thus having a worst transient but a better steady-state performance than hexa-hydrated calcium chloride;
- ➔ Comparing thermal comfort models, it can be seen that Fanger Predicted Mean Vote is the one that assumes worst conditions for all of the scenarios studied, whereas KSU Thermal Sensation Vote is the one having better conditions for all of the scenarios;
- ➔ All thermal comfort models change very slightly in the simulations made, which indicate that only 1 Kg or 2 Kg of PCMs might not be sufficient to prove or disprove a better or worse thermal sensation for the user in the studied conditions.

5. Conclusions and Future Research

5.1. Conclusions

In this study, PCM incorporation in sleeping mats for improvement of homeless thermal comfort in Lisbon was investigated. This study is not enough to have certainty whether PCMs are a good solution. Overall, it seems that PCM sleeping system has a worse thermal transient (the system takes longer to heat up until steady-state) than a non-PCM sleeping system. However, PCMs seem to make a higher steady-state temperature to a maximum of 2 ºC (result of the experimental simulation). This was expectable, as more energy is needed to heat up a system with more mass (in this case, PCM mass), but the PCM can provide the obtained energy to heat up the system throughout the night, when changing its phase, providing a higher steady-state temperature.

An EnergyPlus model was validated for this application. Both models seem to behave in the same way, and it seems that EnergyPlus model estimates the PCM transient behaviour worse than the experimental simulation did and does not produce as good results for PCM steady-state temperature as the experimental part produced.

In terms of economical assessment, hexa-hydrated calcium chloride seems to be a good choice among PCMs, as it is very cheap (about 0.30 €.Kg^{-1}). Although it would be necessary a package for this PCM, the whole product would never cost more than 1 €, which is a very reasonable price.

5.2. Future Work

This idea should be used with other sleeping systems, especially with other sleeping bags, as the sleeping bag used specifically for this implementation was not made for temperatures below 15ºC to 20ºC, and it was simulated for temperatures around 10 ºC.

The most important thing to do to verify and validate this idea would be to simulate both sleeping systems (with and without PCM) in winter outdoor conditions, as it would be the easiest way to really check the feasibility and easiness of this project. In order to remove variability of the study, several experiments should be made in harsh weather conditions. This would also give a perspective of the lifespan of the product and performance of the PCM in different severe meteorological conditions. It might be difficult to find someone willing to do this experiment in real life conditions. It is important to state that the author of this document was the one inside the experimental simulations. One possible solution for this would be doing the simulations with a thermal manikin, so that the humidity and moisture would be analysed as well. Another possibility would be with water, but this would present more assumptions related to human moisture properties and human thermal losses to the surroundings.

It could also be studied the better form of implementation of PCMs in the sleeping system, as it could be better to implement the PCMs closer to the body, like the vests researched in the literature, or PCMs in the sleeping bag, for instance.

The study of the PCM implementation in the sleeping mat can also be improved, in order to be able to produce it faster and easily for larger quantities of sleeping systems and to improve the lifespan of the product.

This idea can and should be investigated in other climates, as PCMs are a very climate-dependent idea in terms of efficacy. Hence, different optimal PCM melting temperatures can be expected for different parts of the world.

Bibliography

American Society of Heating, Refrigerating and Air-Conditioning Engineers (2013) Ashrae Handbook: Fundamentals. Atlanta, Ga.: Ashrae.

AMI (2006), Annual Report, Lisbon.

Amrit, U. (2007). Bedding textiles and their influence on thermal comfort and sleep. *AUTEX Research Journal,* 8 (4).

Azer, N. Z., Hsu, S. (1977). The prediction of thermal sensation from a simple model of human physiological response. *ASHRAE Trans*. 83(1), 88-102.

Bakos, G. (2000). Energy management method for auxiliary energy saving in a passive-solar-heated residence using low-cost off-peak electricity. *Energy and Buildings*, 31, 237-241. https://doi.org/10.1016/S0378-7788(99)00017-1

Baran, G., Sari, A. (2003). Phase change and heat transfer characteristics of a eutectic mixture of palmitic and stearic acids as PCM in a latent heat storage system. *Energy Conversion and Management*, 44, 3227 – 3246. https://doi.org/10.1016/S0196-8904(03)00104-3

Bhat, V., Adhisivam, B., Nivedita, M., Nishad, P., Sridhar, S., Niranjan, T., Manish, K., Sumitha, A., Kumutha, J., Prakash, A., Umamaheswari, B., Manigandan, C., Mintoo, T., Nithya, J., Vasanthan, T. (2017). Manual on therapeutic hypothermia for perinatal asphyxia. India, NNF Publication.

BioPCM Q29 Datasheet. Retrieved 15 July 2018. URL: https://phasechange.com/wp-content/uploads/2018/02/BioPCM-Data-Sheet-Q29.pdf .

Busch, J. (1992). A tale of two populations: thermal comfort in air-conditioned and naturally ventilated offices in Thailand. *Energy and buildings*, 18, 235-249. doi: 0378-7788/92/$5.00

Choi, S., Zhang, Y., Xia, Y. (2010). A temperature-sensitive drug release system based on Phase-Change Materials. *Angew. Chem.* 122, 8076-8080. https://doi.org/10.1002/ange.201004057

de Dear, R.J., Leow, K.G., Ameen, A. (1991). Thermal comfort in the humid tropics. Part I. Climate chamber experiments on temperature preferences in Singapore. *ASHRAE Transactions*, 1, 874-879. doi:10.1007/bf01041840

den Hartog, E., Weder, M., Camenzind, M. (2001). Evaluation of sleeping bags by subjects and a manikin (torso) at low temperature. Proceedings of the *Fourth International Meeting on Thermal Manikins*, Switzerland, pp 1–5.

Doherty, T.J., Arens, E. (1988). Evaluation of the physiological bases of thermal comfort models. *ASHRAE Transactions*, Vol 94, Part 1.

EnergyPlus Engineering Reference Documentation.

EnergyPlus I/O Reference Documentation.

Fanger, P.O. (1970). Thermal comfort. Analysis and applications in environmental engineering. Copenhagen, *Danish Technical Press*.

Feantsa. Information about homeless people in European Union. Retrieved 1 May 2018. URL: *http://www.feantsa.org/en/.*

Fleischer, A.S. (2015). Thermal Energy Storage Using Phase Change Materials, Fundamentals and Applications. London, *Springer*. doi: 10.1007/978-3-319-20922-7_1

Gagge, A.P., Fobelets, A.P., and Berglund, L.G. Wed (1986). A standard predictive index of human response to the thermal environment, United States.

Gao, C., Kuklane, K., Homér, I. (2010). Cooling vests with phase change materials: the effects of melting

temperature on heat strain alleviation in an extremely hot environment. *Applied Physiology*, 111, 1207-1216. Doi: 10.1007/s00421-010-1748-4

Gao, C., Kuklane, K., Wang, F., Holmér, I. (2012). Personal cooling with phase change materials to improve thermal comfort from a heat wave perspective. *Indoor Air*, 22, 523-530. doi:10.1111/j.1600-0668.2012.00778.x

Goldman R (1988) Review of the extreme cold weather sleeping system. Comfort Technology, Norwood, MA.

Haskell, E., Palca, J., Walker, J., Berger, R., & Heller, H. (1981). The effects of high and low ambient temperatures on human sleep stages. *Electroencephalography and Clinical Neurophysiology*, 51(5), 494–501. doi:10.1016/0013-4694(81)90226-1

Hensel, H. (1981). Thermoreception and temperature regulation. London, *Academic Press,* 33-56.

doi: 10.1007/978-3-642-75076-2

Holand B (1999) Comfort temperatures for sleeping bags. Proceedings of *the Third International Meeting on Thermal Manikin Testing*, Sweden, pp 25–28.

House, J., Lunt, H., Taylor, R., Milligan, G., Lyons, J., House, C. (2012). The impact of a phase-change cooling vest on heat strain and the effect of different cooling pack melting temperatures. *Applied Physiology*, 113, 1223-1231. doi: 10.1007/s00421-012-2534-2

Hu, X., Zhang, Y. (2002). Novel insight and numerical analysis of convective heat transfer enhancement with microencapsulated phase change material slurries: laminar flow in a circular tube with constant heat flux. *International Journal of Heat and Mass Transfer*, 45, 3163-3172. https://doi.org/10.1016/S0017-9310(02)00034-0

Huang, J. (2008). Prediction of air temperature for thermal comfort of people using sleeping bags: a review. *Int J Biometeorol*, 52, 717–723. doi: 10.1007/s00484-008-0180-5

Ielmini, D., Lacaita, A.L. (2011). Phase change materials in non-volatile storage. *Materials Today*, 14, 600-607. https://doi.org/10.1016/S1369-7021(11)70301-7

Incropera, F., DeWitt, D. (2016). Fundamentals of Heat and Mass Transfer (6th ed.), New York, John Wiley and Sons.

Iwata, S., Iwata, O., Olson, L., Kapetanakis, A., Kato, T., Evans, S., Araki, Y., Kakuma, T., Matsuishi, T., Setterwall, F., Lagercrantz, H., Robertson, N. (2009). Therapeutic hypothermia can be induced and maintained using either commercial water bottles or a ‘‘phase changing material’’ mattress in a newborn piglet model. *Arch Dis Child,* 94, 387-391. doi:10.1136/adc.2008.143602

Kaygusuz, K. (1994). Experimental and theoretical investigation of latent heat storage for water based solar heating systems. *Energy Conversion Management* Vol. 36(5), 315-323, 1995. doi:10.1016/0140-6701(96)86718

Kreutzmann, J., Havekes, R., Abel, T., Meerlo, P. (2015). Sleep deprivation and hippocampal vulnerability: changes in neuronal plasticity, neurogenesis and cognitive function. *Neuroscience*, 309, 173-190. http://dx.doi.org/10.1016/j.neuroscience.2015.04.053

Jacobs, S., Berg, M., Hunt, R., Tarnow-Mordi, W., Inder, T., Davis, P. (2013). Cooling for newborns with hypoxic ischaemic encephalopathy, *The Cochrane Library*, 3. doi:10.1002/14651858.CD003311.pub3

McCullough, EA (1994). Determining the insulation value and temperature rating of sleeping bags. Proceedings of *Meeting of the Outdoor Retailer Coalition of America*, Reno, NV.

Meteorological observation at Técnico Lisboa. Retrieved 15 August 2018. URL: http://meteo.tecnico.ulisboa.pt/ .

Muzet, A., Libert, J., Candas, V. (1984). Ambient temperature and human sleep. *Experientia*. 15, 425-429. doi: 0014-4754/84/050422-0451.50

OECD. Information about homeless people in OECD countries. Retrieved 8 April 2018. URL:

https://www.oecd.org/els/family/HC3-1-Homeless-population.pdf

Okamoto-Mizuno, K., Mizuno, K., Tanabe, M., Niwano, K. (2016). Effect of cardboard under a sleeping bag on sleep stages during daytime nap. *Applied Ergonomics*, 54, 27–32. doi:10.1016/j.apergo.2015.11.011

Omega, Complete Measurement, Control and Automation Handbook & Encyclopedia.

Pal, D., Joshi, Y. K. (1997). Application of Phase Change Materials to Thermal Control of Electronic Modules: A Computational Study. *Journal of Electronic Packaging*, 119(1), 40. doi:10.1115/1.2792199

Perlman, J. (2004). Brain Injury in the term infant. *Seminars in perinatology*, 28, 415-424. doi:10.1053/j.semperi.2004.10.003

Pilcher, J. J., Morris, M.D., Donnelly, J., Feigl, H.B. (2015). Interactions between sleep habits and self-control. *Neuroscience*, 9, 284. doi: 10.3389/fnhum.2015.00284.

Pina dos Santos, C., Matias, L. (2006). Coeficiente de transmissão térmica de elementos da envolvente dos edifícios. Laboratório Nacional de Engenharia Civil.

Quesada, J., Gil-Calvo, M, Lucas-Cuevas, A., Aparicio, I., Pérez-Soriano, P. (2017). Assessment of a mattress with phase change materials using a thermal and perception test. *Experimental Thermal and Fluid Science*, 81, 358-363. http://dx.doi.org/10.1016/j.expthermflusci.2016.10.024

Rohles FH Jr, Munson DM (1980) Quantifying the thermal protection and comfort characteristics of sleeping bags. *Thermal insulation performance, ASTM STP 718*, 225–236. doi: 10.1520/STP29276S

Seppanen O., McNall, P.E., Munson, D.M., Sprague, C.H. (1972). Thermal insulating values for typical indoor clothing ensembles. *ASHRAE Transactions* 78(1), 120–130.

Sharma, A., Tyagi, V.V., Chen, C.R., Buddhi, D. (2009). *Renewable and Sustainable Energy Reviews*, 13(2), 318–345. doi:10.1016/j.rser.2007.10.005

Spiegel K., Leproult R., Van Cauter E. (1999). Impact of sleep debt on metabolic and endocrine function. Lancet 1999 354, 1435–39. doi:10.1016/S0140-6736(99)01376-8

Technical specifications of Datalogger HOBO® U10-003. Retrieved 15 May 2018. URL:

https://www.inmtn.com/docs/Onset/Spec%20sheets/U10-003%20Detailed%20Specifications.pdf

Thayyil, S., Shankaran, S., Wade, A., Cowan, F., Ayer, M., Satheesan, K., Sreejith, C., Eyles, H., Taylor, A., Bainbridge, A., Cady, E., Robertson, N., Price, D., Balraj, G. (2013). Whole-body cooling in neonatal encephalopathy using phase changing material. *Arch Dis Child*, 2, 35-39. doi:10.1136/archdischild-2013-303840

Thomas, N., Chakrapani, Y., Rebekah, G., Kareti, K., Devasahayam, S. (2015). Phase Changing Material: An Alternative Method for Cooling Babies with Hypoxic Ischaemic Encephalopathy. *Neonatology*, 107, 266-270. doi: 10.1159/000375286

Tyagi, V.V., Buddhi, D. (2008). Thermal cycle testing of calcium chloride hexahydrate as a possible PCM for latent heat storage. *Solar Energy Materials & Solar Cells* 92, 891–899. doi:10.1016/j.solmat.2008.02.021

Wang, X., Zhang, H., Sun, S., Wu, D. (2011). Fabrication of microencapsulated phase change materials based on n-octadecane core and silica shell through interfacial polycondensation. *Colloids and surfaces A: Physicochemical and engineering aspects*, 389, 104-117. https://doi.org/10.1016/j.colsurfa.2011.08.043

Wang, C., Hong, Y., Zhang, M., Hossain, M., Luo, Y., Su, M. (2012). Thermal fingerprint of silica encapsulated phase change nanoparticles. *Nanoscale*, 4, 3237-3241. doi: 10.1039/C2NR30092C

World Health Organization. Retrieved 12 June 2018. URL: http://www.who.int/

Wu, Y. S., & Fan, J. (2009). Measuring the thermal insulation and evaporative resistance of sleeping bags using a supine sweating fabric manikin. *Measurement Science and Technology*, 20(9), 95-108. doi:10.1088/0957-0233/20/9/095108

Xia, Y., Hyun, D.C., Levinson, N.S., Jeong, U. (2014). Emerging applications of Phase-Change Materials: teaching an old dog new tricks. *Angew. Chem. Int. Ed. 2014*, 53, 3780–3795. doi: 10.1002/anie.201305201

Yang, X., Skralabak, S., Li, Z., Xia, Y., Wang, L. (2007). Photoacoustic tomography of a rat cerebral cortex in vivo with Au nanocages as an optical contrast agent. *Nano Lett.*, 2007, *7* (12), 3798–3802.

doi: 10.1021/nl072349r

Zhang, P., Gong, R. (2002). Influence of clothing material properties on rectal temperature in different environments. *International Journal of Clothing Science and Technology*, 14, 299-306. http://dx.doi.org/10.1108/09556220210446112

Zhao, M., Gao, C., Wang, F., Kuklane, K., Holmér, I., Li, J. (2012). The torso cooling of vests incorporated with phase change materials: a sweat evaporation perspective. *Textile Research Journal,* 1-8. doi: 10.1177/0040517512460294

Accuracy of T-thermocouples. Retrieved 15 May 2018. URL:

https://www.thermocoupleinfo.com/type-t-thermocouple.htm

Technical specifications of Onset® Dataloggers. Retrieved 10 June 2018. URL:

https://www.inmtn.com/docs/Onset/Spec%20sheets/U10-003%20Detailed%20Specifications.pdf

Appendices

Appendix A.1.: Input of PCM in EnergyPlus (Hexa-Hydrated Calcium Chloride)

Table A 1 - Enthalpy-temperature of Hexa-hydrated Calcium Chloride

	Units	HH-CC 22	HH-CC 25	HH-CC 28	HH-CC 31
Temperature Coefficient for Thermal Conductivity	$W.m^{-1}.K^{-2}$	0	0	0	0
Temperature 1	ºC	12	15	18	21
Enthalpy 1	$J.Kg^{-1}$	3078.2	3078.2	3078.2	3078.2
Temperature 2	ºC	16	19	22	25
Enthalpy 2	$J.Kg^{-1}$	8034.99	8034.99	8034.99	8034.99
Temperature 3	ºC	18	21	24	27
Enthalpy 3	$J.Kg^{-1}$	11301.13	11301.13	11301.13	11301.13
Temperature 4	ºC	19	22	25	28
Enthalpy 4	$J.Kg^{-1}$	13375.61	13375.61	13375.61	13375.61
Temperature 5	ºC	20	23	26	29
Enthalpy 5	$J.Kg^{-1}$	16171.74	16171.74	16171.74	16171.74
Temperature 6	ºC	21	24	27	30
Enthalpy 6	$J.Kg^{-1}$	19939.98	19939.98	19939.98	19939.98
Temperature 7	ºC	22	25	28	31
Enthalpy 7	$J.Kg^{-1}$	24921.07	24921.07	24921.07	24921.07
Temperature 8	ºC	23	26	29	32
Enthalpy 8	$J.Kg^{-1}$	31706.06	31706.06	31706.06	31706.06
Temperature 9	ºC	24	27	30	33
Enthalpy 9	$J.Kg^{-1}$	40958.94	40958.94	40958.94	40958.94
Temperature 10	ºC	25	28	31	34
Enthalpy 10	$J.Kg^{-1}$	52910.03	52910.03	52910.03	52910.03
Temperature 11	ºC	27	30	33	36
Enthalpy 11	$J.Kg^{-1}$	80911.44	80911.44	80911.44	80911.44
Temperature 12	ºC	28	31	34	37
Enthalpy 12	$J.Kg^{-1}$	95280.95	95280.95	95280.95	95280.95
Temperature 13	ºC	30	33	36	39
Enthalpy 13	$J.Kg^{-1}$	120084	120084	120084	120084
Temperature 14	ºC	32	35	38	41
Enthalpy 14	$J.Kg^{-1}$	137539.9	137539.9	137539.9	137539.9
Temperature 15	ºC	36	39	42	45
Enthalpy 15	$J.Kg^{-1}$	156510.7	156510.7	156510.7	156510.7
Temperature 16	ºC	38	41	44	47
Enthalpy 16	$J.Kg^{-1}$	161446.2	161446.2	161446.2	161446.2

Appendix A.2.: Input of PCM in EnergyPlus (BioPCM)

Table A 2 - Enthalpy-temperature of BioPCM

		BioPCM 22	BioPCM 25	BioPCM 28
Temperature Coefficient for Thermal Conductivity	$W.m^{-1}.K^{-2}$	0	0	0
Temperature 1	ºC	4	7	10
Enthalpy 1	$J.Kg^{-1}$	13000	13000	13000
Temperature 2	ºC	7	10	13
Enthalpy 2	$J.Kg^{-1}$	19200	19200	19200
Temperature 3	ºC	9	12	15
Enthalpy 3	$J.Kg^{-1}$	24000	24000	24000
Temperature 4	ºC	11	14	17
Enthalpy 4	$J.Kg^{-1}$	29200	29200	29200
Temperature 5	ºC	13	16	19
Enthalpy 5	$J.Kg^{-1}$	34500	34500	34500
Temperature 6	ºC	15	18	21
Enthalpy 6	$J.Kg^{-1}$	38000	38000	38000
Temperature 7	ºC	17	20	23
Enthalpy 7	$J.Kg^{-1}$	43500	43500	43500
Temperature 8	ºC	18	21	24
Enthalpy 8	$J.Kg^{-1}$	46500	46500	46500
Temperature 9	ºC	19	22	25
Enthalpy 9	$J.Kg^{-1}$	51000	51000	51000
Temperature 10	ºC	20	23	26
Enthalpy 10	$J.Kg^{-1}$	58700	58700	58700
Temperature 11	ºC	21	24	27
Enthalpy 11	$J.Kg^{-1}$	96000	96000	96000
Temperature 12	ºC	22	25	28
Enthalpy 12	$J.Kg^{-1}$	182000	182000	182000
Temperature 13	ºC	23	26	29
Enthalpy 13	$J.Kg^{-1}$	258000	258000	258000
Temperature 14	ºC	24	27	30
Enthalpy 14	$J.Kg^{-1}$	277000	277000	277000
Temperature 15	ºC	25	28	31
Enthalpy 15	$J.Kg^{-1}$	280000	280000	280000
Temperature 16	ºC	26	29	32
Enthalpy 16	$J.Kg^{-1}$	286000	286000	286000

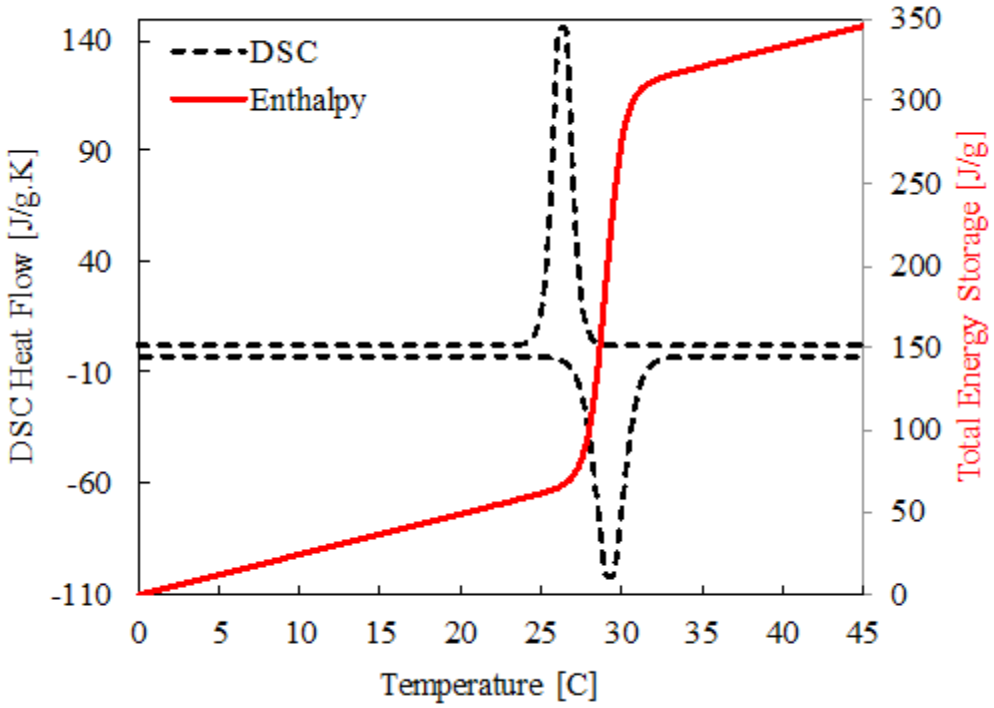

Figure A 1 - Enthalpy curve of Bio PCM (Bio PCM Q29 Datasheet)

Appendix B: Thermocouple information

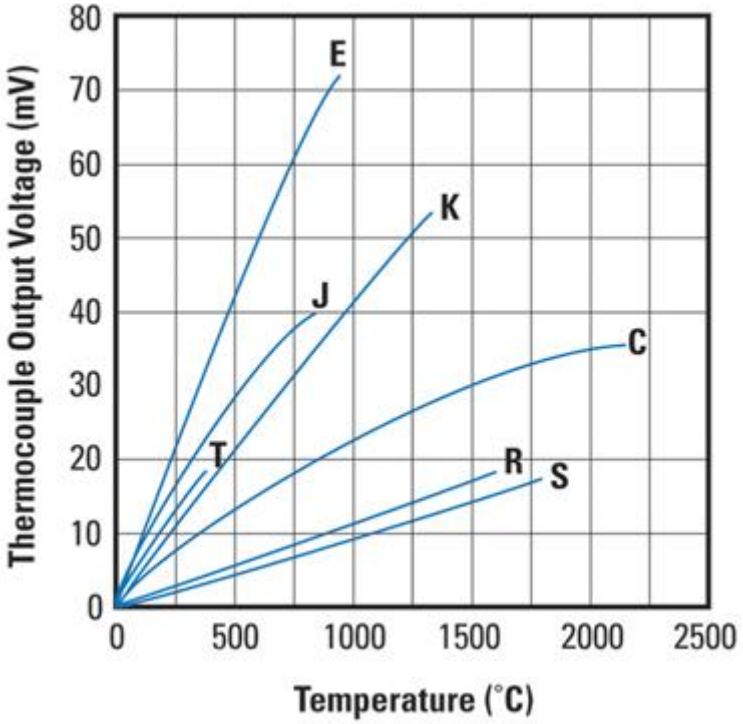

Figure B 1 - Temperature-Millivolt graph for thermocouples (adapted from Omega® Encyclopedia)

Appendix C – Visual Instrument to run NI cDAQ-9172 Datalogger

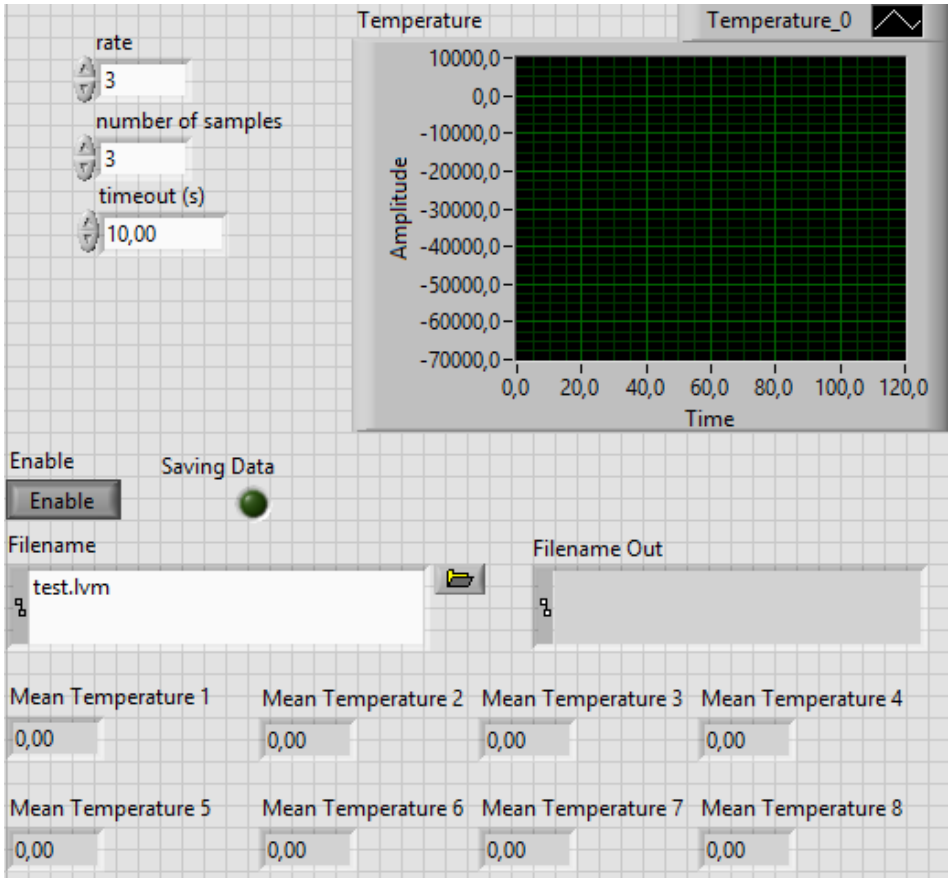

Figure C 1 - VI Front Panel

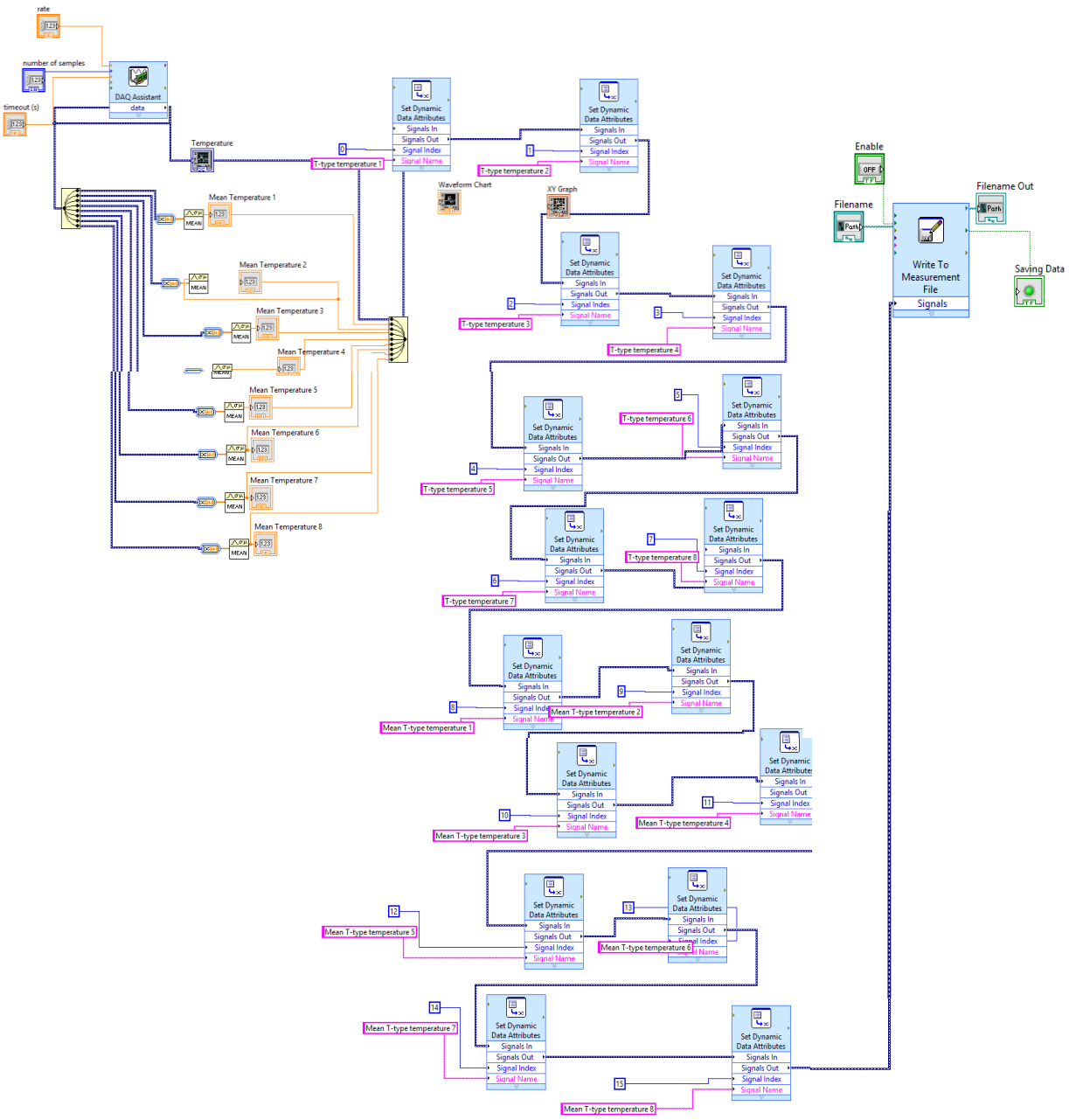

Figure C 2 - VI Block Diagram

Appendix D – Technical specifications of AC unit (Daikin FTXS60)

The version used is Daikin FTXS60-71GV1B:

Table D 1 - AC unit Speed and Power (Daikin FTXS60 Datasheet)

2-1 Technical Specifications				FTXS60GV1B	FTXS71GV1B
Motor	Speed (cooling)	High	rpm	1,330	1,410
		Medium	rpm	1,170	1,220
		Low	rpm	1,010	1,040
		Silent Operation	rpm	920	950
	Speed (heating)	High	rpm	1,360	1,520
		Medium	rpm	1,200	1,330
		Low	rpm	1,040	1,150
		Silent Operation	rpm	950	1,040
Fan	Motor	Output (high)	W	43	43
Cooling	Sound Power	High	dBA	61	62
	Sound Pressure	High	dBA	45	46
		Medium	dBA	41	42
		Low	dBA	36	37
		Silent Operation	dBA	33	34
Heating	Sound Power	High	dBA	60	62
	Sound Pressure	High	dBA	44	46
		Medium	dBA	40	42
		Low	dBA	35	37
		Silent Operation	dBA	32	34

Figure D 1 - Image of AC unit used